POLARIMETRY: THE CHARACTERISATION OF POLARISATION EFFECTS IN EM SCATTERING

by

S.R.Cloude BSc

Thesis submitted to the Faculty of Engineering, University of Birmingham for the degree of Doctor of Philosophy

October 1986

Acknowledgements

I should like to thank my supervisors Prof.R.Shearman and Dr.D.C.Cooper for their help and guidance in writing this thesis. My thanks also to Mr S.E.Gibbs for making this whole project possible and to Dr.G.Gallagher for his patient support during the first 2 years. I am also indebted to Dr.Sands of Dundee University for his useful advice on matters of group theory. Finally, I acknowledge the financial assistance of MOD(PE) who funded me for this degree over the 2 year period August 1982 until August 1984.

Synopsis

This thesis is concerned with the development of a general theory for the characterisation of polarimetric scattering problems.

Traditionally, two main approaches have been used in the literature; the first based on measurement of the coherent scattering matrix (Jones calculus) and the second on measurement of the wave Stokes parameters (Mueller calculus).

This thesis contains three main developments which extend and complement the published work in this area:

1) The representation of nonsymmetric scattering matrices on the Poincaré sphere, using an extension of the fork analysis first introduced by Kennaugh.

2) The construction of a geometry based on the Lorentz transformation for analysing, on the Poincaré sphere, the interaction of partially polarised waves with single targets.

3) The reformulation of polarisation scattering problems in terms of a target spinor and associated coherency matrix. This leads to the construction of a target sphere in 6 dimensions analagous to the Poincaré sphere in 3 dimensions. This new formulation also leads to the development of a decomposition theorem for dynamic targets based on the eigenvectors of the coherency matrix. This decomposition is more fundamental than that used by Huynen and the two are compared and contrasted.

In order to demonstrate many features of the new theory and to highlight its importance to experimental polarimetry, a laser based optical polarimeter was constructed. Results for the measured coherency matrix obtained for transmission through quarter and half wave plates are presented and analysed using the target spinor theory.

LIST OF SYMBOLS

$\underset{\sim}{e}$: instantaneous electric field vector

$\underset{\sim}{E}$: time independent electric field vector

$\underset{\sim}{E}_0$: time and space independent electric field vector

$\underset{\sim}{l}, \underset{\sim}{m}, \underset{\sim}{n}$: unit vectors in a 3 dimensional space

ω : angular frequency

β : wave vector

$\underset{\sim}{E}_1, \underset{\sim}{E}_2$: real and imaginary parts of E_0

$[W_M]$: 2x2 wave matrix

w_1, w_2 : eigenvalues of [W]

θ : inclination angle of major axis of polarisation ellipse

τ : ellipticity angle of polarisation ellipse

$\hat{x}, \hat{y}$: orthonormal polarisation base states

ρ : complex polarisation ratio

α, δ : Deschamps parameters

$\$$: 2 element spinor

$[O_3]$: 3x3 real orthogonal matrix

$[O_6]$: 6x6 real orthogonal matrix

[A] : 3x3 matrix for rotations about l vector

[B] : 3x3 matrix for rotations about m vector

[C] : 3x3 matrix for rotations about n vector

[R] : 2x2 unitary rotation matrix

$\underset{\sim}{\sigma}$: Pauli matrices

$[X_M]$: 2x2 hermitian spin matrix

[L] : Lorentz spin matrix

g : Stokes vector

$[U_2]$: 2x2 unitary matrix

$[U_4]$: 4x4 unitary matrix

[J] : 2x2 wave coherency matrix

j_1, j_2 : eigenvalues of [J]

$\underset{\sim}{b}$: bisectrix vector

$[S]$: 2x2 scattering matrix (conventional coordinates)

$[S_A]$: 2x2 scattering matrix (antenna coordinates)

$[S_D]$: diagonal scattering matrix

$\underset{\sim}{E}_S$: scattered wave spinor

$\underset{\sim}{E}_i$: incident wave spinor

$\underset{\sim}{E}_r$: receiver matched wave spinor

$[P]$: Power scattering matrix

$[U]$: general unitary matrix

$[H]$: general hermitian matrix

$[D]$: diagonal hermitian matrix

$[Q_1]$: matrix of right singular vectors of $[S]$

$[Q_2]$: matrix of left singular vectors of $[S]$

t_1, t_2 : complex singular values of $[S]$

$\varkappa$: target skip angle

γ : target fork angle

P_1, P_2 : Wave probabilities

H_w : wave entropy

D_p : degree of polarisation

$[M]$: 4x4 Mueller matrix

m_{ij} : ijth element of $[M]$

D_{p1} : degree of polarisation for randomly polarised scatter

D_{pc} : critical degree of polarisation

$\hat{\underset{\sim}{k}}$: 4 element wave spinor

$[W]$: 6x6 matrix of minors of $[U]$

$[Q]$: 6x6 permutation matrix

η : set of 16 4x4 target matrices

$[T_c]$: 4x4 target coherency matrix

$\underset{\sim}{p}$: 4 element target vector

Γ : set of first 4 η matrices

H_T : target entropy

$[X]$: matrix of minors of $[T_c]$

LIST OF ILLUSTRATIONS

Overview of Thesis

In Chapter 1 we introduce the main theme of the thesis, namely the use of polarisation information for target identification. This is followed by a brief discussion of the historical background to the subject and a review of the relevant literature.

In Chapter 2 we outline the mathematics required for a description of polarised plane monochromatic waves (called pure states in this thesis) and show how we can formulate such problems in terms of a geometrical quantity known as a spinor. Spinors form the basis for the mapping of pure states onto the Poincaré sphere, the geometry and properties of which are reviewed in section 2.4. Finally, there is a summary of the different coordinate systems used in polarisation problems.

Chapter 3 is concerned with a description of the scattering of pure states from single targets (ie. targets which can be described by a single 2x2 coherent scattering matrix [S]). We deal with the transformation properties of [S] and show how we can map single targets onto the Poincaré sphere via a geometrical construction known as the Polarisation Fork. The main analysis involves a singular value decomposition of [S] with a physical interpretation of the singular vectors as null states. This analysis represents an extension of previous treatments by allowing a geometrical interpretation of nonsymmetric scattering matrices. The implications of using the different coordinate systems of section 2.4 are also explored.

In Chapter 4 we introduce the idea of statistical fluctuations in polarimetry by first considering the representation of partially polarised waves on the Poincaré sphere. We then discuss the interaction of partial states with

single targets via the Mueller matrix and develop a geometrical interpretation of such transformations based on the Lorentz transformation and the Polarisation Fork.

Chapters 5 and 6 represent the core of original work in this thesis. In these chapters we introduce a new formulation of polarisation scattering problems in terms of a target vector (which we show is a spinor in a 6 dimensional space) and coherency matrix. The latter is related to the Mueller matrix and the relationship between them is interpreted in terms of invariants under rotations in 6 dimensions.

With this new formulation we are able to develop a target decomposition theorem for dynamic targets and compare it with the only other such decomposition available in the literature (Huynen 1970). Huynen worked in terms of the Mueller matrix and it is shown, by using the new theorem, that although mathematically correct, his decomposition is but one of an infinite number of other similar analyses and so is not unique.

In Chapter 7 we discuss some experimental results obtained from a coherent optical system designed to investigate many of the new theoretical concepts outlined in the rest of the thesis. Measurements are made of both pure wave states and single targets in the presence of experimental noise. The new coherency matrix formulation is used to analyse the results and extract optimum estimates of the elements of the scattering matrix.

Finally we outline a target classification scheme based on the properties of the target vector and, as an example, consider backscatter from a cloud of identical particles and from a target composed of di and trihedral reflectors.

CONTENTS PAGE

1.1 Introduction

This thesis is concerned with the development of a phenomenological theory for analysing the interaction of polarised electromagnetic (em) waves with dielectric and conducting bodies. Particular emphasis is to be placed on the characterisation and classification of such objects on the basis of the way in which symmetry properties of the target boundary conditions influence the target response to arbitrary incident polarisation.

Although the techniques to be developed are perfectly general, the main application is centred on the analysis of radar target characteristics, covering the frequency range 1-100 Ghz (30cm to 3mm wavelength). Such information is useful in radar systems for enhancing or suppressing radar cross section (Huynen 1970, Poelman 1983) but is also of potential use for solving problems of em inverse scattering (Boerner 1981), where details of target shape and composition are to be inferred from scattered field measurements.

One of the most important features of inverse scattering problems is the sparseness of sampled data (Craig and Brown 1986) and one of the central problems is to quantify just how much target information can be inferred from a limited set of field measurements. It is one of the main objectives of this thesis to examine the potential degrees of freedom present in the polarisation signature of a target and hence to develop measurement and analysis techniques capable of assessing the usefulness or otherwise of polarisation diversity as a source of target information in remote sensing systems.

1.2 Historical background and Literature Survey

The first recorded observation of polarised light was made in 1669 by Erasmus Bartholinus, a Danish philosopher who observed and noted the double images seen through natural crystals of Iceland spar (Calcite). The use of the word "polarisation" to describe the transverse nature of light was first coined by E. Malus in 1808. He made the first qualitative analysis of the reflection of light from surfaces and came to the conclusion that light is to be found in one of two possible forms, analagous to the north and south poles of a magnet; hence the term "polarisation", describing the "polarity" of a light beam.

By 1845, polarised light had been experimentally linked to electromagnetism by Michael Faraday, who observed and noted several electro and magneto optic effects (most notably Faraday rotation). With the theoretical work of James Clark Maxwell to formalise this link, there came a full appreciation of the transverse nature of all electromagnetic waves, and in particular, the realisation that light could exist in any one of an infinite number of different states of elliptical polarisation and not just in the two ways suggested by Malus.

With the advent of Maxwell's field equations, the door was open to a detailed theoretical analysis of depolarisation effects in em scattering problems. Theoretically, it was now possible to solve any problem where target geometry and material properties were known but, in practice, full analytic solutions to such "direct" problems are possible only when the target boundary is expressable in a coordinate system for which the second order vector wave equation is separable. It has been shown that there are only eleven such coordinate systems (Arfken

1970) including cartesian, spherical and cylindrical polar coordinates. This severely restricts the available solutions to such "simple" targets as spheres (first solved by Gustav Mie in 1908) and infinite circular cylinders (Rayleigh in 1881). Most practical problems must then be solved by approximation (the most drastic for our purposes being scalar diffraction theories which ignore entirely the polarisation properties of the scattering process) or, more recently, by numerical techniques.

If direct problems are seen to be difficult, then inverse problems are even more intractable (see Craig and Brown 1986), all of which points to the need for the development of a phenomenological theory, based not on a detailed analysis of the underlying differentio-integral equations, but on a characterisation of the process through measurement of several key field parameters which themselves are derived from a set of minimally restrictive assumptions about the process (eg. linearity, far field scattering etc.). Indeed, the development of such phenomenological theories has formed the basis for study in many areas of physical science, notably quantum optics, where a theory for the absorption and emission of photons by atoms was developed long before quantum mechanics developed to the stage where the absorption and emission coefficients could be calculated for given systems (see Loudon 1983).

Although Maxwell's field equations signalled the beginning of research aimed at a quantitative understanding of polarisation phenomena, a significant theoretical breakthrough had been made in 1852 by George Stokes, Professor of Mathematics at Cambridge. He developed an important description of polarised light based on the propagation of waves in a mechanical medium and, although he had no idea then of the link between light and electromagnetism, his work still remains of fundamental

importance to a qualitative analysis of polarisation phenomena, not only in em scattering but also in the quantum mechanical description of spin dependent scattering (see Fano 1957, Farago 1971). A second important development of the late nineteenth century was the work of the French mathematician H.Poincaré, who developed a mapping of polarisation states onto the surface of a sphere, a geometrical representation which has found widespread application in polarisation analyses.

In the twentieth century the em theory of Maxwell had to be reviewed in light of the new theory of quantum mechanics. In particular, the concept of polarisation, usually ascribed as a wave property, had to be reinterprted in terms of the particulate photon nature of light. At risk of oversimplifying, the essential difference arises in the fact that quantum mechanics ascribes polarisation to the interaction of photons with matter, rather than to free oscillations of the field. Accordingly, photons are found in one of 2 spin states corresponding to the 2 spin states of an electron (the photon is a spin 1 particle with zero rest mass and so its possible spin states are $\pm h$). These 2 possible spins are usually interpreted as the photon being circularly polarised (either left or right) since circularly polarised light does impart angular momentum to a target (Beth 1936). However, the reader must not think that a polarised wave is then composed of well defined left and right handed photons. According to quantum mechanics, we must treat all photons as identical until we make a measurement on the wave. In other words, each photon exists in both states simultaneously, the different observed polarisations being a macroscopic manifestation of the fact that on making a spin measurement, there are different probabilities for the photon to be found in a left or right circularly polarised state. It is in

such probabilistic terms that we must consider polarised waves in quantum optics.

Turning now to the importance of polarisation in em scattering, we begin by noting its discovery in zoology. In the 1950's the Austrian zoologist Karl Frisch discovered that the bee has a compound eye which is sensitive to the polarisation of skylight (Wehner 1976). Such information is used by the insect for navigation to pollen sites. The bee is not the only animal to use polarisation information in this way, some ants and fish also have the capability to detect the polarisation of scattered light. Indeed, the human eye is weakly sensitive to polarisation as evidenced by the Haidinger brush (Scientific American 1976).

These discoveries, combined with interests in the scattering of light by planetary atmospheres, revitalised interest in vector diffraction theories capable of predicting full polarisation effects. In particular, optimisation of radar system performance in the presence of strong clutter, as well as the possibility of using radars for target identification, led to an increased awareness of the importance of polarisation in the microwave scattering problem.

With the development of complex matrix algebra and its application to linear system theory, a phenomenological matrix description was made possible. Early work on developing such matrix theories was performed by R Clark Jones who published a series of seminal papers on the subject between 1941 and 1947. By using Stokes description of polarised waves, Perrin published a paper in 1942 outlining a 4x4 matrix algebra for handling partially polarised scattering, a theory which was further developed by H. Mueller in 1948.

In radar scattering, the Jones calculus was first related to the radar cross section in the range equation by Sinclair (1945) and as such the 2 x 2 scattering matrix, called the Jones matrix in optics, is sometimes called the Sinclair matrix in the radar literature. Pioneering work in the radar area was carried out by E.M.Kennaugh (1952) who derived an elegant geometrical interpretation for backscatter (the most prevalent case for radar) based on the concept of target null states and their mapping on the Poincaré sphere. Experimental and theoretical work continued, notably by Copeland (1960), Graves (1956), Huynen (1965), Déschamps (1951) and Gent (1954) but the full potential of radar polarimetry was never fully realised, due in no small part to technological problems. A summary of this early work is contained in a special issue of Proc IEEE in August 1965. It contains many papers on scattering matrix measurement and on elementary use of the matrix information for target classification.

In the 1970's interest in polarimetric techniques was revived, encouraged by significant advances in signal processing and antenna technologies. The most significant result of this era was the development by J.R. Huynen (1970) of a set of decomposition theorems for analysing fluctuating targets. Although his work contains some important conceptual errors, his ideas form the basis for the decomposition theorems developed in this thesis and must be considered an important step towards the development of a useful phenomenological theory for polarimetric scattering.

Finally, it is worth mentioning some major developments in polarimetry outwith the radar applications.

Mathematically, the problems of polarisation are formulated in terms of spinors and among the very many texts on

spinor algebra, the paper by Payne (1953) and chapter 41 of the book by Wheeler (1973) are useful for gaining physical insight into the geometrical significance of spinors. The use of Stokes parameters for describing statistical effects has also been extended to generalised linear system theory and in particular, the interpretation of the Mueller matrix in terms of a Lorentz transformation has found use in many areas outwith em scattering (Bolinder 1959).

The coherency matrix description of polarised waves was first described by Wolf (1965) and its relation to the Stokes parameters is usually credited to Fano (1957) although both originate in the work of Wiener (1930) on generalised harmonic analysis.

2.1 Plane Waves

We begin by considering a three dimensional plane wave solution to Maxwell's equations, having an electric field vector of the form

$$\underset{\sim}{e} = \mathrm{Re}[\underset{\sim}{E}\exp(i\omega t)] \qquad - 2.1$$

where

$$\underset{\sim}{E} = \underset{\sim}{E_0}\exp(-i\,\underset{\sim}{\beta}.\underset{\sim}{r})$$

$$\underset{\sim}{E_0} = E_{0x}\underset{\sim}{l} + E_{0y}\underset{\sim}{m} + E_{0z}\underset{\sim}{n}$$

E_{0x}, E_{0y} and E_{0z} are complex eg. $E_{0x} = E_{1x}+iE_{2x}$

$\underset{\sim}{r} = x\underset{\sim}{l} + y\underset{\sim}{m} + z\underset{\sim}{m}$: the position vector of a point

$\underset{\sim}{\beta} = \beta_x\underset{\sim}{l} + \beta_y\underset{\sim}{m} + \beta_z\underset{\sim}{n}$: the wave vector

$w = 2\pi f$: the angular frequency

$\underset{\sim}{l}$, $\underset{\sim}{m}$ and $\underset{\sim}{n}$ are unit vectors, forming a right handed cartesian coordinate system.

There is no loss of generality in using such solutions, since an arbitrary wave can be expressed as a sum of plane waves by use of the Fourier integral (Born and Wolf 1970).

We will show that plane waves of this type are characterised by having an electric field vector which traces out an ellipse in a plane as a function of time.

It is important to note that the geometrical parameters of this ellipse are constant ie. the ellipticity and major axis angles do not vary. Such waves will be called pure states of polarisation, to be distinguished from partial states, where the geometry of the polarisation ellipse varies as a function of

time (these states will be the subject of chapter 4).

To show that the locus of $\underset{\sim}{e}$ is elliptical, and to find the geometrical structure of the ellipse given $\underset{\sim}{E}_0$, we define two real vectors

$$\underset{\sim}{E}_1 = E_{1x}\underset{\sim}{l} + E_{1y}\underset{\sim}{m} + E_{1z}\underset{\sim}{n} \qquad - 2.2$$

$$\underset{\sim}{E}_2 = E_{2x}\underset{\sim}{l} + E_{2y}\underset{\sim}{m} + E_{2z}\underset{\sim}{n} \qquad - 2.3$$

where $\underset{\sim}{E}_0 = \underset{\sim}{E}_1 + i\underset{\sim}{E}_2$

and $\underset{\sim}{e} = Re[\underset{\sim}{E}_0 \exp(i\phi)] = \cos(\phi)\underset{\sim}{E}_1 - \sin(\phi)\underset{\sim}{E}_2 \qquad -2.4$

N.B. $\phi = \omega t - \underset{\sim}{\beta}.\underset{\sim}{r}$

From 2.4 it is evident that $\underset{\sim}{e}$ lies in a plane defined by the two vectors $\underset{\sim}{E}_1$ and $\underset{\sim}{E}_2$. The locus of $\underset{\sim}{e}$ is an ellipse, as may be shown by eliminating ϕ from 2.4 (this is achieved by taking the cross product of $\underset{\sim}{e}$ with $\underset{\sim}{E}_1$ and $\underset{\sim}{E}_2$, squaring the result and adding). This leads to the following equation for $\underset{\sim}{e}$

$$(\underset{\sim}{e} \times \underset{\sim}{E}_1)^2 + (\underset{\sim}{e} \times \underset{\sim}{E}_2)^2 = (\underset{\sim}{E}_1 \times \underset{\sim}{E}_2)^2 \qquad - 2.5$$

This equation certainly represents a plane quadric curve, but it is not immediately obvious that the curve is an ellipse. We can easily demonstrate that it is by considering the special case where $\underset{\sim}{E}_1$ is perpendicular to $\underset{\sim}{E}_2$ and lies parallel to the $\underset{\sim}{l}$ unit vector. In this case $e_z = 0$ and

$$(\underset{\sim}{e} \times \underset{\sim}{E}_1)^2 = \underset{\sim}{E}_1^2 \underset{\sim}{e}_y^2$$

$$(\underset{\sim}{e} \times \underset{\sim}{E}_2)^2 = \underset{\sim}{E}_2^2 \underset{\sim}{e}_x^2$$

$$(\underset{\sim}{E}_1 \times \underset{\sim}{E}_2)^2 = \underset{\sim}{E}_1^2 \underset{\sim}{E}_2^2$$

Substituting in 2.5, we obtain the more usual form for the equation of an ellipse

$$\frac{e_x^2}{\underset{\sim}{E}_1^2} + \frac{e_y^2}{\underset{\sim}{E}_2^2} = 1$$

Equation 2.5 is just a generalisation of this result, allowing for arbitrary direction of $\underset{\sim}{E}_1$ and $\underset{\sim}{E}_2$.

We can determine the lengths and directions of the major and minor axes of the polarisation ellipse by expressing $\underset{\sim}{e}$ as a linear combination of $\underset{\sim}{E}_1$ and $\underset{\sim}{E}_2$, ie.

$$\underset{\sim}{e} = \alpha \underset{\sim}{E}_1 + \beta \underset{\sim}{E}_2 \qquad - 2.6$$

and from 2.5

$$\alpha^2 + \beta^2 = 1 \qquad - 2.7$$

The major and minor axes correspond with the extrema of $|\underset{\sim}{e}|^2$ subject to the constraint of 2.7. By using the method of Lagrange multipliers, it can be shown (see Chen 1985) that the lengths of the major and minor axes are given by the eigenvalues of the symmetric matrix

$$[W_M] = \underset{\sim}{E}_r^T . \underset{\sim}{E}_r \qquad - 2.8$$

where $\underset{\sim}{E}_r$ is the 3x2 matrix whose columns comprise $\underset{\sim}{E}_1$ and $\underset{\sim}{E}_2$ ie. $\underset{\sim}{E}_r = (\underset{\sim}{E}_1 , \underset{\sim}{E}_2)$.

If w_1 and w_2 are the eigenvalues of $[W_M]$ then

$$Tr([W_M]) = w_1 + w_2 = \underset{\sim}{E}_1^2 + \underset{\sim}{E}_2^2 \qquad - 2.9$$

$$det([W_M]) = w_1 . w_2 = (\underset{\sim}{E}_1 \times \underset{\sim}{E}_2)^2 \qquad - 2.10$$

and

$$|\underset{\sim}{e}|^2_{max} = w_1$$

$$|\underset{\sim}{e}|^2_{min} = w_2$$

The directions of the major and minor axes can be found from the eigenvectors of $[W_M]$. In particular

$$\underset{\sim}{e}_{max} \parallel [\underset{\sim}{E}_2 \times (\underset{\sim}{E}_1 \times \underset{\sim}{E}_2) - w_1 \underset{\sim}{E}_1] \qquad - 2.11$$

$$\underset{\sim}{e}_{min} \parallel [\underset{\sim}{E}_1 \times (\underset{\sim}{E}_2 \times \underset{\sim}{E}_1) - w_2 \underset{\sim}{E}_2] \qquad - 2.12$$

In many instances, it is important to directly calculate the geometrical parameters of the ellipse ie. the ellipticity and

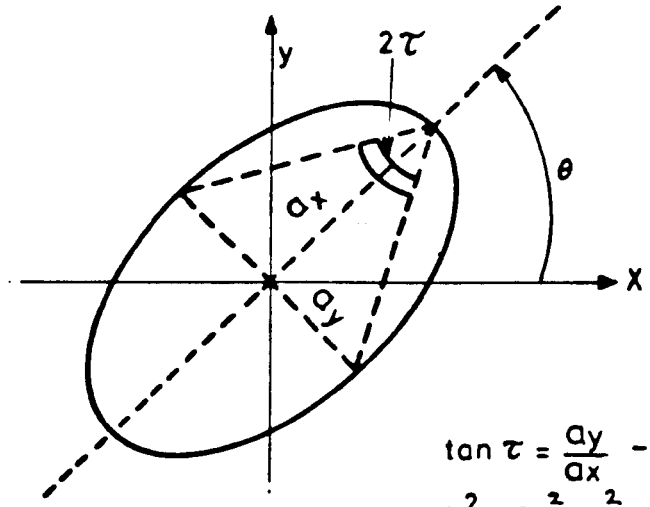

$-45° < \tau < 45°$

$\tan \tau = \frac{a_y}{a_x}$ - Ellipticity angle

$a^2 = a_x^2 + a_y^2$ - Wave amplitude

θ = Inclination angle

FIG.1 POLARISATION ELLIPSE

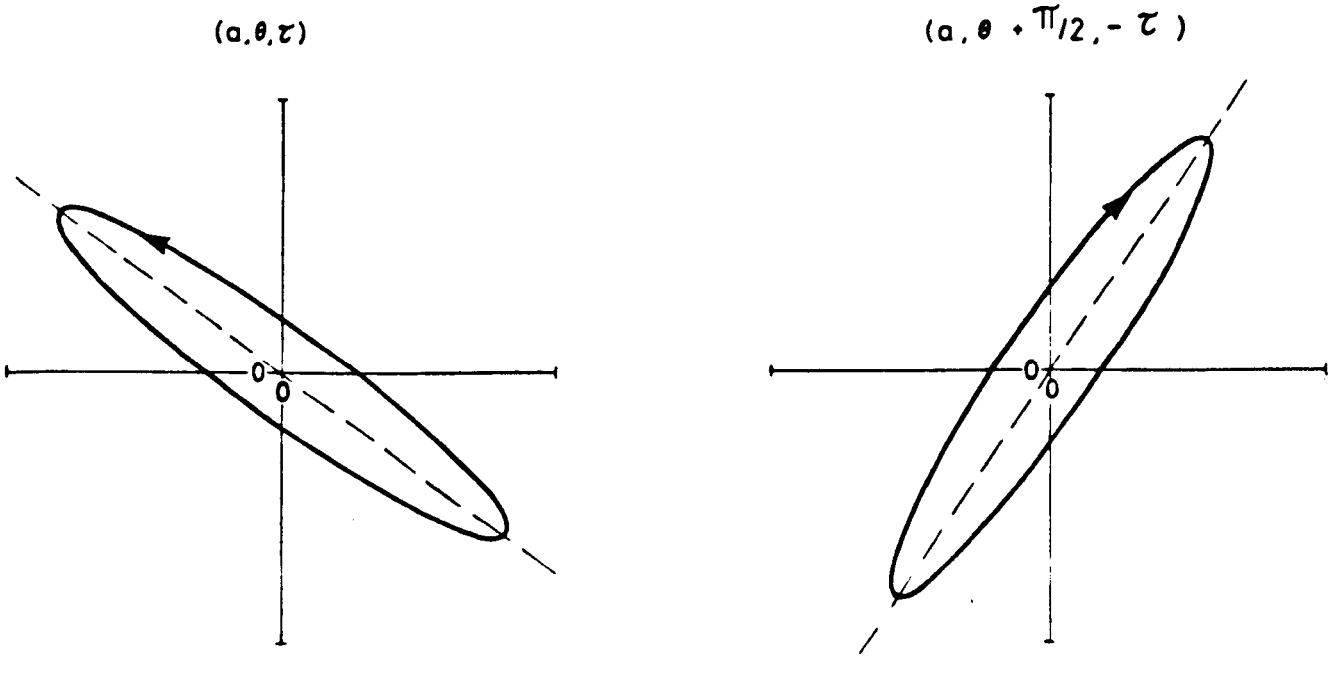

FIG. 2 ORTHOGONAL POLARISATIONS

major axis inclination angles τ and θ (see figure 1). These can be derived from the eigenvalues and eigenvectors of $[W_H]$ as

$$\tan(\tau) = (w_2/w_1)^{1/2} \qquad - 2.13$$

$$0 < \tau < 45°$$

$$\cos(\theta) = [(\underset{\sim}{E}_2 \times (\underset{\sim}{E}_1 \times \underset{\sim}{E}_2) - w_1 \underset{\sim}{E}_1)]_x \qquad - 2.14$$

$$-90° < \theta < 90°$$

where $[]_x$ is the x component of the normalised vector.

Two cases are of special importance:

a) $\det([W_H]) = 0$ defines the condition for linear polarisation ie. $\tau = 0°$

b) If $w_1 = w_2$, $[W_H]$ has degenerate eigenvalues and the wave is circularly polarised ie. $|\tau| = 45°$

Note that for each ellipse, specified by the three parameters w_1, θ and τ, we can define two polarisation states depending on the sense of rotation of $\underset{\sim}{e}$ as a function of time. To account for these we define the sense of polarisation as left or right, depending on the sense of rotation.

To be more specific, when defining the sense we have to decide on the following conventions:

1) Whether to look at the temporal variation of the vector $\underset{\sim}{e}$ in a fixed plane or to examine the spatial variation of $\underset{\sim}{e}$ for fixed time. These are not the same ie. a clockwise temporal variation corresponds to an anticlockwise spatial variation and vice versa.

2) Whether to define the sense of rotation by looking along (parallel) or against (antiparallel) the direction of propagation. Evidently, the sense of rotation will depend on which convention is used.

3) Finally, we have to decide whether left sense polarisations

correspond to clockwise or anticlockwise rotations of $\underset{\sim}{e}$.

In this thesis the angular momentum convention will be adopted because of its widespread use in physics and antenna engineering. According to this convention, the sense is defined by looking at the time variation of $\underset{\sim}{e}$ in a fixed plane (given by z=0). When looking against the direction of propagation the following definitions then apply:

clockwise rotation is left handed

anticlockwise rotation is right handed

As an example, left and right circular are written

$$\underset{\sim}{e}_L = \cos(\omega t)\underset{\sim}{l} + \cos(\omega t + \pi/2)\underset{\sim}{m} \quad \text{or} \quad \underset{\sim}{E}_0^T = (1,i,0) \qquad - 2.15$$

$$\underset{\sim}{e}_R = \cos(\omega t)\underset{\sim}{l} + \cos(\omega t - \pi/2)\underset{\sim}{m} \quad \text{or} \quad \underset{\sim}{E}_0^T = (1,-i,0) \qquad - 2.16$$

This convention parallels that of high energy physics, where the direction of intrinsic angular momentum, or spin, of a photon is defined according to a right hand rule: a right circular photon has angular momentum +h (where h is Planck's constant) and so its spin is directed parallel to the direction of propagation, while a left circular photon has angular momentum -h and its spin points in a direction opposite to that of the propagation vector.

The matrix formulation outlined above follows that of Chen (1985), where further details may be found (Nye (1983) uses a similar idea but a slightly different matrix). This approach has three clear advantages over other formulations (such as detailed by Born and Wolf 1970):

1) It uses a wave matrix which provides a link with other

aspects of polarisation algebra. This is important when studying the spatial and temporal structure of polarised fields, as detailed by Nye (1983). He examines the spatial variation around points of circular polarisation by perturbing the wave matrix.

2) It employs real vectors $\underset{\sim}{E}_1$ and $\underset{\sim}{E}_2$ in place of the complex quantity $\underset{\sim}{E}_0$, so a geometrical interpretation is straight forward.

3) It is perfectly general, being applicable for any plane wave propagating in space, independent of the reference axes chosen.

In many instances the third feature is not essential, since we can arrange the reference axes so that $E_{0z} = 0$ eg. a plane TEM wave propagating along the optic axis.

In this case we can write

$$\underset{\sim}{E}_1 = E_{1x}\underset{\sim}{l} + E_{1y}\underset{\sim}{m}$$

$$\underset{\sim}{E}_2 = E_{2x}\underset{\sim}{l} + E_{2y}\underset{\sim}{m}$$

This simplification allows an important new formulation to be used, for which we define a complex vector

$$\underset{\sim}{E}_0 = \begin{bmatrix} E_x \\ E_y \end{bmatrix} \qquad -2.17$$

where

$$E_x = E_{1x} + iE_{2x}$$

$$E_y = E_{1y} + iE_{2y}$$

We can still use the matrix $[W_H]$ to find the polarisation ellipse, but in this case it pays to treat $\underset{\sim}{E}_0$ as a single geometrical quantity known as a complex vector or <u>spinor</u>(see Payne 1953).

A spinor has potentially four degrees of freedom (derived from the 2 complex coefficients E_x and E_y) ie.

$$\underset{\sim}{E}_0 = E_x \hat{x} + E_y \hat{y}$$

where $\hat{x}$ and $\hat{y}$ are orthonormal complex vectors (which may or may not equal the space vectors $\underset{\sim}{l}$ and $\underset{\sim}{m}$)

$$\text{ie. } \hat{x}^{*T}.\hat{x} = \hat{y}^{*T}.\hat{y} = 1 \text{ and } \hat{x}^{*T}.\hat{y} = 0 \qquad - 2.18$$

$\hat{x}$ and $\hat{y}$ are called the polarisation base states and (x,y) defines the reference base for $\underset{\sim}{e}$. As an example, we very often express every polarisation as a linear combination of horizontal and vertical linear base states, for which the base vectors $\hat{x}$ and $\hat{y}$ are real and may be expressed in terms of the two spatial unit vectors $\underset{\sim}{l}$ and $\underset{\sim}{m}$ as

$$\hat{x} = \hat{h} = \begin{bmatrix} 1 \\ 0 \end{bmatrix} \qquad \hat{y} = \hat{v} = \begin{bmatrix} 0 \\ 1 \end{bmatrix}$$

We can easily generate a range of other base states,

$$\hat{x} = \begin{bmatrix} \cos(A) \\ -\sin(A) \end{bmatrix} \qquad \hat{y} = \begin{bmatrix} \sin(A) \\ \cos(A) \end{bmatrix}$$

by rotating the reference axes through an angle A. These real states correspond to orthogonal linearly polarised waves. We can also create a new base by allowing orthogonal elliptical polarisations (figure 2), in which case $\hat{x}$ and $\hat{y}$ are complex. For example, we can choose left and right circular as a reference base by using the base vectors (still expressed in terms of $\underset{\sim}{l}$ and $\underset{\sim}{m}$)

$$\hat{x} = \frac{1}{\sqrt{2}}\begin{bmatrix} 1 \\ i \end{bmatrix} \qquad \hat{y} = \frac{1}{\sqrt{2}}\begin{bmatrix} 1 \\ -i \end{bmatrix}$$

Clearly, we cannot transform from linear to elliptical base states via a simple plane rotation.

As an attempt at finding a geometrical interpretation of the change of base, we might try to map polarisation states onto

the complex plane. To do this we have to represent $\underset{\sim}{e}$ by a single complex number, and not by the spinor E_0. We can do this by defining the complex polarisation ratio, ρ, as:

$$\rho = E_y/E_x = \tan(\alpha)\ \exp(i\delta) \qquad - 2.19$$

where $0 < \alpha < \pi/2$ and $0 < \delta < 2\pi$

ρ is the ratio of the components of $\underset{\sim}{E}_0$ and has only two degrees of freedom, as expressed by the parameters α and δ, known as the Deschamps parameters (Deschamps 1951). As defined, ρ is insensitive both to the absolute phase of E_x and to the amplitude of the ellipse. Despite this, we can still calculate the geometry of the polarisation ellipse from ρ (as we will show later) and this, combined with the ability to represent polarisations as points on the complex plane, makes ρ a useful parameter in polarisation analyses (see Rumsey 1951, Boerner 1981).

However, the change of base is still not simply related to a rotation in the complex plane and to develop a more complete geometrical model, we have to return to $\underset{\sim}{E}_0$ and examine the properties of spinors in more detail.

In the next section, we will consider the way in which rotations in three dimensional space are described via quaternions. By considering the properties of spinors and their relation to quaternions, we will arrive at a one to one correspondence between the set of all possible polarisation states and the surface of a 3-sphere, a result which means that the transformation of base is geometrically equivalent to a rotation in a real 3-dimensional space.

In polarisation algebra this sphere is called the Poincaré sphere and we will return to examine its properties in section 2.4.

2.2 Spinor Algebra

Spinors are complex quantities, $, which transform under complex matrix operators [S] as

$$\$' = [S].\$ \qquad - 2.20$$

where

$$\$ = \begin{bmatrix} \$_x \\ \$_y \end{bmatrix} = \begin{bmatrix} \cos\alpha.\exp(i\nu_x) \\ \sin\alpha.\exp(i\nu_y) \end{bmatrix} \qquad - 2.21$$

and x,y are orthonormal basis vectors, with

$$[S] = \begin{bmatrix} S_{xx} & S_{xy} \\ S_{yx} & S_{yy} \end{bmatrix} \qquad S_{ij} \text{ are complex}$$

The name spinor derives from the close association between unitary transformations of $, where $[S]^{*T} = [S]^{-1}$,and rotations of a real vector, $\underset{\sim}{r} = x\underset{\sim}{l} + y\underset{\sim}{m} + z\underset{\sim}{n}$ in a 3 dimensional space. In the former case $\$^{*T}.\$$, the magnitude of the spinor, is an invariant, while in the latter, $\underset{\sim}{r}^2$ is an invariant under transformations of the form

$$\underset{\sim}{r}' = [O_3].\underset{\sim}{r} \qquad - 2.22$$

where $[O_3]$ is a real orthogonal matrix, specified by three Euler angles a,b and c so that

$$[O_3] = [A].[B].[C]$$

where

$$[A] = \begin{bmatrix} 1 & 0 & 0 \\ 0 & \cos(a) & \sin(a) \\ 0 & -\sin(a) & \cos(a) \end{bmatrix}$$

$$[B] = \begin{bmatrix} \cos(b) & 0 & -\sin(b) \\ 0 & 1 & 0 \\ \sin(b) & 0 & \cos(b) \end{bmatrix}$$

$$[C] = \begin{bmatrix} \cos(c) & \sin(c) & 0 \\ -\sin(c) & \cos(c) & 0 \\ 0 & 0 & 1 \end{bmatrix}$$

and a, b and c represent rotations about the x, y and z axes. NB. Goldstein (1980) details 12 different conventions for the Euler angles, the above being known as the Tait-Bryan or engineering convention.

The laws for combining transformations of the spinor $ are related to those for combining rotations in 3-space and it is the purpose of this section to investigate the nature of this relation.

It is well known (see Misner 1973) that rotations in 3 dimensional space cannot be descibed by scalars or vectors, and that the laws for combining them are formulated in terms of a quantity known as a spin matrix or quaternion. In this formulation a rotation of x degrees about an axis which lies in a direction specified by the three angles α, β and γ is written

$$\begin{aligned} [R] &= \cos(x/2)\sigma_0 - i\sin(x/2)[\sigma_1\cos\alpha + \sigma_2\cos\beta + \sigma_3\cos\gamma] \\ &= \cos(x/2)\sigma_0 - i\sin(x/2)[\underline{\sigma}.\underline{n}] \\ &= \exp(-ix[\underline{\sigma}.n]/2) \end{aligned} \qquad - 2.23$$

where σ_0 is the 2x2 identity, $\underline{n}$ the vector of direction cosines and $\underline{\sigma}$ the Pauli matrices given by

$$\sigma_1 = \begin{bmatrix} 1 & 0 \\ 0 & -1 \end{bmatrix} \qquad \sigma_2 = \begin{bmatrix} 0 & 1 \\ 1 & 0 \end{bmatrix} \qquad \sigma_3 = \begin{bmatrix} 0 & -i \\ i & 0 \end{bmatrix} \qquad - 2.24$$

which satisfy the following relations

$$\sigma_i^{*T} = \sigma_i$$

$$\sigma_i\sigma_j + \sigma_j\sigma_i = 2\delta_{ij}\sigma_0$$

$$\sigma_i\sigma_j = i\varepsilon_{ijk}\sigma_k$$

where δ_{ij} is the Kronecker symbol, ε_{ijk} the permutation symbol and σ_0 the 2x2 identity matrix.

In particular, for a rotation of x about the x, y, and z axes, respectively, we have

$$[R]_y = \begin{bmatrix} \cos(x/2) & -i\sin(x/2) \\ -i\sin(x/2) & \cos(x/2) \end{bmatrix} \quad [R]_z = \begin{bmatrix} \cos(x/2) & -\sin(x/2) \\ \sin(x/2) & \cos(x/2) \end{bmatrix}$$

and

$$[R]_x = \begin{bmatrix} \exp(-ix/2) & 0 \\ 0 & \exp(ix/2) \end{bmatrix}$$

Note that [R] is a 2x2 complex unitary matrix

ie. $[R]^{*T} = [R]^{-1}$ and $\det([R])=1$

When written in this form, the law for combining rotations $[R_1]$ and $[R_2]$ to produce a third, $[R_3]$, is particularly simple and given by Hamilton's formula

$$[R_3] = [R_2].[R_1] \qquad - 2.25$$

In order that [R] operate on a real vector $\underset{\sim}{r}$, we construct a spin matrix [X] from $\underset{\sim}{r}$, given by

$$[X] = x\sigma_x + y\sigma_y + z\sigma_z$$

$$= \begin{bmatrix} x & y-iz \\ y+iz & -x \end{bmatrix} = \underset{\sim}{\sigma}.\underset{\sim}{r} \qquad - 2.26$$

and under the operation of [R], [X] transforms as

$$[X]' = [R].[X].[R]^{*T} \qquad - 2.27$$

where $\det([X]') = \det([R]).\det([X]).\det([R]^{*T}) = \det([X]) = \underset{\sim}{r}'.\underset{\sim}{r}$

By direct comparison with the Euler angle formulation discussed earlier, we can see evidence of a close correspondence between 2x2 unitary matrices, [R], and 3x3 real orthogonal matrices, $[O_3]$. For example, the matrix [A] corresponds to R_x, in that both represent rotations about the x-axis (similarly [B] and [C] correspond to R_y and R_z).

We can formalise this correspondence by defining the groups SU(2) and O_3^+ as, respectively, the group of all 2x2 unitary and 3x3 real orthogonal matrices, both having determinant = +1. Further, if two groups X and Y have a one to one correspondence between their elements then they are said to be <u>isomorphic</u>, while if the correspondence is two (or many) to one, we say that the groups are <u>homomorphic</u> (see Arfken).

The correspondence between SU(2) and O_3^+ is not a simple one to one relationship because of the appearance of the half angle in [R]. For example

$$[C(c+360°)] = [C(c)]$$

but $$[R(c/2+180°)]_z = -[R(c/2)]_z$$

hence both $[R(c/2)]_z$ and $-[R(c/2)]_z$ correspond to [C(c)]. For this reason SU(2) and O_3^+ are 2-to-1 or homomorphic.

By definition, the spinor \$ transforms under [R] as

$$\$' = [R].\$$$

from which we can show that \$ and the vector $\underset{\sim}{r}$ are related via the spin matrix

$$[X] = \$.\$^{*T} \qquad - 2.28$$

so that $\underset{\sim}{r} = 1/2\ \mathrm{Tr}([X].\underset{\sim}{\sigma})$

ie. $x = 1/2(\$_1.\$_2^{*}-\$_2.\$_2^{*})$

$y = \mathrm{Re}(\$_1.\$_2^{*})$

$z = \mathrm{Im}(\$_1.\$_2^{*})$

$\underset{\sim}{r} = (x,y,z)$, is called the associated longitudinal vector of the spinor (see Payne 1953).

Before looking at the interpretation of these ideas in the context of polarisation, we must first extend the concept of a rotation matrix to incorporate Lorentz transformations of a four vector, g. We will need such transformations when considering partial states and target operators in chapter 4. We can proceed by defining a four vector

$$\underset{\sim}{g}^{T} = (g_0, g_1, g_2, g_3)$$

where $g_0^2-g_1^2-g_2^2-g_3^2 = d_4$ is to be an invariant.
We can fit this with our previous ideas by generalising the concept of a spin matrix to

$$[X] = g_0.\sigma_0+\underset{\sim}{g}_r.\underset{\sim}{\sigma} \qquad - 2.29$$

$$= \begin{bmatrix} g_0+g_1 & g_2-ig_3 \\ g_2+ig_3 & g_0-g_1 \end{bmatrix}$$

where $g_0 = 1/2(\$_1.\$_1^{*}+\$_2.\$_2^{*})$, transforms like a scalar while $\underset{\sim}{g}_r = (g_1, g_2, g_3)$ is the longitudinal vector of $\$$.
Remembering that $\det(X) = d_4$ must be a transformation invariant, we can postulate a transformation of the form (Misner 1973)

$$[X]' = [L].[X].[L]^{*T} \qquad \det([L]) = 1 \qquad - 2.30$$

where [L] is called the Lorentz spin matrix and is obtained from [R] by allowing complex angles of rotation such that

$$[L] = \exp[(-i\chi\underline{n}+\alpha\underline{k}).\underline{\sigma}/2] \qquad - 2.3$$

where χ is a real angle of rotation and $\alpha\underline{k}$ is a vector specifying the direction and magnitude of a "boost" for the spinor $\underline{E}_0$ (see section 4.3 for more details).

2.3 The Wave Spinor

In this section we will look at the implications of using spinor algebra for the description of polarised waves.

We will begin by identifying E_0 as a spinor (see 2.17) and hence associate the Deschamps parameters with 2.21 (where we define $\delta = r_y - r_x$). As mentioned in section 2.1, we can express $\underline{E}_0$ in terms of an infinite number of orthonormal base states, (x,y), and in order to make use of spinor algebra we must look more closely at the details of the change of base transformation.

The change from (x,y) to (x',y') is a linear transformation in C2, the complex 2 dimensional space. The only constraint is the invariance of the orthonormal conditions, 2.18, which force the transformation matrix, $[U_2]_s$, to be unitary. Hence (see Goldstein 1980)

$$\begin{bmatrix}\hat{x}'\\ \hat{y}'\end{bmatrix} = \begin{bmatrix}\cos\alpha.\exp(i\theta) & \sin\alpha.\exp(i\delta)\\ -\sin\alpha.\exp(-i\delta) & \cos\alpha.\exp(-i\theta)\end{bmatrix}\begin{bmatrix}\hat{x}\\ \hat{y}\end{bmatrix} \qquad - 2.32$$

θ represents a phase reference for the new base states and is

not important in determining the geometrical parameters of $\hat{x}'$ and $\hat{y}'$. In many instances it is factored from the matrix, which becomes

$$[U_2]_B = \begin{bmatrix} \exp(i\theta/2) & 0 \\ 0 & \exp(-i\theta/2) \end{bmatrix} \begin{bmatrix} \cos\alpha & \sin\alpha.\exp(i\delta) \\ -\sin\alpha.\exp(-i\delta) & \cos\alpha \end{bmatrix} \quad - 2.33$$

The first component is just $[R]_x$, which as we saw in section 2.2, corresponds to a rotation of 0^0 about the x axis in a 3-dimensional space. By ignoring this rotation, we can express the transformation matrix in terms of the complex polarisation ratio, ρ , as

$$[U_2]_B = (1+\rho\rho^*)^{-1/2} \begin{bmatrix} 1 & \rho \\ -\rho^* & 1 \end{bmatrix} \quad - 2.34$$

We can write an arbitrarily polarised wave as

$$\underset{\sim}{e} = E_x\hat{x} + E_y\hat{y}$$

or

$$\underset{\sim}{e} = E_x'\hat{x}' + E_y'\hat{y}'$$

By substituting for $\hat{x}'$, $\hat{y}'$ and equating, we obtain an equation for the transformation of coefficients (as opposed to base states)

$$E_0 = [U_2]_C . E_0' \quad - 2.35$$

where $[U_2]_C = [U_2]_B^T$. In all further calculations we will drop the "B" and "C" subscripts and write $[U_2]$ for the matrix describing the change of <u>components</u> ie $[U_2]_C$.

Note that ρ is the complex polarisation ratio defining $\hat{x}'$ in terms of $\hat{x}$ and $\hat{y}$ eg. if (x,y) is horizontal and vertical linear, (h,v), and we wish to transform to left and right circular ,(l,r), then $\rho = i$ and

$$[U_2] = 2^{-1/2}\begin{bmatrix} 1 & 1 \\ i & 1 \end{bmatrix}$$

Having established the unitary nature of the change of base transformation, we can use the results of section 2.2 to identify $[U_2]$ with [R] and say that the change of base is equivalent to a rotation in a real 3-dimensional space. We can also calculate the vector $\underset{\sim}{r}$, associated with $\underset{\sim}{E}_0$, from 2.28 and so associate a unique point in 3-space with any given polarisation state. In addition, all states of the same amplitude must lie on the surface of a sphere, called the Poincaré sphere.

In summary, by using a homomorphic relationship between two groups we have turned a complex problem into an equivalent real space problem. This result is of paramount importance because it enables us to solve polarisation problems by considering only rotations of a sphere in 3-space.

The only remaining problem is to relate the Euler angles a, b and c to the geometrical structure of the polarisation ellipse.

We saw in section 2.1 that the polarisation ellipse can be specified by three parameters, namely a, θ and τ. If we assume, initially, that the major axis is aligned with the reference x direction, taken as the unit vector $\underset{\sim}{1}$, then we can express $\underset{\sim}{e}$ in terms of τ as follows:

$$e = \begin{bmatrix} a\cos(\tau).\cos(\phi) \\ -a\sin(\tau).\sin(\phi) \end{bmatrix} = Re\begin{bmatrix} a\cos(\tau) \\ ia\sin(\tau) \end{bmatrix} \exp(i\phi) \qquad - 2.36$$

where $\phi = \omega t - \beta.r$ and

$$E_0 = a\begin{bmatrix} \cos(\tau) \\ i\sin(\tau) \end{bmatrix} \qquad - 2.37$$

If the major axis makes an angle θ with the reference x axis, we can modify this equation quite easily to give

$$E_0 = a\begin{bmatrix} \cos(\theta) & -\sin(\theta) \\ \sin(\theta) & \cos(\theta) \end{bmatrix}\begin{bmatrix} \cos(\tau) \\ i\sin(\tau) \end{bmatrix} \qquad - 2.38$$

By forming E_x^2 and equating with $\cos^2\alpha$ we can derive an equation relating α to the geometrical parameters:

$$\cos(2\alpha) = \cos(2\theta).\cos(2\tau) \qquad - 2.39$$

In order to relate δ to θ and τ, we must consider the change of base matrix, $[U_2]$, in terms of a change of ellipticity, τ_c, and inclination angle, θ_c. This has the form

$$[U_2] = \begin{bmatrix} \cos(\tau_c) & i\sin(\tau_c) \\ i\sin(\tau_c) & \cos(\tau_c) \end{bmatrix}\begin{bmatrix} \cos(\theta_c) & -\sin(\theta_c) \\ \sin(\theta_c) & \cos(\theta_c) \end{bmatrix} \qquad - 2.40$$

Note that the τ_c component is derived from

$$\begin{bmatrix} \cos(\tau+\tau_c) \\ i\sin(\tau+\tau_c) \end{bmatrix} = \begin{bmatrix} \cos(\tau_c) & i\sin(\tau_c) \\ i\sin(\tau_c) & \cos(\tau_c) \end{bmatrix}.\begin{bmatrix} \cos(\tau) \\ i\sin(\tau) \end{bmatrix}$$

By comparing this with 2.23 we can show that (see Deschamps 1951)

$$\tan(\delta) = \tan(2\tau).\csc(2\theta) \qquad - 2.41$$

The inverse relationships may be similarly derived as

$$\tan(2\theta) = \tan(2\alpha).\cos(\delta) \qquad - 2.42$$

$$\sin(2\tau) = \sin(2\alpha).\sin(\delta) \qquad - 2.43$$

Equation 2.40 is the key result, when we write it in the form

$$[U_2] = \exp(i2\tau.\sigma_y).\exp(i2\vartheta.\sigma_z) \qquad - 2.44$$

we can make a direct comparison with 2.23 and hence arrive at our desired relationship between the Euler angles and the geometrical parameters of the polarisation ellipse.

This result indicates that, starting from a reference linear polarisation, we can move to any other state (specified by θ and τ) on the Poincaré sphere by undertaking two rotations: first, 2θ about the z axis (longitude on the sphere) and secondly, 2τ about the new y axis (latitude).

Realising that 2τ and 2θ are just the latitude and longitude of points on the Poincaré sphere, we can use equations 2.39 and 2.41 to prove that the Deschamps parameters are related to the geometrical parameters by the formation of a right angled spherical triangle (see figure 3).

In order to move from point to point on the sphere, we need only know two angles, but, as we saw earlier, we need three Euler angles to describe an arbitrary rotation in 3 dimensions. We must therefore examine the physical significance of the

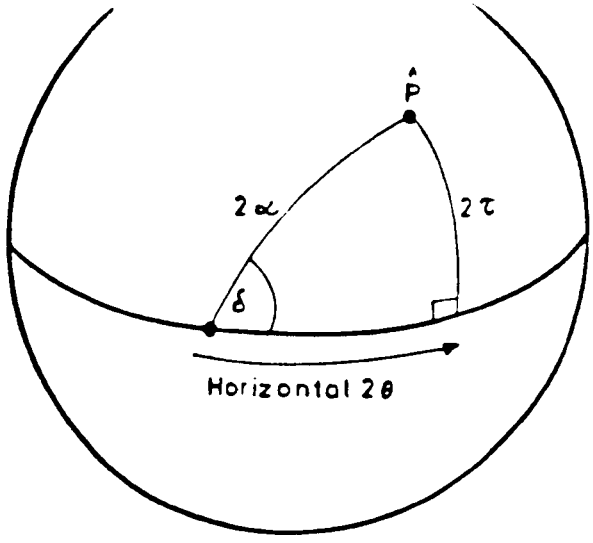

δ = Phase of polarisation ratio

$\tan\alpha$ = Amplitude of polarisation ratio

θ = Inclination angle of polarisation ellipse

τ Ellipticity angle

FIG 3 DÉSCHAMPS SPHERE

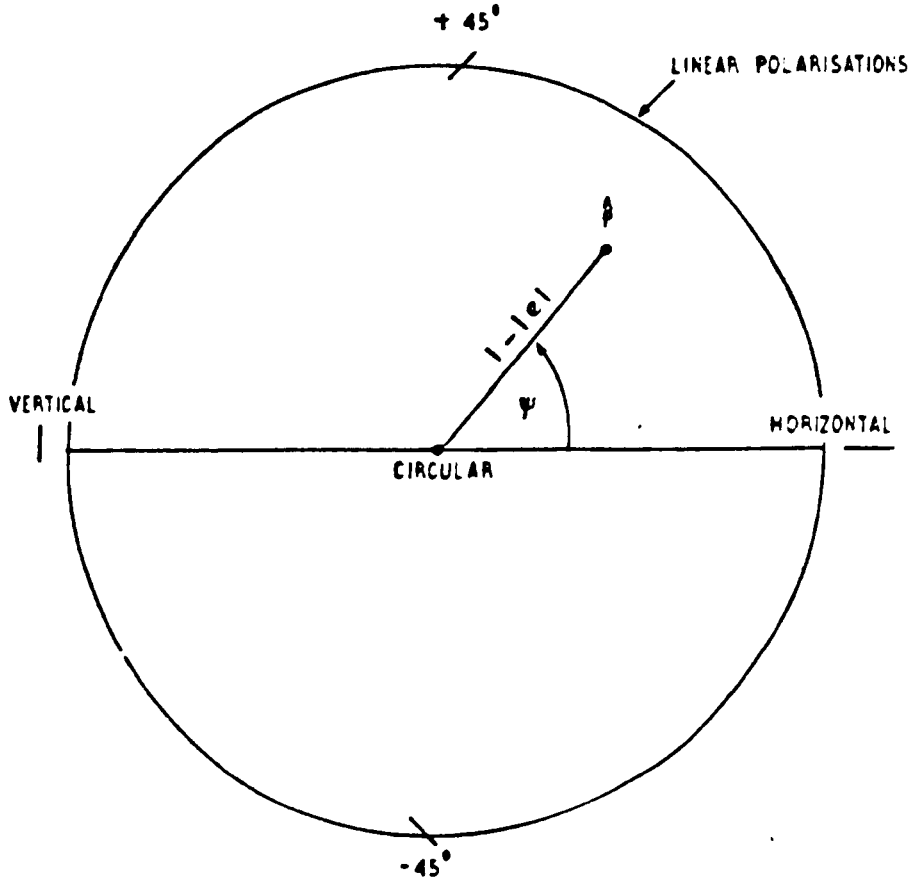

RADIUS FROM $C-\hat{P} = 1-|e|$ $|e|$ IS ECCENTRICITY OF POLARISATION ELLIPSE $(0 \leq |e| \leq 1)$

ANGLE $\psi = 2\theta$ θ IS THE ORIENTATION ANGLE OF POLARISATION ELLIPSE $(-\pi/2 \leq \theta \leq \pi/2)$

FIG 4 POLARISATION CHART

third component, $[R]_3$.

This angle specifies a rotation of the whole coordinate system about the final x axis (ie. about a line joining the centre of the sphere to the point representing the new polarisation state). As mentioned earlier (see 2.33), this angle depends only on the phase reference taken for the new base states.

2.4 Stokes Parameters And The Poincaré Sphere

In the last section we saw that by using the results of spinor algebra, we could map all polarisation states onto the surface of the Poincaré sphere. The latitude and longitude of points on this sphere are simply the double angles 2τ and 2θ, where τ and θ are the ellipticity and inclination angles of the polarisation ellipse. We also found a simple relationship between the geometrical and Deschamps parameters, as given by equations 2.39 and 2.41.

In this section we will look more closely at the distribution of states over the surface of the sphere and at the relationship between the angular and cartesian coordinates of points in polarisation space. In the process we will discover a generalised form of the law of Malus, concerning the polarisation efficiency of receiving systems; discuss some of the different coordinate systems used for describing the sphere and introduce the concept of polarisation filtering.

There is a great deal of symmetry in the distribution of polarisation states over the Poincaré sphere (see figure 6). These properties may be summarised as follows:

1) The set of all linear polarisations map onto the equator, which separates two symmetrical hemispheres, the upper representing left hand elliptical polarisations and the lower, a

similar set of right handed states.

2) Orthogonal polarisations have an inclination angle difference of 90 degrees and opposite sense (with the same magnitude of ellipticity), and so are antipodal on the sphere.

3) Left circular lies at the north pole (τ = 45°) with right circular at the south pole (τ = -45°), as consistent with the angular momentum convention (see 2.1).

4) The radius of the sphere is proportional to the amplitude of the wave ie. $E_x^2+E_y^2$. Usually, we normalise this amplitude to unity and consider only transformations of θ and τ. In many instances, amplitude information is of secondary importance (eg. when looking for polarisations which produce a null measurement) in which case, normalising the radius of the sphere is unimportant and allows a convenient representation of the degree of polarisation of partial states (see 4.1).

In order to calculate the cartesian coordinates of points in polarisation space, we can use equations 2.26 and 2.28 to create a polarisation spin matrix, [J], called the wave coherency matrix (Born and Wolf 1970)

$$[J] = \underset{\sim}{E_o}.\underset{\sim}{E_o}^{*T} \qquad - 2.45$$

[J] is the starting point for a discussion of partial states, which are the subject of chapter 4, and for now we need only recognise the fact that we can calculate the elements of the longitudinal vector, $\underset{\sim}{g_s}$, from

$$\underset{\sim}{g}_i = \tfrac{1}{2}\mathrm{Tr}([J].\sigma_i) \qquad i = 1,2,3 \qquad - 2.46$$

where $\underset{\sim}{\sigma}$ are the Pauli matrices (see 2.24). The components are given explicitly as

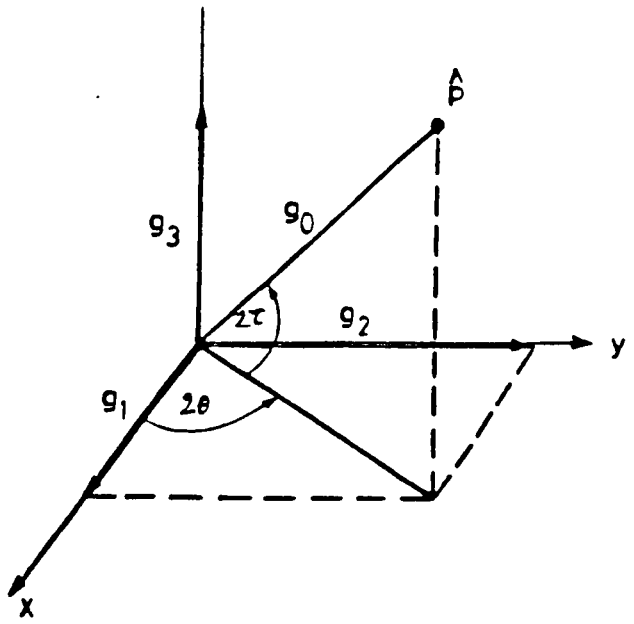

$\underline{g} = (g_0\ g_1\ g_2\ g_3)$ $\qquad g_0^2 = g_1^2 + g_2^2 + g_3^2$

(1, 1, 0, 0) = Horizontal
(1,-1, 0, 0) = Vertical
(1, 0, 1, 0) = +45° Linear
(1, 0, 0, 1) = Left Circular

FIG. 5 STOKES PARAMETERS AND POLARISATION SPACE

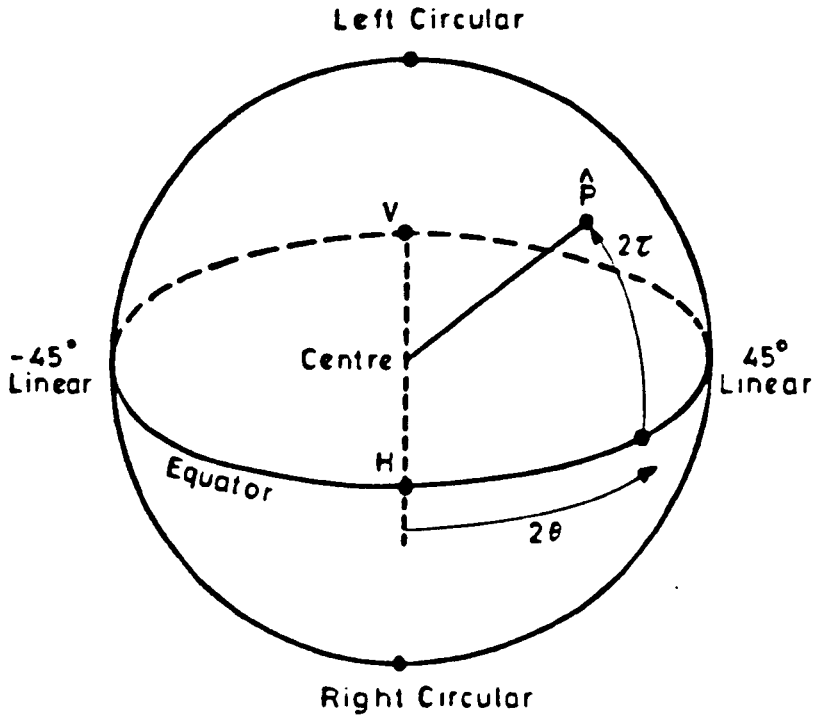

FIG. 6 POINCARÉ SPHERE

$$g_1 = \frac{1}{2}(E_x^2 - E_y^2) = a\cos(2\theta)\cos(2\tau) \qquad -2.47$$

$$g_2 = \mathrm{Re}(E_x.E_y^*) = a\sin(2\theta)\cos(2\tau) \qquad -2.48$$

$$g_3 = \mathrm{Im}(E_x.E_y^*) = a\sin(2\tau) \qquad -2.49$$

These are the x, y and z cordinates of a point on the Poincare sphere and clearly

$$g_1^2 + g_2^2 + g_3^2 = a^2$$

We can combine "a" with g_R to form a single 4-vector, called a Stokes vector, given by

$$\underset{\sim}{g} = (g_0, g_1, g_2, g_3)$$

where

$$g_i = \frac{1}{2}\mathrm{Tr}([J].\sigma_i) \qquad i = 0,1,2,3 \qquad -2.50$$

and $d_4 = 0$ (see 2.29 and figure 5)

A clear measure of the proximity of two points, with normalised position vectors $\underset{\sim}{r}_P$ and $\underset{\sim}{r}_Q$, is the inner product

$$r_P.r_Q = \cos(x) \qquad -2.51$$

where x is the angular separation of points on the sphere. If we form the dot product of the normalised Stokes vectors representing these states we obtain

$$\underset{\sim}{g}_P.\underset{\sim}{g}_Q = 1+\cos(x) = 2\cos^2(x/2) \qquad -2.52$$

This is a generalisation of Malus' law (Hecht and Zajac 1980), usually derived for linear polarisations but which in this case applies to any two points on the surface of the sphere.

When making measurements on a polarised wave, the

receiver will usually be weighted (intentionally or not) to be more responsive to some polarisation states than to others. For example, in optical systems we very often use linear or circular polaroid in combination with a detector such as a photodiode or photomultiplier. In radar systems we receive the reflected signal via a receiving antenna which may, for example, be a dipole or helix. In either case, we will refer to the receiver as a polarisation filter and can study its properties on the Poincare sphere using equation 2.52.

The first point to note is that the loci of constant response for such a filter are circles centred on the receiver matched polarisation (defined as the incident state for which the received power is maximum).

To plot polarisation states in a convenient form, we very often use plane projections of the Poincare sphere, and because of the existence of these circular loci, it is useful to consider projections which transform circles on the sphere into circles on the plane. One very common such projection is the Polarisation Chart (see figure 4). Note that two such charts are needed, one for each hemisphere and, although similar to an polar orthographic projection (which projects all states onto the g_1, g_2 plane), there is a subtle difference caused by a change in radial scale. Nonetheless, its general features are the same, with circular mapped in the centre and all linear polarisations around the outer circumference. We will present experimental results on such a chart in chapter 7.

Finally, we will spend some time considering the different coordinate systems used for describing polarisation states and the Poincaré sphere. We have already met one possible source of confusion over the choice of convention for circular polarisation (see 2.1), but there are two other main areas of

convention to be decided.

In radio engineering, care is needed when defining the matched polarisation of an antenna. The problem arises because it is conventional to define the polarisation of an antenna as that which it transmits ie. from a right handed coordinate system with positive z direction pointing away from the antenna. This poses no problem for transmitted states but, when the antenna is used as a receiver, we have a conflict of coordinates: the wave state is referenced to a right handed set, with positive z in the opposite direction to the antenna (figure 7). If we call the antenna coordinates $(l,m,n)_{TX}$ and the wave coordinates $(l,m,n)_{RX}$, we have the following relationship between them

$$\begin{bmatrix} l \\ m \\ n \end{bmatrix}_{TX} = \begin{bmatrix} 1 & 0 & 0 \\ 0 & -1 & 0 \\ 0 & 0 & -1 \end{bmatrix} \begin{bmatrix} l \\ m \\ n \end{bmatrix}_{RX} \qquad - 2.53$$

This result has two main consequences for the wave spinor E_0. In the first place we have to use $(l,-m)$ instead of (l,m) for the reference linear base. This has the effect of turning a, θ, τ into a, $-\theta$, $-\tau$ in the antenna coordinates (Huynen 1970).

We have still to account for the change in z coordinate, which corresponds to a change in sense and can be included by taking the conjugate of $\underset{\sim}{E}_0$.

In summary, to change from the wave to antenna coordinates we have to transform E_0 as

$$\underset{\sim}{E}_{0TX} = \begin{bmatrix} 1 & 0 \\ 0 & -1 \end{bmatrix} \underset{\sim}{E}_{0RX}^{*} \qquad - 2.54$$

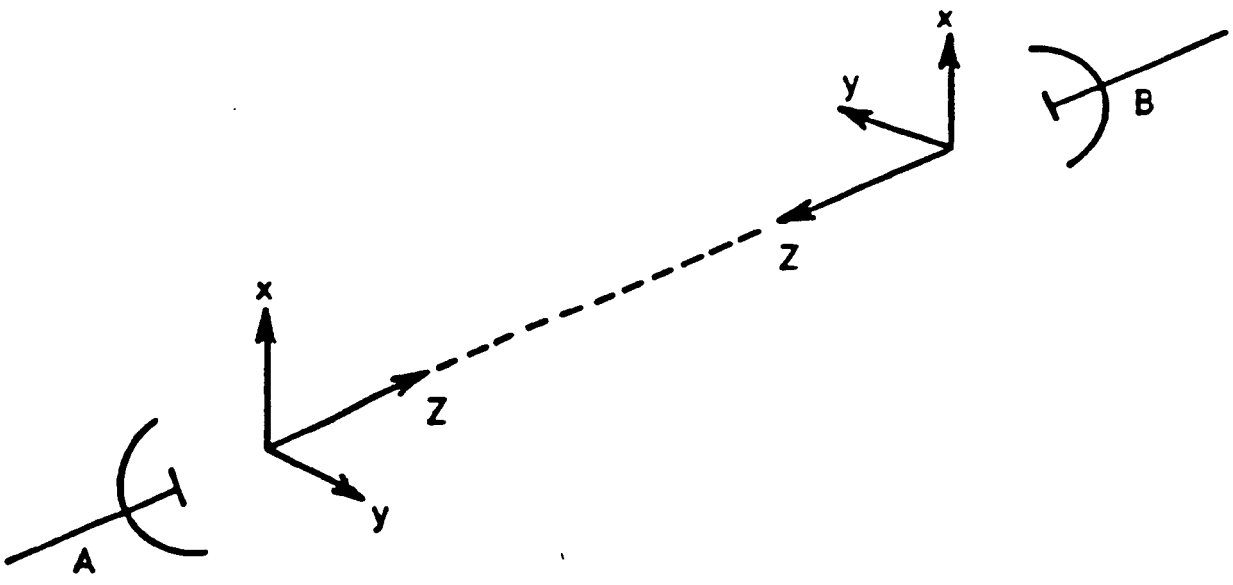

$$\begin{bmatrix} x \\ y \end{bmatrix}_A = \begin{bmatrix} 1 & 0 \\ 0 & -1 \end{bmatrix} \begin{bmatrix} x \\ y \end{bmatrix}_B$$

FIG. 7 ANTENNA CO-ORDINATE SYSTEMS

The net result of this transformation is to turn a, θ, τ into $a, -\theta, \tau$ (note that the sense does not change because of the combined effect of negating the y and z axes). This transformation is often made implicitly in the radar literature and can lead to confusion when comparing results with other areas of polarisation analysis.

However, by making it, we can use the same point on the Poincare sphere to represent an antenna, whether it be used for transmitting or receiving. We will return to this transformation later, when discussing the coherent scattering matrix.

In section 2.2 we introduced the Pauli matrices which led to the definition of a Stokes vector, $\underline{g}$, as given by 2.50. Unfortunately, this choice of notation is not universal, there being two other main conventions for both the Pauli matrices and the Stokes vector.

We have used the <u>traditional</u> ordering, as used by Stokes in his original formulation, but in some optical texts (Marathay), the so called <u>natural</u> ordering is used which defines the Pauli matrices as

$$\sigma_0 = \begin{bmatrix} 1 & 0 \\ 0 & 1 \end{bmatrix} \quad \sigma_1 = \begin{bmatrix} 0 & 1 \\ 1 & 0 \end{bmatrix} \quad \sigma_2 = \begin{bmatrix} 0 & -i \\ i & 0 \end{bmatrix} \quad \sigma_3 = \begin{bmatrix} 1 & 0 \\ 0 & -1 \end{bmatrix} \qquad - 2.55$$

and leads to a reordered Stokes vector $\underline{g} = (g_0, g_2, g_3, g_1)$. This convention amounts to a composite rotation of the Poincaré sphere of 90 degrees about the z axis followed by 90 degrees about the x axis.

The second convention in widespread use is the <u>radar</u> ordering (see Huynen 1970), for which the Pauli matrices are defined as

$$\sigma_0 = \begin{bmatrix} 1 & 0 \\ 0 & 1 \end{bmatrix} \sigma_1 = \begin{bmatrix} 0 & -1 \\ 1 & 0 \end{bmatrix} \quad \sigma_2 = \begin{bmatrix} 0 & i \\ i & 0 \end{bmatrix} \quad \sigma_3 = \begin{bmatrix} -i & 0 \\ 0 & i \end{bmatrix} \qquad - 2.56$$

giving rise to a complex Stokes vector $\underset{\sim}{g} = (g_0, ig_3, -ig_2, ig_1)$.

In order to convert between the various systems, the following matrix transformations can be used

$$\begin{bmatrix} g_0 \\ g_1 \\ g_2 \\ g_3 \end{bmatrix}_R = \begin{bmatrix} 1 & 0 & 0 & 0 \\ 0 & 0 & 1 & 0 \\ 0 & 0 & 0 & 1 \\ 0 & 1 & 0 & 0 \end{bmatrix} \begin{bmatrix} g_0 \\ g_1 \\ g_2 \\ g_3 \end{bmatrix}_T = \begin{bmatrix} 1 & 0 & 0 & 0 \\ 0 & 0 & 0 & i \\ 0 & -i & 0 & 0 \\ 0 & 0 & -i & 0 \end{bmatrix} \begin{bmatrix} g_0 \\ g_1 \\ g_2 \\ g_3 \end{bmatrix}_R \qquad - 2.57$$

The traditional ordering will be used throughout this thesis, as it is the most convenient for discussing transformations of the Poincaré sphere.

3.1 SINGLE TARGETS

In this chapter we deal with the interaction of pure states with single targets, the definition of singular being that incident pure states remain pure after scattering ie. the target may alter the state of polarisation, but the scattered wave can still be represented by a wave spinor, $\underset{\sim}{E}_{os}$.

The scattering problems will be referenced to the geometry shown in figure 8. The target will remain as general as possible throughout and will be characterised by a set of observable scattering parameters rather than by a specific scattering model. This phenomenological approach is a deliberate attempt to keep the techniques as broadly applicable as possible.

The bistatic angle ψ, incident wave vector $\underset{\sim}{\beta}_i$ and scattered wave vector $\underset{\sim}{\beta}_s$ are defined in figure 8. The plane containing the two wave vectors is called the scattering plane and the line in this plane which bisects the angle between $\underset{\sim}{\beta}_i$ and $\underset{\sim}{\beta}_s$ is called the bisectrix $\underline{b}$, where

$$\underline{b} = \frac{\underset{\sim}{\beta}_s - \underset{\sim}{\beta}_i}{|\beta_s - \beta_i|} \qquad - 3.1$$

The (h,v) linear polarisation base may then be conveniently defined as those components lying in, and perpendicular to, the scattering plane.

For $\psi = 0^\circ$ we have the case of backscatter or monostatic scattering, which, although the most common operating condition for radar systems, will be treated here as only a special case of the more general bistatic problem.

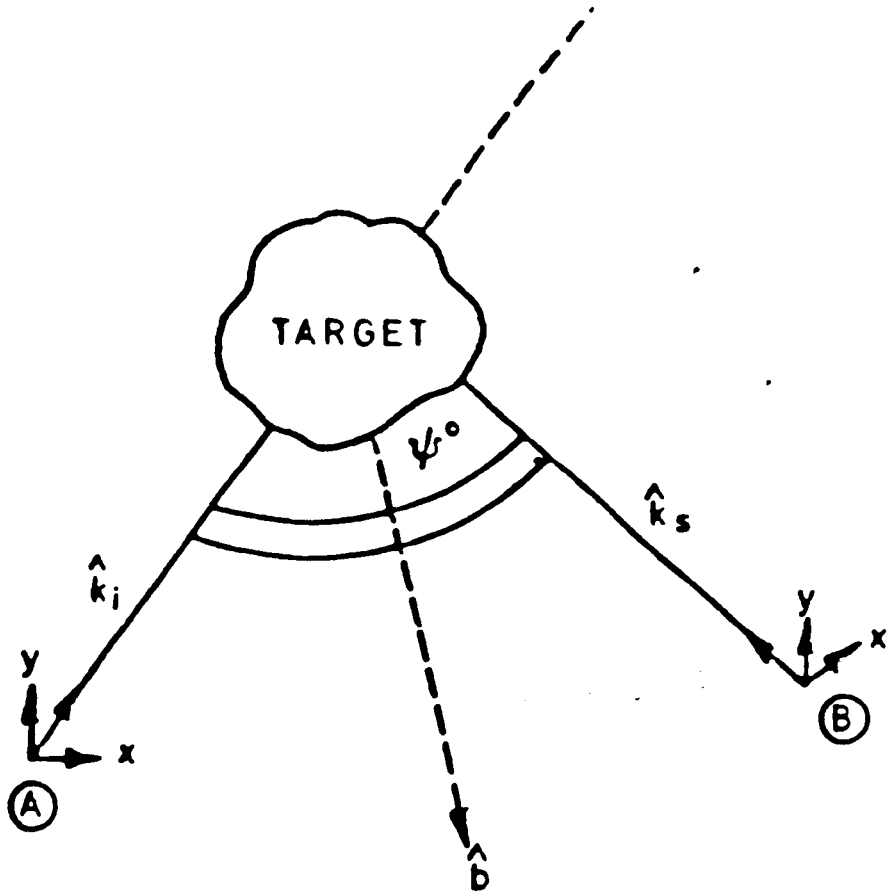

$$\begin{bmatrix} x \\ y \end{bmatrix}_A = \begin{bmatrix} 1 & 0 \\ 0 & -1 \end{bmatrix} \begin{bmatrix} x \\ y \end{bmatrix}_B$$

$\hat{b}$ - BISECTRIX

(A) - TRANSMITTER

(B) - RECEIVER

$-180^\circ < \psi < 180^\circ$

$\hat{k}_i$ - INCIDENT WAVE DIRECTION

$\hat{k}_s$ - SCATTERED WAVE DIRECTION

$\hat{k}_{i,s} = (k_x, k_y, k_z)$

FIG. 8 SCATTERING GEOMETRY

In general terms the target may be described as a polarisation transformer: it operates on the incident wave spinor, $\underset{\sim}{E_{oi}}$, to produce a scattered wave which, generally, will have an altered state of polarisation. The nature of this transformation will depend on the geometry, surface properties and material composition of the object and for a typical target will be a function not only of polarisation but of bistatic angle and frequency. We will assume that all parameters, except the incident wave polarisation, are fixed. The more general case of fluctuating targets will be discussed in chapter 6.

Given the constraints of single target scattering, we can represent the wave target interaction as a spinor transformation of the type 2.20, where the matrix [S] is called the coherent scattering matrix and may or may not be unitary (figure 9).

As noted earlier, [S] is complex and so requires eight measurements for its determination. The four amplitudes, $S_{ij}(i,j=1,2)$, may be obtained by polarising the incident wave alternately in the $\hat{x}$ and $\hat{y}$ states and measuring the amplitude of the scattered wave by using a receiver which, as a polarisation filter, is matched, in turn, to $\hat{x}$ and $\hat{y}$. The four phase angles, θ_{ij}, may be obtained in a similar manner with the use of a coherent receiver (see Chapter 7).

The power of this representation is that by measuring [S] in the base (x,y), we can calculate the scattering matrix for any other polarisation state by using the change of base matrix developed in 2.3 . When we do this we will see that, for each matrix, there are several special states, called the null polarisations, which show a great deal of symmetry when mapped on the Poincare sphere and can be used as the basis for a geometrical model of the target on the sphere.

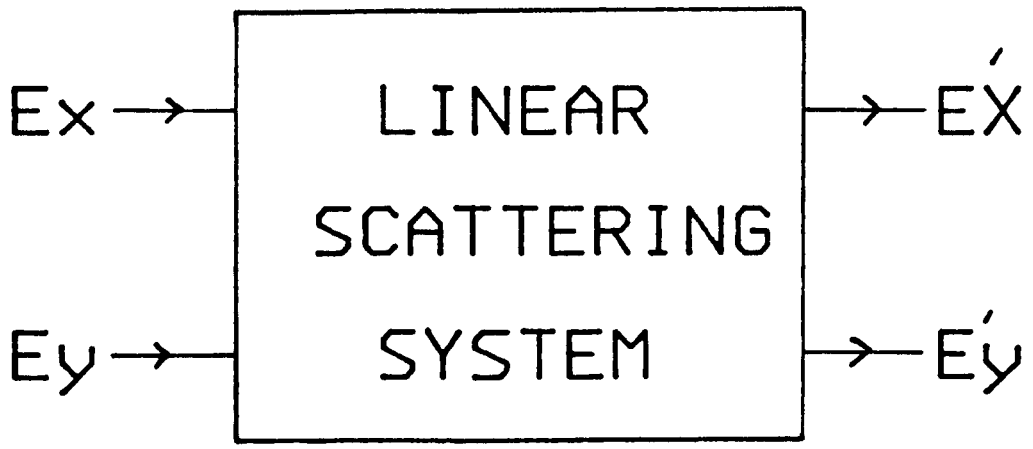

$$E'x = Sxx.Ex + Sxy.Ey$$

$$E'y = Syx.Ex + Syy.Ey$$

$$\underset{\sim}{E}' = [S].\underset{\sim}{E}$$

IN ANTENNA COORDINATES

$$\underset{\sim}{E}^{*} = [Sa].\underset{\sim}{E}$$

FIG.9: THE SCATTERING MATRIX

3.2 The Singular Value Decompoeition and Null Statee

In this section we examine the nature of the change of base transformation for the scattering matrix and show that, by performing a singular value decomposition (SVD) of [S], we can express the matrix in diagonal form (see Atkinson (1978) for a discussion of SVD). From the singular vectors we can obtain the null polarisations, and from the singular values, obtain a second set of characteristic polarisation states, known as the Copolar Nulls.

From 2.20 we have

$$\underset{\sim}{E}_s = [S].\underset{\sim}{E}_i \qquad - 3.2$$

where all quantities are expressed in terms of the same polarisation base, (x,y).

If the receiver is matched to a pure state $\underset{\sim}{E}_r$, then the received voltage may be written in terms of a complex inner product of spinors as

$$V = \underset{\sim}{E}_r.\underset{\sim}{E}_s^{*} = \underset{\sim}{E}_r.[S]^{*}.\underset{\sim}{E}_i^{*} \qquad - 3.3$$

Before proceeding, let us consider how these equations are modified if we adopt the antenna coordinate transformations outlined in 2.53. In this case 3.2 becomes

$$\underset{\sim}{E}_s^{*} = [S_A].\underset{\sim}{E}_i \qquad - 3.4$$

where $[S_A] = [\sigma_R].[S]$ and 3.3 becomes

$$V = \underset{\sim}{E}_r.[S_A].\underset{\sim}{E}_i \qquad - 3.5$$

Most treatments of the change of base transformation (see Boerner (1981), Kennaugh (1952) and Graves 1956) assume that the

reference polarisation base is the same for both transmit and receive states. We will find this too restrictive and so will define two change of base matrices, $[U_{2T}]$ for the incident wave and $[U_{2R}]$ for the receiver (eg. we might choose to reference all incident states to a linear base, (h,v), with a circular base, (l,r), for the receiver). The following relationships then apply

1) For the incident wave

$$\underset{\sim}{E}_i = [U_{2T}].\underset{\sim}{E}_i' \qquad - 3.6$$

2) For the scattered wave

$$\underset{\sim}{E}_s = [U_{2R}].\underset{\sim}{E}_s'' \qquad - 3.7$$

3) From the definition of [S]

$$\underset{\sim}{E}_s = [S].\underset{\sim}{E}_i$$
$$= [S].[U_{2T}].\underset{\sim}{E}_i' \qquad - 3.8$$

and from 2)

$$\underset{\sim}{E}_s'' = [U_{2R}]^{*T}.[S].[U_{2T}].\underset{\sim}{E}_i' \qquad - 3.9$$

In the antenna coordinate system, this transformation becomes (see Boerner 1981)

$$\underset{\sim}{E}_s'' = [U_{2R}]^{T}.[S_A].[U_{2T}].\underset{\sim}{E}_i' \qquad - 3.10$$

We can make the following observations based on these transformation formulae:

1) In the antenna coordinate system, if $[U_{2T}] = [U_{2R}]$ then the quantity $S_{XY}-S_{YX}$ is a transformation invariant. In particular,

if the scattering matrix is symmetric in one base, then it will remain symmetric in all other bases. Note that this is not true in the conventional coordinate system.

2) Det([S]) is a transformation invariant in both 3.9 and 3.10, since $\det([U_{2T}]) = \det([U_{2R}]) = 1$. This result will be of use when considering [S] as a spinor transformation.

3) The Span([S]), which is the sum of the squared magnitudes of [S], is another transformation invariant, being the total power available to a pair of orthogonally polarised filters. This quantity is also defined by the trace of the power scattering matrix, [P], given by (see Graves 1956)

$$[P] = [S]^{*T}.[S] \qquad - 3.11$$

We can proceed by noting that any spinor transformation of the form 3.2 may be written as the product of three composite transformations (Payne 1952), to be called class 1, 2 and 3, where:

Class 1 is a unitary matrix, [U], which, as we showed in section 2.2, corresponds to a rotation of the spinor in 3-space
Class 2 is a unimodular Hermitian matrix, [H], which, as we will see, corresponds to the complex angle α in the Lorentz spin matrix (see 2.31) and as such represents a contraction or extension of the magnitude of the spinor.
Class 3 is multiplication by a single complex quantity, det([S]), which amounts only to a rotation of the spinor about its own axis (Payne).

We will assume, in what follows, that [S] is nonsingular and

leave the special case of targets for which det([S]) = 0 until 3.4. Further, since class 3 transformations are of little importance to us (being analagous to the R_1 transformation of 2.2), we will assume that det([S]) = 1, so enabling us to write a general matrix as

$$[S] = [U].[H] \qquad - 3.12$$

In some texts (Graves 1956) this is called the polar decomposition of [S], being analagous to the polar representation of a complex number: [U] corresponds to the "phase" of the matrix and [H], the "magnitude".
Clearly

$$\begin{aligned}[S]^{*T}.[S] &= [H]^{*T}.[U]^{*T}.[U].[H] \\ &= [H]^{*T}.[H] \\ &= ([H])^2 = [P] \end{aligned} \qquad - 3.13$$

From this we can conclude that [H] and [P] have the same eigenvectors, since Hermitian matrices commute with their square ie.$[H,H^2] = 0$. Further, the eigenvalues of [H] are real and given by the square root of the eigenvalues of [P].
We can also show that

$$[S].[S]^{*T} = [U].[P].[U]^{*T} \qquad - 3.14$$

Note that 3.13 and 3.14 have the same eigenvalues but different eigenvectors.

Both 3.13 and 3.14 are Hermitian matrices and can be diagonalised by a similarity transformation of the form (Arfken 1970)

$$[D] = [Q].[H].[Q]^{*T} \qquad - 3.15$$

where [Q] is unitary, [H] Hermitian and

$$[D] = \begin{bmatrix} l_1 & 0 \\ 0 & l_2 \end{bmatrix}$$

where l_1, l_2 are real positive eigenvalues.

Let $[Q_1]$ and $[Q_2]$ be the unitary matrices which diagonalise 3.13 and 3.14 respectively. We will show that these matrices also diagonalise [S] by a transformation of the form

$$[S_D] = [Q_2].[S].[Q_1]^{*T} \qquad - 3.16$$

where

$$[S_D] = \begin{bmatrix} t_1 & 0 \\ 0 & t_2 \end{bmatrix}$$

and t_1 and t_2 are the complex singular values of [S], $[Q_2]$ is the matrix of left singular vectors and $[Q_1]$, the right singular vectors.

Proof

By definition

$$[Q_1].[P].[Q_1]^{*T} = [D]$$

and

$$[Q_2].[U].[P].[U]^{*T}.[Q_2]^{*T} = [D]$$

Hence

$$[Q_1] = [Q_2].[U] \qquad - 3.17$$

or

$$[U] = [Q_1].[Q_2]^{*T}$$

Returning now to the transformation of [S], we have

$$[S_D] = [Q_2].[S].[Q_1]^{*T}$$

$$= [Q_2].[U].[H].[Q_1]^{*T}$$

$$= [Q_1].[H].[Q_1]^{*T} = [D]^{1/2}$$

This constitutes a proof of 3.16 and provides a systematic method for finding $[Q_1]$ and $[Q_2]$ via the diagonalistion of two Hermitian matrices.

By comparing this result with 3.9, we arrive at the important conclusion that we can always find a mixed base representation for [S] in which the scattering matrix is diagonal.

To see the physical significance of this result, we start by asking under what conditions is $[Q_1] = [Q_2]$? In this special case, we can diagonalise the scattering matrix by using the <u>same</u> reference base for transmit and receive and so interpret the diagonalisation as an eigenvalue equation.

For $[Q_1] = [Q_2]$ we must have

$$[S][S]^{*T} = [S]^{*T}[S]$$

or

$$[U].[P].[U]^{*T} = [P]$$

This is equivalent to saying that [U] must commute with [P] ie [U,P] = 0. In chapter 6 we will examine more closely the nature of these constraints but, for the moment, we note only that hermitian and unitary matrices fall into this category.

In the antenna coordinates the requirements are somewhat different; here we wish to diagonalise $[S_A]$ by a transformation of the form 3.10. We also wish to have the same base for transmit and receive and so require

$$[S_{AD}] = [Q]^T.[S_A].[Q] \qquad - 3.18$$

We have just proved 3.16, and to satisfy 3.18 as well, we have to find the conditions under which $[Q] = [Q_1]^{*T} = [Q_2]^T$. It is easy to show that this is satisfied by $[S_A] = [S_A]^T$ ie. by <u>symmetric</u> scattering matrices (to show this, simply take the transpose of 3.16 and use the symmetry of $[S_A]$ and $[S_{AD}]$ to show that 3.18 is satisfied (Graves 1956)).

In conclusion, if the scattering matrix is symmetric (in the antenna coordinate system), we can diagonalise it by using the same base for transmit and receive. This result is of particular importance in radar systems, where very often the transmitter and receiver are fed through the same antenna (ie. monostatic). By using the reciprocity theorem, it can be shown (Graves 1956) that the scattering matrix is symmetric for such systems and hence, for this large class of problems, we can use 3.18 to obtain a diagonal matrix.

Physically, if we transmit one of the diagonal states, then the scattered wave will have an unchanged polarisation ie. these states are target <u>eigenpolarisations</u>. Similarly, if we transmit one state and receive its orthogonal, we will obtain a null measurement. For this reason the eigenstates are sometimes called the <u>Crosspolar Nulls</u> (Boerner 1981).

Note that the eigenvalue equation corresponding to 3.18 is

$$[S_A].\underset{\sim}{E}_1 = t.\underset{\sim}{E}_1^* \qquad - 3.19$$

as opposed to the usual form of eigenvalue problem

If we map the eigenstates on the Poincaré sphere then, because they are orthogonal, they will be antipodal. The diameter joining the null states is called the eigenaxis of the target. The relative orientation of this axis is an important target feature, forming the basis for a geometrical target classification scheme to be discussed in section 3.4.

For the more general case of nonsymmetric matrices in normal or antenna coordinates, the concept of eigenstates needs some modification. In this case, the left and right singular vectors are not equal and so there are two eigenaxes on the sphere; one for transmit and a different one for receive. This result is still of some practical use because, by using these states, orthogonality is preserved ie. if the two right singular vectors of [S] are transmitted, then the scattered wave states will be the left singular vectors.

In addition, we very often wish to maximise or minimise the received power from a target, and the eigenpolarisations specify which transmitter/receiver combination best be used, since by diagonalising [S], we are maximising the Hermitian form for received power (Graves 1956).

3.3 Copolar Nulls

We saw in the last section that, for symmetric matrices, there exist special states of polarisation which have the useful property of remaining unchanged when scattered from a target. Even when the matrix is not symmetric, we saw that we could still define two sets of base states such that orthogonality was preserved.

We now ask the question whether other states exist which have the property of being transformed into their orthogonal

state. We will see that, in the antenna coordinates, two such Copolar Nulls exist, and that they can be calculated from knowledge of the singular values of [S].

They also show a symmetric displacement from the eigenaxis on the Poincaré sphere such that all four null states lie in a plane and give rise to a structure known as the polarisation fork.

NB. In this section we will be using the antenna coordinates.

We begin by considering a change of base transformation for the <u>diagonal</u> [S]

$$[S]' = [U_2]^T . [S_{AD}] . [U_2] \qquad - 3.21$$

where from 2.34

$$[U_2] = A \begin{bmatrix} 1 & -\rho^* \\ \rho & 1 \end{bmatrix} \qquad - 3.22$$

with $A = 1/(1+\rho\rho^*)$ and ρ, the complex polariston ratio.

By expanding 3.21 we obtain the following general form for [S]'

$$\begin{bmatrix} t_1+\rho^2 t_2 & t_2-\rho^* t_1 \\ t_2-\rho^* t_1 & t_2+\rho^{*2} t_1 \end{bmatrix}$$

For this transformed matrix to have a Copol Null, we require

$$t_1+\rho^2 t_2 = 0 \qquad - 3.23$$

or $$\rho^2 = -t_1/t_2 = \tan^2\alpha . \exp(12\delta) \qquad - 3.24$$

From this result, we can write $[S_D]$ in the parametric form

$$[S_0] = \begin{bmatrix} m\exp[i(\phi+\chi)] & 0 \\ 0 & m.\tan^2(\tau)\exp[i(\phi-\chi)] \end{bmatrix} \quad - 3.25$$

where $0 < \tau < 45°$, $-90° < \chi < 90°$

and $m = t_1$, $\tau = 90°-\alpha$ and $\chi = \delta - 90°$

The two solutions for ρ are

$$\rho_1 = i(t_1/t_2)^{1/2} = \tan(\alpha).\exp(i\delta) \quad - 3.26$$

$$\rho_2 = -i(t_1/t_2)^{1/2} = -\tan(\alpha).\exp(i\delta) \quad - 3.27$$

These two points have Deschamps coordinates $(2\tau, -\chi)$ and $(-2\tau, -\chi)$, referenced to the minimum eigenpolarisation, and $(2\alpha, \chi)$ and $(-2\alpha, \chi)$ when referenced to the maximum eigenstate.

Physically, when transmitted by an antenna and incident on the target, these 2 states are transformed such that the scattered wave is orthogonally polarised to the antenna.

Note that these points are not so simply interpreted in the normal coordinate system, where the scattered and transmitted waves will not be orthogonal (see 2.53). Because of this, the concept of Copolar Null states is only of particular significance when considering the antenna coordinate system. Given this restriction however, they are still of great practical importance, a typical application being the use of circularly polarised radars for rain clutter suppression (Skolnik 1980).

We will now consider, more closely, the geometrical properties of the null states on the Poincare sphere and derive a geometrical model for targets which we can use as the basis for target classification.

3.4 The Polarisation Fork

In this section we will look more closely at the relative positions of the null polarisations on the Poincaré sphere and show that they form a highly symmetric arrangement, known as a polarisation fork. We will treat both symmetric and nonsymmetric target operators and will show that the former is a special case of the latter. By examining the properties of this fork, we will explore the structure of unitary targets and singular operators as well as developing a set of geometrical rules for calculating the change of state.

We begin by looking at the properties of symmetric targets, using the antenna coordinate system so as to include the case of Copolar Nulls. We saw earlier that, for a symmetric scattering matrix, there is just one eigenaxis on the sphere, its position specified by two angles: Θ and τ, being the inclination and ellipticity angles of the maximum eigenpolarisation.

When discussing the Copolar Nulls, we discovered that there were two such states, with Deschamps coordinates related to the singular values of [S] via 3.26 and 3.27. From this result, we see that the Copolar Nulls are symmetrically displaced about the eigenpolarisations, being closer to the minimum eigenstate. Thus, all four null states form a plane in polarisation space, the eigenaxis bisecting the angle between the Copolar Nulls. If we draw radii from the centre of the sphere to the Copol points, and draw the diameter joining the eigenstates, then the resulting structure is known as a polarisation fork (see figure 10).

To specify the plane of the fork we need to know three angles; two we have already mentioned, locating the eigenaxis, but a third is required to specify the orientation of the plane.

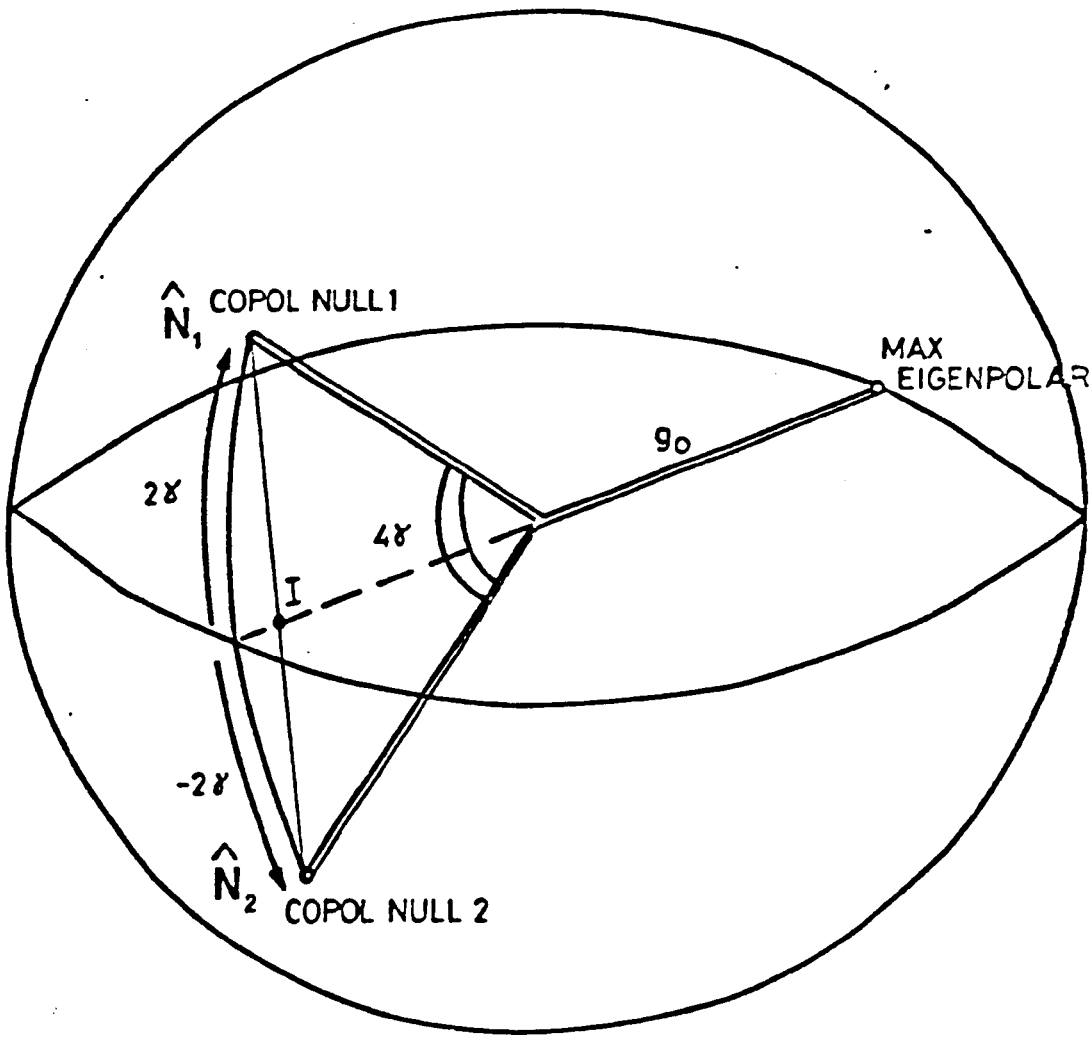

THE FORK LIES IN A PLANE DEFINED BY
(θmax τmax, γ)
REPRESENTING ROTATIONS ABOUT Z, Y, X AXES RESPECTIVELY

FIG10 POLARISATION FORK

This third angle is called the skip angle, and, from examination of 3.26 and 3.27, is given by half the phase difference between the singular values of [S] (χ in 3.25). If χ = 0 (remember we are using the antenna coordinate system), the fork plane is normal to the equator. At the opposite extreme, if χ = 90° then the plane is parallel to the equator.

The angle between the copolar nulls is called the fork angle (γ in 3.25). This angle depends on the arctangent of the amplitude ratio of singular values, being 45° if they are equal and 0° for the case where one singular value is zero.

Before proceeding, we must identify two other parameters of special importance: the radius of the Poincaré sphere is very often made equal to m (although Kennaugh uses t_1+t_2), since this represents the largest obtainable amplitude of scattered radiation for fixed polarisation measurement.

The second geometrical point of special interest is the intersection of the chord joining the Copol Nulls and the eigenaxis, the point I in figure 10. This point figures prominently in the rules for changing base (see below) and in the treatment of partial state interaction, to be discussed in Chapter 4.

Let us now return to a discussion of the fork angle, γ. For the case $t_1 = t_2$, the fork angle is maximum and we say the fork is "opened out" (4γ = 180°). In this rather special case the Copol Nulls are orthogonal (in general of course they are not) and because of the unusual symmetry, the eigenstates become, not just two isolated points, but a family of polarisations lying along a great circle formed by the intersection of the sphere with a plane. This plane is perpendicular to the plane of the fork and contains the eigenaxis.

Unitary targets fall into this category, since they have

a diagonal matrix of the form (Murnaghan 1962)

$$[S_b] = \begin{bmatrix} \exp(i\emptyset_1) & 0 \\ 0 & \exp(i\emptyset_2) \end{bmatrix} \qquad - 3.27$$

Unitary targets are very important in practice because they are pure transformers, lacking any differential attenuation, and hence form the basis for lossless polarisation control in optical and microwave circuits. We will meet examples of these in chapter 7.

The second important category of targets are those specified by $r = 0$ ie.those targets with a singular scattering matrix, det([S]) = 0. These targets have a "collapsed" fork and again, are very common, examples being dipole and helix antennae in radar and linear polaroid in optics. Their prime characteristic is that they transform all incident polarisations into just one state (linear polarisation in the case of a dipole or polaroid).

Geometrically, we have the situation where all possible input states, represented by the surface of the Poincare sphere, are mapped into just one point.

This leads us on to discuss the general problem of establishing a set of geometrical rules for predicting how an arbitrary input state will be transformed by a target, given that we know the parameters of the fork. Such a set were formulated by Kennaugh (1952) and involve three simple stages:

1) Map the input state E_i on the Poincare sphere.

2) Invert E_i through the point I, which, as mentioned earlier, lies at the intersection of the chord joining the Copol Nulls and the eigenaxis.

NB. In the case of Unitary matrices, I lies at the centre of the Poincare sphere and so E_1 is mapped into its orthogonal state. For singular matrices, the point lies at the minimum eigenstate and so all input states are mapped into this one polarisation.

3) Rotate the result of 2) by 180° about an axis normal to the eigenaxis, but lying in the plane of the fork. The coordinates of this point then give the polarisation of the scattered wave.

NB. For unitary targets, the final state will depend on the skip angle, while for singular matrices, all polarisations get mapped into the maximum eigenstate.

So far, we have considered only symmetric matrix operators, and to develop the concept of a polarisation fork for the more general case, we have to return to the considerations of 3.3 and the calculation of Copol Nulls.

We saw in 3.2 that we could express a nonsymmetric matrix in diagonal form by using a mixed base representation, giving rise to two eigenaxes on the sphere, one for transmit states and a second for receive.

Given the existence of a diagonal scattering matrix, $[S_{AB}]$, we can, then, still apply a transformation of the form 3.21 and obtain a quantitatively similar result to the above ie. by applying the <u>same</u> transformation matrix to the <u>different</u> transmit and receive bases, we can still find two values of p for which the mixed base matrix will have $S_{xx} = 0$. We define these as the Copol Nulls, even though their interpretation in terms of a mixed base configuration is somewhat different to the simple case of symmetric operators.

The nulls are still symmetrically displaced about their respective eigenstates, and as a result, we can define two forks: one for transmit, centred on the transmit eigenaxis, and

a second for receive, centred on the receive eigenaxis. It is important to note that although the two forks lie in different planes, they have the same fork and skip angles, because these depend only on the singular values, not on the singular vectors, of [S].

However, the whole point of using the fork structure in the first place was to devise a simple geometrical representation of targets on the Poincare sphere. This simplicity is manifest for symmetric operators where the transmit and receive forks overlap, but, for the more general case, where we have seen the need for two forks, the simplicity begins to disappear.

For example, we can still use the geometrical rules outlined above for predicting the change of state, but now, we have the added complication that the coordinates of the final point are not to be referenced to the same base as the input, but to a different one, obtained by a rotation of the reference axes through two angles, which themselves depend on the difference in ellipticity and inclination of the singular vectors of [S]!

Even for the simpler symmetric case, the fork is still a multipoint respresentation of the target in, what is essentially, a wave space and so when, for example, we discuss target dynamics, we will find that tracking the loci of all four null points on the sphere is extremely complicated. This will drive us to search for a single point target represention on a real hypersphere, so that we can not only characterise target dynamics, but achieve a simpler target representation for both symmetric and nonsymmetric operators.

In summary, we have seen that we can characterise any target by an eight element target descriptor

$$T = (\theta_T, \tau_T, \theta_R, \tau_R, r, x, m, \phi) \qquad - 3.28$$

where

θ_T = inclination angle of transmit eigenstate

τ_T = ellipticity of transmit eigenstate

θ_R = inclination angle of receive eigenstate

τ_R = ellipticity of receive eigenstate

These four parameters locate the eigenaxes

x = skip angle or phase between singular values

r = fork angle, or amplitude ratio of singular values.

These two specify the plane and shape of the fork

m = magnitude of t_1, the maximum singular value of [S].

ϕ = absolute phase reference of [S]

For the special case of symmetric targets, $\theta_T = \theta_R$ and $\tau_T = \tau_R$ ie. the transmit and receive forks overlap.

Knowledge of these parameters forms the basis for a classification scheme for targets and, through knowledge of the properties of the associated null polariations, target scattering may be minimised or maximised through the techniques of polarisation filtering (Poelman 1983).

4.1 Wave Coherency matrix

In this chapter we will study the interaction of partial states with single targets. Partial states are distinguished from the pure states of Chapter 2 by virtue of the former having a polarisation ellipse which varies as a function of time. Such waves are also termed "partially polarised" (pp) and are important in many applications in radar and passive imaging (Gruner 1982, Ko 1962, Deschamps 1973).

We cannot represent partial states by a single spinor $\underset{\sim}{E}_o$, and have to modify our description of polarised waves to allow for the characterisation of statistical fluctuations. In this section we will see how to represent such states by the wave coherency matrix [J], introduced in equation 2.45.

We could, of course, characterise a fluctuating wave by using a receiver capable of instantaneous measurement of E_x and E_y, and hence obtain Θ and τ directly as a function of time. This is often possible, especially with radar systems and by doing just this, Nye (1983) has studied some interesting temporal structural properties of polarised fields. More usually, however, equipment limitations or the requirements of data reduction, force us to consider some kind of average measurement of the field. The question is: what minimal set of measurements are required to characterise the statistics of the wave?

Forming $\langle \underset{\sim}{E}_o \rangle$ is of little practical use, because it tells us nothing of the correlation properties of E_x and E_y. In particular, we are most interested in information on the cross correlation, since this determines the degree of polarised structure in the field.

We can obtain such information by forming $\langle[J]\rangle$, the time average of the wave coherency matrix (see Born and Wolf 1970). In particular, the off diagonal element $J_{XY} = \langle E_X . E_Y^* \rangle$ yields information on the statistical dependence of the field components E_X and E_Y.

At one extreme, $J_{XY} = 0$, the fluctuations are uncorrelated, there is no polarised structure, and the wave is said to be randomly polarised (rp). In this case, [J] is diagonal with equal diagonal terms $J_{XX} = J_{YY} = I$, where I is the wave intensity.

At the other extreme θ and τ are constant, so

$$J_{XY} . J_{YX} = J_{XX} . J_{YY}$$

and the wave is a pure state. Evidently, for such states, $\det([J]) = d_4 = 0$ and there is maximum correlation between E_X and E_Y.

Between these two extremes we have the case of partial polarisation, where $\det([J]) > 0$ and there is some degree of statistical dependence. We can develop a convenient model for such partial states by performing an eigenvector analysis of the Hermitian matrix [J]. There are two variations of this model in common use, one derived directly from [J] and the second from the associated Stokes vector. These models are collectively known as Wave Decomposition Theorems, and we can study them by looking at the way in which [J] transforms under a change of base. Using 2.35 and 2.45 we can show that

$$[J]' = [U_2]^{*T} . [J] . [U_2] \qquad - 4.1$$

From 4.1 and 3.15, we arrive at the important result that we can

always find a polarisation base for which [J] is diagonal ie.

$$[J_p] = \begin{bmatrix} J_1 & 0 \\ 0 & J_2 \end{bmatrix}$$

where $J_1 > J_2$,are the real positive eigenvalues of [J] and $\underset{\sim}{w}_1$, $\underset{\sim}{w}_2$, the corresponding orthogonal eigenvectors.

Combining this result with our discussion of the statistical significance of a diagonal coherency matrix, leads us to the following wave decomposition theorems:

1) <u>The Two State Model</u>: We can write $[J_p]$ as

$$[J_p] = J_1 \, \underset{\sim}{w}_1 . \underset{\sim}{w}_1^{*T} + J_2 \, \underset{\sim}{w}_2 . \underset{\sim}{w}_2^{*T} \qquad - 4.2$$

which may be interpreted as the <u>noncoherent</u> superposition of tw orthogonal pure states, $\underset{\sim}{w}_1$ and $\underset{\sim}{w}_2$. Further,we can develop the relative probability of occurence of these two states by defining

$$P_1 = J_1/(J_1+J_2) \qquad - 4.3$$

$$P_2 = J_2/(J_1+J_2) \qquad - 4.4$$

where $P_1 + P_2 = 1$ and $P_{1,2}$ are the probabilities that, on making an instantaneous measurement of polarisation, the wave will be found in state $\underset{\sim}{w}_1$ or $\underset{\sim}{w}_2$ respectively.

As a formal measure of the degree of statistical disorde in the wave, we can define the wave entropy, H_w, as

$$H_w = -P_1 \log_2 P_1 - P_2 \log_2 P_2 \qquad -4.5$$

Clearly, $H_w = 0$ when $j_2 = 0$ ie. for a pure state, and $H_w = 1$ when $j_1 = j_2$ ie. for a randomly polarised wave.

We can also define the degree of polarisation, D_p, as

$$D_p = (j_1 - j_2)/(j_1 + j_2) \qquad - 4.6$$

$D_p = 1$ for a pure state and 0 for a randomly polarised wave. In terms of invariants of [J]

$$D_p = [1 - (4.\det([J])/Tr([J])^2)] \quad 0 < D_p < 1 \qquad - 4.7$$

This model is important because it allows the problem of target illumination by pp waves to be tackled as two independent single target scattering problems (see section 4.3).

2)<u>The Pure State Plus Noise Model</u>: We can also write $[J_0]$ as

$$[J_0] = [J_{PS}] + [J_{RP}] = \begin{bmatrix} j_1 - j_2 & 0 \\ 0 & 0 \end{bmatrix} + \begin{bmatrix} j_2 & 0 \\ 0 & j_2 \end{bmatrix} \qquad - 4.8$$

where $[J_{PS}]$ represents a pure state, and $[J_{RP}]$, an rp wave. In this model we express [J] as the noncoherent superposition of a pure state plus a "noise" term.

This model is more usually formulated in terms of a Stokes vector $\langle g \rangle$ (see 2.46). The Stokes vector of a pp wave has the property that

$$g_0^2 = g_1^2 + g_2^2 + g_3^2 \neq g_0^2.$$

In fact

$$d_4 = \det([J]) = g_0^2 - g_R^2 > 0 \qquad - 4.9$$

This decomposition generates two auxiliary Stokes vectors from $\underset{\sim}{g}$:

$$\underset{\sim}{g}_{PS} = (g_R, g_1, g_2, g_3) \qquad - 4.10$$

$$\underset{\sim}{g}_{RP} = (g_0 - g_R, 0, 0, 0) \qquad - 4.11$$

where 4.10 corresponds to $[J_{PS}]$ and 4.11 to $[J_{RP}]$. Note that the degree of polarisation is given by

$$D_P = g_R/g_0 \qquad - 4.12$$

The main advantage of this decomposition is that we can use 4.10 and 4.11 to map partial states in polarisation space and provide a link with the Poincaré sphere formalism of chapter 2. The key difference between partial states and the pure states considered earlier, is that we now have to map polarisations throughout the <u>volume</u> of the Poincaré sphere and not just over its surface (Deschamps 1973). Thus a pp wave has coordinates g_R, the radius of the Poincaré sphere is g_0 and $g_R < g_0$. If we normalise g_0 to unity, the relative length of the spinor is given by D_P ie. unity for pure states and zero for randomly polarised waves.

We will use this model in section 4.3 to generate a geometrical interpretation for the scattering of pp waves from single targets.

These two decomposition theorems are collectively known as the <u>Wave Dichotomy</u> (Van De Hulst 1980) since there is no particular preference to be made over the choice of model: they represent two different ways of looking at the same wave. This ability to choose two apparently different models for the same statistical process will be a recurring theme in our discussion

of polarised scattering. In Chapter 6 we will see that, while it is possible to develop a decomposition for fluctuating targets analogous to the two state model, we are unable to develop a unique decomposition analogous to the pure state plus noise model.

4.2 The Mueller Matrix

In Chapter 3 we characterised the target by a 2x2 complex scattering matrix [S]. However, when discussing the interaction of partial states, we cannot use the spinor $\underline{E}_o$ to represent the wave and so cannot use [S] to represent the target. Instead, we must develop a new target descriptor based on the Stokes vector or on the wave matrix [J], either of which can be used to represent partial states.

In this new formalism, both the incident and scattered waves can be represented by Stokes vectors and so we begin by simply representing the target by a 4x4 real matrix, [M], relating incident and scattered wave Stokes vectors (figure 11). [M] is known as the target Mueller matrix after H. Mueller, who developed the main features of this calculus in the 1940's (see Perrin (1942) and Mueller (1948)). It is derived from the assumption of linear scattering and its formulation is a logical step following consideration of the Stokes vector representation of partial states. As we will see however, this apparently simple formulation of the scattering problem leads to extreme difficulties in analysis. These difficulties will become apparent as we progress through this section and will drive us to consider yet another formulation of the scattering problem in Chapter 5.

The Mueller matrix has 16 <u>real</u> elements, which means that it can be obtained by amplitude only measurements of the field ie. there is no need for phase measurement as there was for [S]

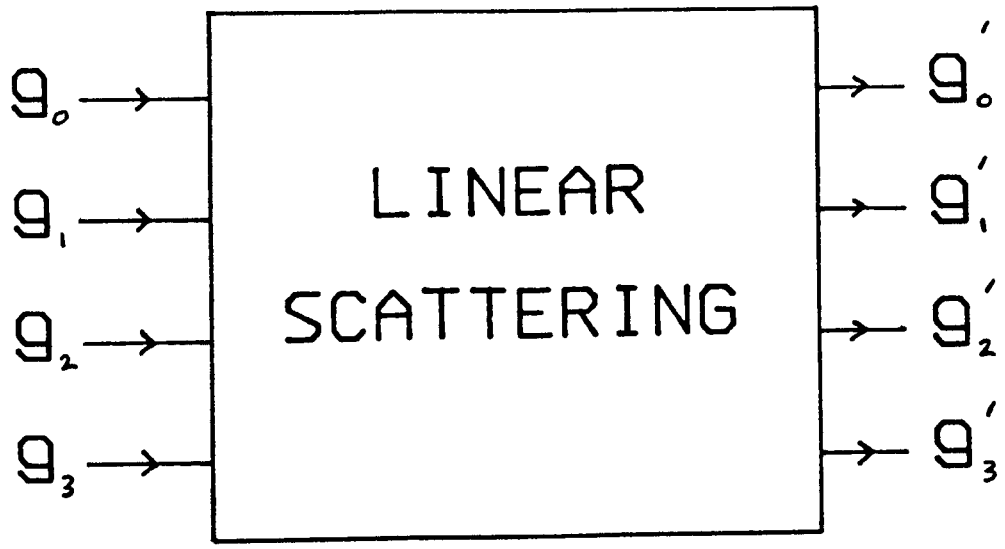

$$g_0' = m_{00} g_0 + m_{01} g_1 + m_{02} g_2 + m_{03} g_3$$

$$g_1' = m_{10} g_0 + m_{11} g_1 + m_{12} g_2 + m_{13} g_3$$

$$g_2' = m_{20} g_0 + m_{21} g_1 + m_{22} g_2 + m_{23} g_3$$

$$g_3' = m_{30} g_0 + m_{31} g_1 + m_{32} g_2 + m_{33} g_3$$

$$\underset{\sim}{g}' = [M] . \underset{\sim}{g}$$

FIG. 11 THE MUELLER MATRIX

(the important relative phase relationships are "built into" the real coefficients of [M]). For this reason, Mueller calculus has found its most widespread use in high frequency problems (particularly optics) where accurate phase measurement is difficult or impossible. More generally, the Mueller matrix is of use, not only because we don't need phase measurement, but also because of its ability to characterise dynamic scattering (see Chapter 6).

According to Mueller calculus, if the incident wave has Stokes vector $\underset{\sim}{g}$, the scattered wave will have a modified vector $\underset{\sim}{h}$, given by

$$\underset{\sim}{h} = [M].\underset{\sim}{g} \qquad - 4.13$$

If the receiver is matched to a polarisation $\underset{\sim}{g}_R$, then the received <u>power</u> will be

$$P = \underset{\sim}{g}_R.\underset{\sim}{h} = \underset{\sim}{g}_R.[M]\ \underset{\sim}{g} \qquad - 4.14$$

The target information contained in [M] must bear some relation to that in [S], except that there can be no dependence on the absolute phase, $\emptyset$, only on the relative phase between the elements of [S].

We saw in chapter 3 that [S] has 7 degrees of freedom (ignoring $\emptyset$), but [M] appears to have 16 and so must either contain more information than [S], or have fewer degrees of freedom than its number of elements. We will see in chapter 6 that the extra degrees of freedom are used for characterising the fluctuation statistics of dynamic targets but, for the present case of pure state illumination of single targets, there is indeed redundancy in [M], and a one to one correspondence

between the Mueller and scattering matrices. As a result, given [S], we can always calculate an equivalent [M], but can only go in the reverse direction if [M] satisfies certain constraints. In this section we will discuss the detailed form of this mapping and also derive the constraint equations.

The mapping of [S] into [M] is derived in Appendix 1, the key result being that if

$$[S] = \begin{bmatrix} a & b \\ c & d \end{bmatrix}$$

and we write $a.a^* = a^2$, $Re(a) = (a+a^*)/2$, $Im(a) = i(a-a^*)/2$ etc. then

$$2m_{11} = a^2+b^2+c^2+d^2 \qquad 2m_{12} = a^2-b^2+c^2-d^2$$

$$m_{13} = Re(a^*b+c^*d) \qquad m_{14} = Im(a^*b+c^*d)$$

$$2m_{21} = a^2+b^2-c^2-d^2 \qquad 2m_{22} = a^2-b^2-c^2+d^2$$

$$m_{23} = Re(a^*b-c^*d) \qquad m_{24} = Im(a^*b-c^*d)$$

$$m_{31} = Re(a^*c+b^*d) \qquad m_{32} = Re(a^*c-b^*d)$$

$$m_{33} = Re(a^*d+b^*c) \qquad m_{34} = Im(a^*d-b^*c)$$

$$m_{41} = -Im(a^*c+b^*d) \qquad m_{42} = -Im(a^*c-b^*d)$$

$$m_{43} = -Im(a^*d+b^*c) \qquad m_{44} = Re(a^*d-b^*c)$$

Note that in the antenna coordinates, c, d and the fourth row of [M] must all be multiplied by -1.

We can see from these equations that it is difficult to predict the effect on [M] of a change in the elements of [S], and vice versa. This makes a physical interpretation of the elements of [M] difficult and is one price to be paid for

adopting such a simple phenomenological model of the scattering process. We will see in the next chapter that we can develop an alternative formulation whose elements have a more direct relationship to those of [S].

The Mueller matrix may be expressed in any one of an infinite number of reference polarisation base states, (x,y), and from our discussion of spinor algebra in 2.2 and 2.4 we can easily show that [M] transforms as

$$[M]' = [O_{3A}]^T . [M] . [O_{3A}] \qquad - 4.15$$

where $[O_{3A}]$ is an augmented matrix obtained from $[O_3]$ as

$$\begin{bmatrix} 1 & 0 & 0 & 0 \\ 0 & & & \\ 0 & & [O_3] & \\ 0 & & & \end{bmatrix}$$

where the Euler angles (see equation 2.22) are a = $\emptyset$ (the absolute phase) b = τ (the ellipticity angle) and c = Θ (the inclination angle of the new base state).

Of particular interest is the form of [M] when [S] is diagonal. From Appendix 1, if

$$[S_0] = \begin{bmatrix} t_1 & 0 \\ 0 & t_2 \end{bmatrix}$$

then

$$[M_0] = 1/2 \begin{bmatrix} t_1^2+t_2^2 & t_1^2-t_2^2 & 0 & 0 \\ t_1^2-t_2^2 & t_1^2+t_2^2 & 0 & 0 \\ 0 & 0 & 2t_1t_2\cos(2x) & 0 \\ 0 & 0 & 0 & 2t_1t_2\cos(2x) \end{bmatrix} \qquad - 4.16$$

Notice that [M] is not in diagonal form unless $t_1 = t_2$. In general therefore, [M] cannot be diagonalised by the orthogonal rotation matrix $[O_{3A}]$, and it is not possible to set up an eigenvalue equation for [M] as we did for [S]. The consequences of this result for a geometrical interpretation of the transformation of Stokes vectors will be explored in section 4.3.

As well as expressing $[O_{3A}]$ in terms of the Euler angles ϕ, θ and τ, we can use the results of Appendix 1 to express the rotation matrix in terms of ρ, the complex polarisation ratio and hence close the loop on the equivalence between Unitary transformations of the wave spinor and real orthogonal transformations of the Stokes vector. We can do this by substituting

$$[S] = A\begin{bmatrix} 1 & \rho^* \\ -\rho & 1 \end{bmatrix} \qquad - 4.17$$

into the equation for [M] (this is just the conjugate transpose of 2.34, the change of base matrix for the spinor $\underset{\sim}{E_o}$). By direct substitution we obtain

$$[M] = A^2\begin{bmatrix} 1+\rho\rho^* & 0 & 0 & 0 \\ 0 & 1-\rho\rho^* & 2Re(\rho) & -2Im(\rho) \\ 0 & -2Re(\rho) & Re(1-\rho^2) & Im(\rho^2) \\ 0 & 2Im(\rho) & Im(\rho^2) & Re(1+\rho^2) \end{bmatrix} \qquad - 4.18$$

Hence, given

$$\rho = \tan(\alpha).\exp(i\delta)$$

we can determine the three Euler angles representing a rotation

of coordinates in polarisation space. In section 2.3 we showed how θ and τ are related to α and δ via the construction of a right angled spherical triangle, but what of the third Euler angle, ϕ? As discussed earlier, this represents a rotation about the x axis and locates the plane of zero phase in the new base.

This bring us to the question of how to define the phase of an elliptically polarised wave, especially when the field vector never passes through zero. For linear waves, the phase can be measured unambiguously from some defined zero crossing but, for elliptical polarisation, we can't do this and have to choose an arbitrary direction in the plane of polarisation and define the phase as zero whenever the electric field vector crosses this axis.

We will see that for 4.18 to be consistent with 2.22, we must define ϕ as a function of θ and τ, an unfortunate complication, but one which is essential if we are to express the change of base matrix in terms of the single parameter, ρ. By comparing elements of 4.18 with 2.22, and in particular, the (3,4) and (4,3) elements, which must be equal, we obtain

$$\cos(\tau)\sin(\phi) = \cos(\phi)\sin(\tau)\sin(\theta) - \cos(\theta)\sin(\phi) \qquad - 4.1$$

or

$$\tan(\phi) = [\sin(\tau)\sin(\theta)/(\cos(\tau)+\cos(\theta))] \qquad - 4.20$$

This is a bivalued function of θ and τ, since $0 < \phi < 360°$. The two solutions are separated by 180° and fix the sense of the positive z axis in the new coordinate system. The choice of value depends on the sign of the phase of ρ and again, by direct comparison of 4.18 and 2.22, we choose ϕ such that

$$\phi > 0 \text{ if } \sin(2\delta) < 0$$

$\phi < 0$ if $\sin(2\delta) > 0$

Finally, we will consider the conditions imposed on [M] such that it have an equivalent [S]. These may be derived from the condition for physical realisabilty of a Stokes vector, $\underset{\sim}{g}$, namely

$$g_0^2 - g_1^2 - g_2^2 - g_3^2 > 0$$

[M] must be constrained so that the scattered Stokes vector, $\underset{\sim}{h}$, satisfies this condition. Further, for [M] to have an equivalent [S], the equality must hold so that $\underset{\sim}{h}$ is a pure state. We can express this condition in matrix form by defining $[D]_{(M)}$ as

$$[D] = \begin{bmatrix} 1 & 0 & 0 & 0 \\ 0 & -1 & 0 & 0 \\ 0 & 0 & -1 & 0 \\ 0 & 0 & 0 & -1 \end{bmatrix} \qquad - 4.21$$

Then we can write the condition of physical realisability as

$$[D]\underset{\sim}{g}.\underset{\sim}{g} > 0 \qquad - 4.22$$

For the scattered wave, [M] must satisfy

$$[D][M]\underset{\sim}{g}.[M]\underset{\sim}{g} = 0$$

but $$[M]\underset{\sim}{g}.\underset{\sim}{h} = \underset{\sim}{g}.[M]^T\underset{\sim}{h}$$

so $$[M]^T[D][M]\underset{\sim}{g}.\underset{\sim}{g} = 0$$

Since $\underset{\sim}{g}$ is arbitrary, we have

$$[M]^T[D][M] = [E] = 0 \qquad -4.23$$

If [E] contains components in its diagonal which are proportional to [D] then, since

$$[D]\underset{\sim}{g}.\underset{\sim}{g} = 0$$

these components do not contribute to 4.23. With these removed we have

$$[E] = [E_0] + 1[D] \qquad - 4.24$$

Where 1 is a scalar and $[E_0]$ a 4x4 matrix, providing a set of sixteen equations, quadratic in the elements of [M], which are constraints on the Mueller matrix having a single equivalent scattering matrix [S]. We will leave further discussion of the relationship between [M] and [S] until Chapters 5 and 6, when we will return to 4.24 and see a clear physical interpretation of these constraint equations. To analyse these results any further using Mueller calculus is difficult, both algebraically and physically, and so we will not attempt such an analysis here (see Huynen 1970 for a detailed treatment in terms of Mueller calculus).

4.3 Lorentz Geometry And The Polarisation Fork

In the last section we saw how the Mueller matrix is related to [S] and discovered a rather surprising result: although we can diagonalise the scattering matrix using SVD analysis, we cannot diagonalise [M] using the real orthogonal rotation matrix $[O_{3A}]$.

In this section we will see that this result stems from the fact that [M] represents a Lorentz transformation of the

incident Stokes four vector and, by examining the link between this transformation and the polarisation fork discussed in 3.4, we will extend our geometrical model to include the scattering of partial states from single targets.

In Chapter 3, we asked the question: how do states on the surface of the sphere transform under interaction with a single target? We must now ask the more general question as to how states throughout the volume of the Poincaré sphere transform, as well as those on the surface. We can see immediately that as well as a rotation about the origin, we now have the possibility of contraction or extension of the length of the spinor, indicating a change in the degree of polarisation of the wave. It is this extra degree of freedom that leads to the Lorentz transformation. Before discussing the geometry in detail, we will construct a suitable model for the scattering process, based on the Wave Decomposition Theorems and SVD analysis of [S].

We can use the Two State Model for the incident wave to express it as the noncoherent superposition of two pure states, each of which interacts with [S] in the manner descibed in Chapter 3. We also know the relative probability of occurrence of these two states from knowledge of the eigenvalues of [J]. We will call the two states w_1 and w_2 and their probabilities, P_1 and P_2 (see 4.1).

Because the two states are statistically independent, we can treat them separately and simply add the resulting pure state coherency matrices to find the overall state of the scattered wave.

Consider w_1 incident on the target: we can express it in terms of the right singular vectors of [S], which, remember, form an orthonormal reference base (x,y), in which

$$\underset{\sim}{w}_1 = \begin{bmatrix} w_{1x} \\ w_{1y} \end{bmatrix}$$

where $w_{1x} = \underset{\sim}{w}_1 . \underset{\sim}{x}^*$ and $w_{1y} = \underset{\sim}{w}_1 . \underset{\sim}{y}^*$

After scattering, $\underset{\sim}{w}_1$ becomes a new state, $\underset{\sim}{z}_1$, given by

$$\underset{\sim}{z}_1 = \begin{bmatrix} t_1 w_{1x} \\ t_2 w_{1y} \end{bmatrix}$$

where t_1 and t_2 are the singular values of [S].

A similar argument for $\underset{\sim}{w}_2$ yields a second scattered state $\underset{\sim}{z}_2$ given by

$$\underset{\sim}{z}_2 = \begin{bmatrix} t_1 w_{2x} \\ t_2 w_{2y} \end{bmatrix}$$

We know that $\underset{\sim}{w}_1$ and $\underset{\sim}{w}_2$ occur with probabilities P_1 and P_2 and so the scattered wave has a final coherency matrix

$$[J]_s = P_1 \underset{\sim}{z}_1 \underset{\sim}{z}_1^{*T} + P_2 \underset{\sim}{z}_2 \underset{\sim}{z}_2^{*T} \qquad - 4.25$$

The details of this transformation are complicated because $\underset{\sim}{z}_1$ and $\underset{\sim}{z}_2$ are not, in general, orthogonal. Nonetheless we can develop a geometrical model for 4.25, based on the properties of the Lorentz transformation.

We will begin by considering a simple two dimensional problem, where the incident wave has a Stokes vector of the form

$$\underset{\sim}{g} = (g_0, g_1, 0, 0)$$

and $$g_1 = D_P g_0 \qquad - 4.26$$

If $D_P = 0$, $\underset{\sim}{g} = (g_0, 0)$ and the wave is randomly polarised. On the other hand, if $D_P = 1$, $g_0 = g_1$ and the wave represents a pure state: $\underset{\sim}{w}_1$ if $g_1 = g_0$ and $\underset{\sim}{w}_2$ if $g_1 = -g_0$.

On the Poincare sphere these states lie along a single radius whose direction is set by the reference base of $\underset{\sim}{g}$. Alternatively, we can plot all such points on the g_0, g_1 plane (see figure 12). The area on this diagram between the two solid lines represents partial states: in the right plane the wave is partially $\underset{\sim}{w}_1$ polarised, and in the left plane, partially $\underset{\sim}{w}_2$ polarised. The area in shade corresponds to points for which $g_0 > g_1$ ie. states which are not physically realisable. The two solid lines at 45° to the axes represent the two pure states, $\underset{\sim}{w}_1$ and $\underset{\sim}{w}_2$ (forming the polarisation equivalent of the light cone of special relativity (see French 1982)). Note that the range of D_P has to be extended to include negative values so that $-1 < D_P < 1$ (this is a precursor to the introduction of a vector degree of polarisation in 4.4).

We may now ask what happens when these partial states interact with a target, characterised by a scattering matrix [S] (or its equivalent Mueller matrix [M])? We begin by determining the invariants of $\underset{\sim}{g}$, from which we can deduce the geometrical form of the transformation. For example, if $g_0^2+g_1^2$ is found to be invariant, then the target causes a plane rotation of the $\underset{\sim}{g}$ axes in figure 12.

To find a suitable invariant, we assume [S] has unit determinant (see section 3.2) and can then easily show that the diagonal wave coherency matrix associated with $\underset{\sim}{g}$ is transformed as

$$[J]' = [S][J_s][S]^{*T} \qquad - 4.27$$

Figure 12 Minkowski diagram for transformation of Stokes Vectors

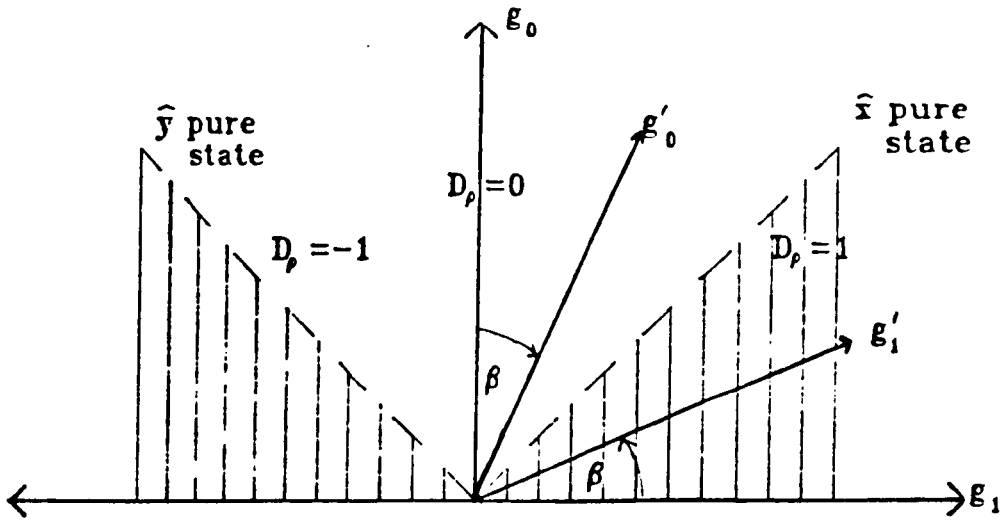

Input Stokes vector=$(g_0,g_1,0,0)$ $g_1=D_p g_0$

Transformed Stokes vector=$(g_0',g_1',0,0)$ $g_1'=D_p' g_0'$

where $\det([J]') = g_0^2 - g_1^2 = d_4 = \det([J_t])$.

For the sake of simplicity, we will further assume that [S] is diagonal in (w_1, w_2), which means that [J]' in 4.27 is also diagonal and we can map both the incident and scattered wave states on the same diagram (figure 12) (we will consider the more general case where $(x,y) \neq (w_1, w_2)$ in 4.4). We can write the diagonal scattering matrix, $[S_{AD}]$, in the form (see 3.25)

$$[S_{AD}] = \begin{bmatrix} m & 0 \\ 0 & m\tan^2(r) \end{bmatrix} = A \begin{bmatrix} 1/\tan(r) & 0 \\ 0 & \tan(r) \end{bmatrix} \qquad - 4.28$$

where $A = \det([S]) = m^2\tan^2(r)\exp(i\theta)$ and $r > 0$.

Under these conditions, equation 4.27 represents a set of linear transformations which increase (or decrease) the g_1 component at the expense of power to g_0 (just as long as d_4 remains unchanged). Physically, this means that the degree of polarisation of the wave is the only parameter which can change on scattering from the target (remember we are assuming $(w_1, w_2) = (x,y)$). Geometrically, we are rotating the $g_1 = 0$ axis (ie. locus of randomly polarised input states) so that it lies at some angle to the vertical (the angle β in figure 12) where

$$\tan(\beta) = D_{P1} \qquad - 4.29$$

Points which lie on the straight line $g_0 = D_{P1}g_1$ are transformed to $(g_0', 0)$ ie. to randomly polarised waves, while randomly polarised inputs are scattered with a modified degree of polarisation equal to D_{P1}.

We can analyse the details of this transformation by considering an infinitessimal change in degree of polarisation, δD_{P1}. We can then write the transformation as

$$g_1' = g_1 + \partial D_{F1} g_0$$

and by symmetry

$$g_0' = g_0 + a\partial D_{F1} g_1$$

where "a" is some constant to be determined from $d_4 = 0$. Clearly

$$g_1'^2 = g_1^2 + 2\partial D_{F1} g_0 g_1 + \partial D_{F1}^2 g_0^2$$

$$g_0'^2 = g_0^2 + 2a\partial D_{F1} g_0 g_1 + a^2\partial D_{F1}^2 g_1$$

By ignoring second order terms and setting $d_4 = 0$, we can show that $a = 1$. In matrix form

$$g' = (\sigma_0 + \partial D_{F1}\sigma_V)g \qquad - 4.30$$

where σ_0 and σ_V are the Pauli matrices (see 2.2).

For a finite rotation, we define $\alpha = N\partial D_{F1}$ and 4.30 becomes (Arfken)

$$g' = (\sigma_0 + (\alpha/N)\sigma_V)^N \qquad - 4.31$$

In the limit as N tends to infinity we have

$$\lim_{N \to \infty} (\sigma_0 + (\alpha/N)\sigma_V)^N = \exp(\alpha\sigma_V) \qquad - 4.32$$
$$= \sigma_0 + \alpha\sigma_V + (\alpha\sigma_V)^2/2 + ...$$
$$= \sigma_0 \cosh(\alpha) + \sigma_V \sinh(\alpha)$$

where we have used a Maclaurin expansion for the exponential and the last step was obtained by using $\sigma_V^2 = \sigma_0$.

Note that in most texts on special relativity (French 1982, Arfken 1970), the Minkowski metric is used which employs

ig_0 instead of g_0 (this means that the invariant d_4 can be written as $g_0^2+g_1^2$). In this case 4.32 becomes a function of σ_2 instead of σ_1. Our notation follows that of Misner (1973) and Payne (1953) and displays more clearly the underlying difference between Lorentz transformations and plane rotations.

Writing 4.32 in full, we have

$$\begin{bmatrix} g_0' \\ g_1' \end{bmatrix} = \begin{bmatrix} \cosh(\alpha) & \sinh(\alpha) \\ \sinh(\alpha) & \cosh(\alpha) \end{bmatrix} \begin{bmatrix} g_0 \\ g_1 \end{bmatrix} \qquad - 4.33$$

In order to appreciate the physical significance of α, we have to relate it to D_{P1} and hence to r, which is one of the target parameters discussed in Chapter 3.

The former relation is straightforward; we know that D_{P1} is the slope of the line $g_1' = 0$ and so from 4.33

$$0 = \sinh(\alpha)g_0 + \cosh(\alpha)g_1$$

or $$\tanh(\alpha) = -g_1/g_0 = -D_{P1} \qquad - 4.34$$

From which we can show that

$$\sinh(\alpha) = D_{P1}/(1-D_{P1}^2)^{1/2}$$

$$\cosh(\alpha) = 1/(1-D_{P1}^2)^{1/2}$$

These equations may be related to those of special relativity by noting that D_{P1} corresponds to a pure "boost" (ie. the velocity parameter) and α is an imaginary angle of rotation in Lorentz space (from 4.29 and 4.34 we can see that $\tan(\beta) = \tanh(\alpha)$). The difference between polarisation algebra and special relativity

is that in the latter, the "boost" parameter is the velocity of the coordinate frame relative to "c", the velocity of light, while in polarisation terms D_{Pl} is the degree of polarisation required of an incident wave such that the scattered wave is randomly polarised.

The only remaining task is to relate D_{Pl} to the fork angle γ. We can do this by identifying 4.33 as part of a Mueller matrix [M] given by

$$[M] = \begin{bmatrix} \cosh(\alpha) & \sinh(\alpha) & 0 & 0 \\ \sinh(\alpha) & \cosh(\alpha) & 0 & 0 \\ 0 & 0 & 1 & 0 \\ 0 & 0 & 0 & 1 \end{bmatrix} \qquad - 4.35$$

which compares directly with 4.16 and confirms yet again that we cannot diagonalise the Mueller matrix by a real rotation. Using the result of Appendix 1 we can show that equation 4.35 corresponds to a diagonal scattering matrix of the form

$$[S_{ab}] = \begin{bmatrix} \exp(\alpha/2) & 0 \\ 0 & \exp(-\alpha/2) \end{bmatrix} = \begin{bmatrix} 1/\tan(\gamma) & 0 \\ 0 & \tan(\gamma) \end{bmatrix} \qquad - 4.36$$

where the last equality comes from 4.28. From this result we can see that

$$\exp(-\alpha) = \tan^2(\gamma) \qquad - 4.37$$

and since

$$\tanh(\alpha) = \frac{e^{\alpha} - e^{-\alpha}}{e^{\alpha} + e^{-\alpha}}$$

then by 4.34

$$D_{Pl} = -\frac{1 - \tan^4(\gamma)}{1 + \tan^4(\gamma)} \qquad - 4.38$$

NB. $0 < \gamma < 45°$ and $-1 < D_{Pl} < 0$.

This is our key result, relating the target fork angle to the "boost" parameter of a Lorentz transformation (see Figure 13)

So far we have only dealt with one special value of degree of polarisation for the incident wave, but using 4.33 we can look at the general transfer characteristic relating the degree of polarisation of the scattered wave for arbitrary input state (still under the assumption $(x,y) = (w_1,w_2)$). In Appendix 2 it is shown that this characteristic can be written as

$$D_P' = \frac{\tanh(\alpha) + D_P}{1 + \tanh(\alpha)D_P} = \frac{D_P - D_{P1}}{1 - D_P D_{P1}} \qquad - 4.39$$

Figure 14 shows a plot of this function for various values of fork angle. As can be seen, $D_{P1} = 0$ ($\gamma = 45°$) yields no change in degree of polarisation (Unitary targets being an important example) but generally there is a nonlinear change: some states become more polarised (to be called "expansion") while others show a decrease in D_P ("compression"). To illustrate this idea, Figure 15 shows the gradient of the transfer characteristic, again as a function of γ (see Appendix 2). Expansion occurs for $\partial D_P'/\partial D_P < 1$ and compression for $\partial D_P'/\partial D_P > 1$. A point of particular interest is the value of D_P for which the slope of the characteristic is unity, since at this point, $D_P' = \pm D_P$ and we have a transition from compression to expansion (note that pure states ie. $D_P = \pm 1$, are always scattered as pure states, as expected from the single target approximation). Figure 16 is a plot of D_{Pc}, the value of D_P for which the slope of 4.39 is unity, as a function of γ. It is shown in Appendix 2 that this critical value of D_P is simply related to the fork angle as

$$D_{Pc} = - \cos(2\gamma) \qquad - 4.40$$

Geometrically, this point lies along the radius joining the centre of the Poincaré sphere to the minimum eigenpolarisation

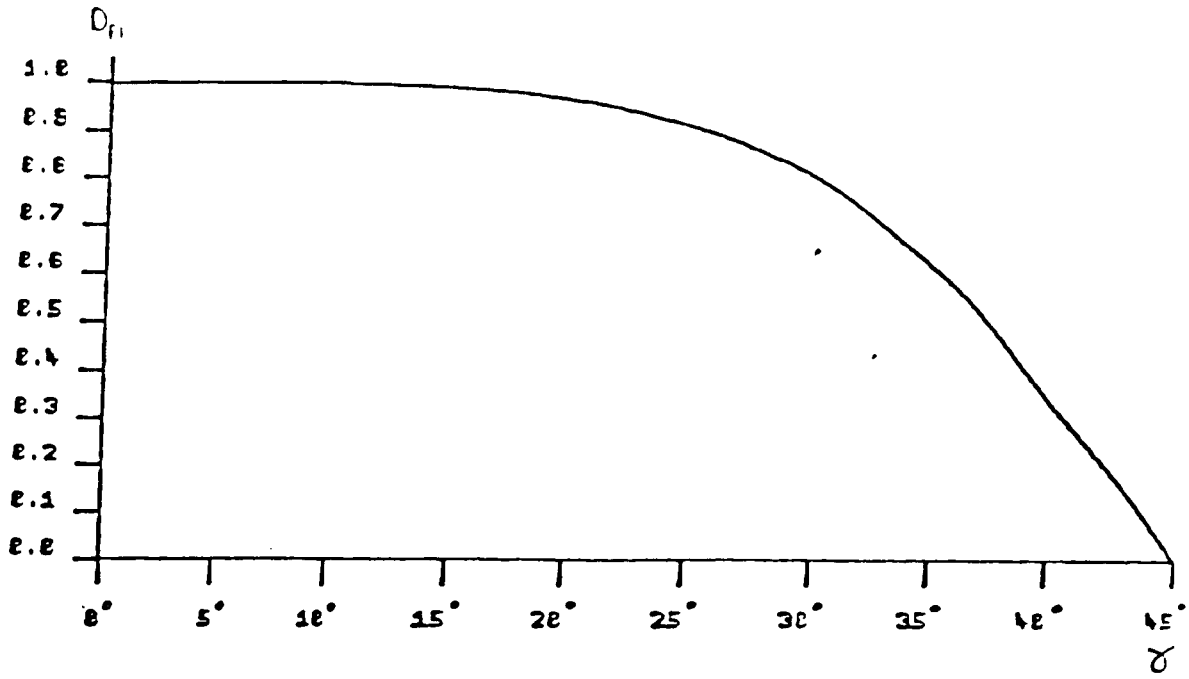

FIGURE 13: D_{f1} VS FORK ANGLE

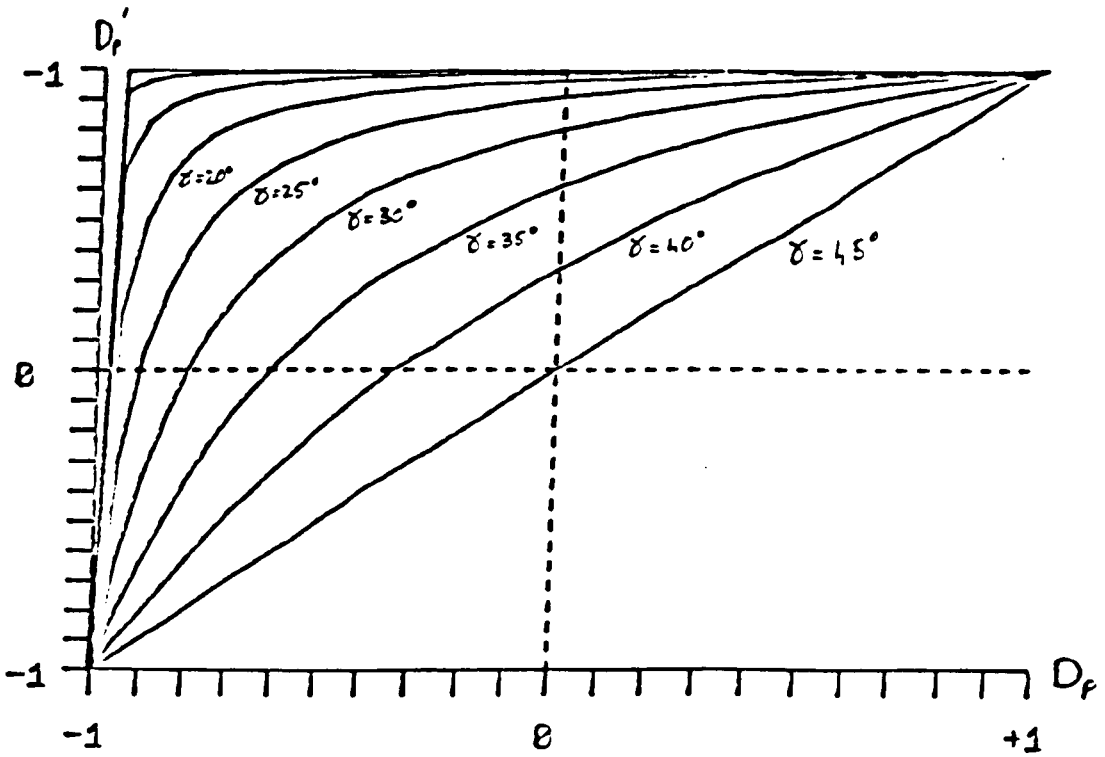

FIGURE 14: D_f' VS D_f

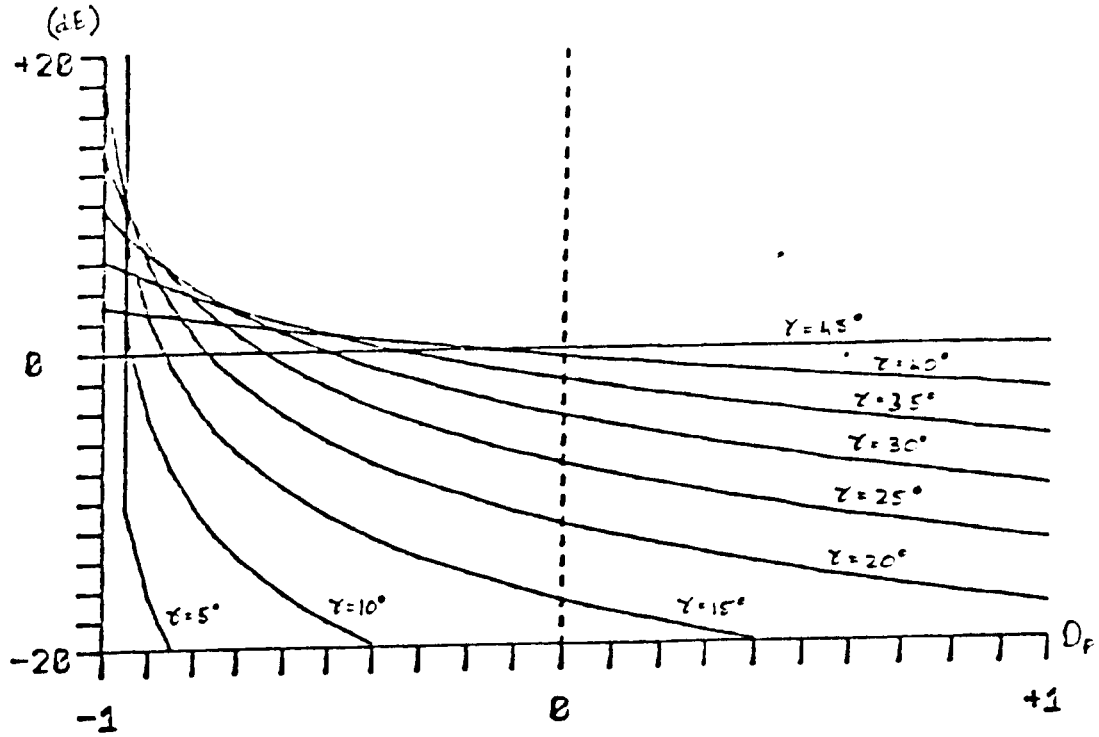

FIGURE 15: GRADIENT OF D_p' VS D_p

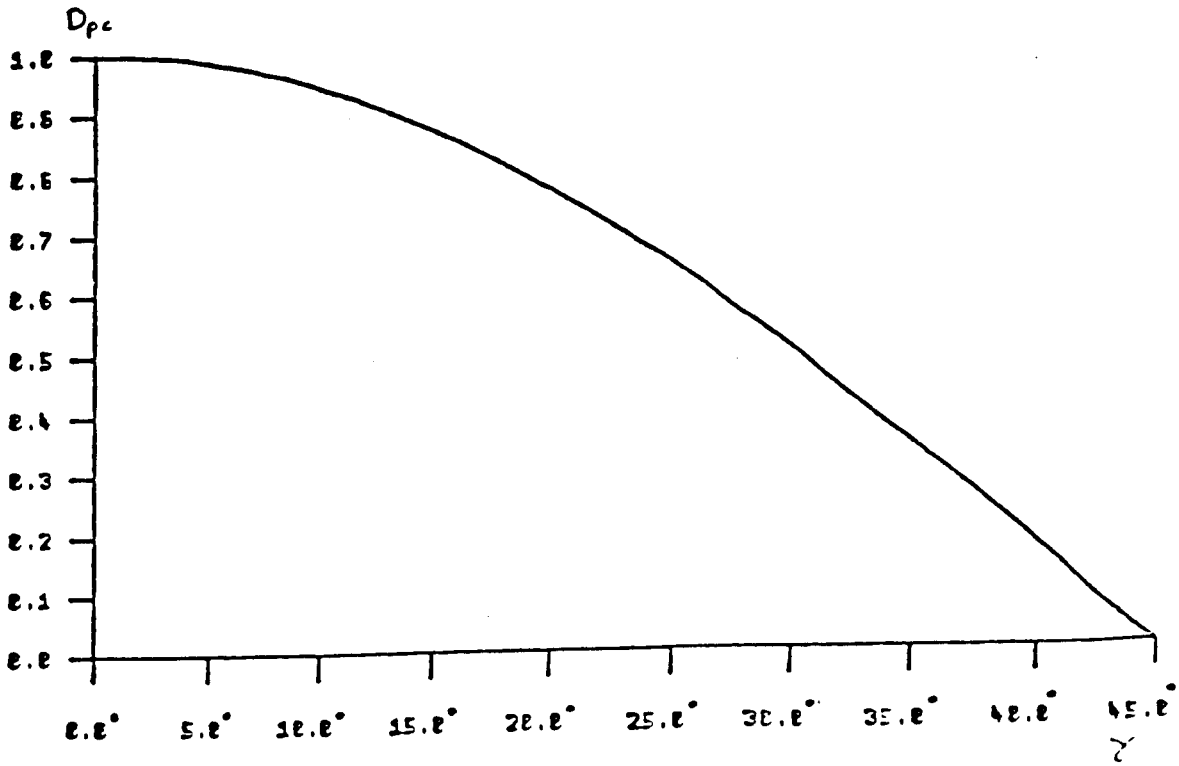

FIGURE 16: D_{FC} VS γ

and marks the intersection of the chord joining the two Copol Nulls with this radius (Figure 17). This point figured prominently in the rules for transformation of pure states in Chapter 3 and is now seen as an important point in the prediction of partial state transformations. Points which lie beyond this are compressed while all others are expanded. Note that if $r = 0$, all states are expanded; in fact all states are reflected with $D_r = 1$ ie. as pure states. This is the case, for example, in scattering from a dipole or for transmission through linear Polaroid and is a general characteristic of targets with a collapsed fork.

4.4 Generalised Lorentz Geometry

In 4.3 we assumed that the eigenvectors of [J] were equal to the target eigenpolarisations and so considered only those incident states which lie along the target eigenaxis. In this section we will extend the results of 4.3 to consider the behaviour of arbitrary incident state.

In section 3.2 (equation 3.12) we saw that, under a unimodular assumption, we could write [S] as the product of two composite matrices

$$[S] = [U][H]$$

where [U] is Unitary and hence homomorphic to a rotation matrix in 3 dimensions. We now concern ourselves with the Hermitian matrix [H] and show that it is homomorphic to "pure" Lorentz transformations, where "pure" indicates the use of a boost parameter, a, but no spatial rotation of coordinates. The more

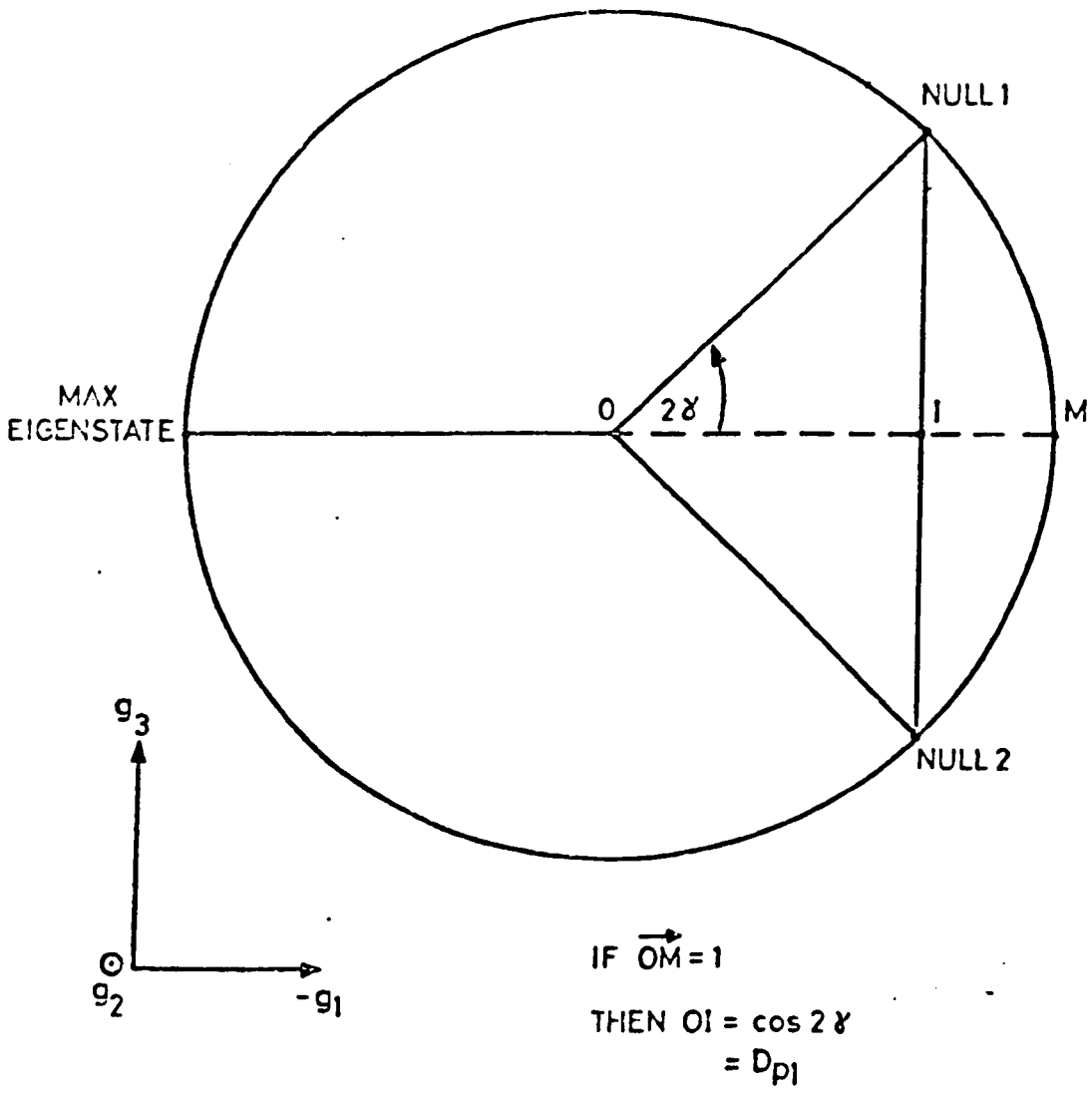

FIG 17 DETERMINATION OF D_{pl} FROM POLARISATION FORK

general combination of rotation and pure boost represented by 3.12, forms a wider group of so called "restricted" Lorentz transformations (see Goldstein Chapter 7). However, we will see that a very important class of scattering problems can be modelled by a pure boost only.

A pure Lorentz transformation may be written in exponential form as (Goldstein 1970)

$$\exp(\underset{\sim}{k}.\underset{\sim}{\sigma}a/2) \qquad - 4.41$$

where $\underset{\sim}{k}$ is a direction vector, $\underset{\sim}{\sigma}$ are the Pauli matrices and a a complex angle indicating the magnitude of the boost. We have already met an equation of this type: 4.36 represents the special case of a boost in the x direction and may be written

$$\cosh(a/2)\sigma_0 + \sinh(a/2)\sigma_1 \qquad - 4.42$$

which corresponds to 4.41 with $\underset{\sim}{k} = (1,0,0)$.

In general, a boost in an arbitrary direction may be written as a 2x2 Hermitian matrix in the form (Payne).

$$\begin{bmatrix} \cosh(a/2)+\sinh(a/2)\cos(A) & \sinh(a/2)\cos(B)-i\sinh(a/2)\cos(C) \\ \sinh(a/2)\cos(B)+i\sinh(a/2)\cos(C) & \cosh(a/2)-\sinh(a/2)\cos(A) \end{bmatrix}$$

which is equivalent to 4.41 with $\underset{\sim}{k} = (\cos(A),\cos(B),\cos(C))$, the vector of direction cosines and A, B and C the angles formed by the axis of the boost relative to some reference coordinate system.

We have thus established the homomorphism between Hermitian matrices and pure Lorentz transformations and clearly, for the target scattering matrix to be written in this form, it

must be Hermitian. We saw in section 3.2 that Hermitian scattering matrices have only one eigenaxis and, in the more useful antenna coordinate system, correspond to symmetric matrices $[S_A]$. From this result, we can associate the direction of the boost in 4.41 with the target eigenaxis, since by definition, this is the orthogonal base for which $[S_A]$ is diagonal. Further, from our discussion in 4.3, we know that the magnitude of the boost is a function of the fork angle, γ, given by 4.37.

In conclusion we can say that for symmetric scattering matrices in the antenna coordinate system (as is the case for monostatic radar scattering) the transformation of arbitrary incident partial state is homomorphic to a pure Lorentz transformation of the incident Stokes 4-vector, the direction of the boost being parallel to the target eigenaxis.

Before considering the implications of this result for a geometrical model of the change of partial state, let us consider the form of transformation when [S] is not symmetric.

In this case we have to return to equation 3.12 and write the scattering matrix as the product of two exponentials

$$[S] = \exp(-ix[\underline{\sigma}.\underline{n}]/2).\exp(\alpha[\underline{\sigma}.\underline{k}]/2) \qquad - 4.4$$
$$= \exp[(-ix\underline{n}+\alpha\underline{k}).\underline{\sigma}/2]$$

which represents a combination of boost and rotation and corresponds to a "restricted" Lorentz transformation (Goldstein). Equation 4.43 is the same as the Lorentz spin matrix discussed in 2.2. Note that the restricted transformation has 8 degrees of freedom: two direction vectors, $\underline{n}$ and $\underline{k}$, and 2 angles α and x whereas the pure Lorentz transformation has only four, corresponding to three for the location of the eigenaxis

and one for the boost parameter or fork angle.

We will leave further discussion of the restricted transformation until chapter 5 and now return to the rather special, but important, case of pure transformations.

We wish to develop a simple set of transformtion equations, based on the polarisation fork, for predicting the change of θ, τ and D_P for arbitrary incident partial state. By using the homomorphism outlined above, we can examine the general form of this transformation in close analogy to that used for the transformation of velocity in special relativity (see French, Chapter 5).

We begin by expressing the incident Stokes vector, $\underset{\sim}{g}$, in the target eigenpolarisation base. We can always do this because the eigenpolarisations are orthogonal for symmetric matrices $[S_A]$. In this base, [M] can be written in the form 4.35 and hence we can write the change of state as

$$\underset{\sim}{g}' = \begin{bmatrix} \cosh(\alpha) & \sinh(\alpha) & 0 & 0 \\ \sinh(\alpha) & \cosh(\alpha) & 0 & 0 \\ 0 & 0 & 1 & 0 \\ 0 & 0 & 0 & 1 \end{bmatrix} \underset{\sim}{g} \qquad -4.44$$

We can define the input state as a vector degree of polarisation

$$\underset{\sim}{D_P} = (D_{P1}, D_{PV}, D_{P2}) \qquad -4.45$$

where

$$D_{P1} = g_1/g_0 \quad D_{PV} = g_2/g_0 \quad D_{P2} = g_3/g_0$$

D_{P1} is the "inline" component ie. parallel to direction of boost (D_{PV}, D_{P2}) is the "transverse" component ie. perpendicular to direction of boost.

The reason for employing this separation of D_P is that the inline component will transform as in section 4.3 ie.

$$D_{P2}' = \frac{D_{P2} - D_{P1}}{1 - D_{P2}D_{P1}} \qquad - 4.46$$

where D_{P1} is given by 4.38.

We now just have to find how the transverse components transform and we will be able to predict the change of state for any incident polarisation. Consider, initially, the D_{PV} component. From 4.44, it transforms as

$$D_{PV}' = \frac{g_2'}{g_0'} = \frac{g_2}{\cosh(\alpha)g_0 + \sinh(\alpha)g_1}$$

$$= \frac{D_{PV}/\cosh(\alpha)}{1 + D_{P2}\tanh(\alpha)} = \frac{D_{PV}(1 - D_{P1}^2)^{1/2}}{1 - D_{P2}D_{P1}} \qquad - 4.47$$

Similarly, we can show that

$$D_{P2}' = \frac{D_{P2}/\cosh(\alpha)}{1 + D_{P2}\tanh(\alpha)} = \frac{D_{P2}(1 - D_{P1}^2)^{1/2}}{1 - D_{P2}D_{P1}} \qquad - 4.48$$

We can see from these equations that the transverse components of D_P are functions of the "inline" component, D_{P2} as well as of the fork angle r. Predicting the final position of D_P' in polarisation space is made difficult by this coupling of "inline" and "transverse" components but, nonetheless, equations 4.46, 4.47 and 4.48 provide the basis for calculation of the change of partial state as a function of the boost parameter D_{P1} introduced in 4.3.

As an example, consider the special case of states for which $g_1 = 0$ ie. those states lying in a plane normal to the eigenaxis and passing through the origin (figure 18). For all such states $D_{P1} = 0$ and so

$$D_{P2}' = D_{P1} = -\tanh(r)$$

From 4.47 and 4.48 we have

$$D_{PV}' = D_{PV}(1 - D_{P1}^2)^{1/2}$$

$$D_{P2}' = D_{P2}(1 - D_{P1}^2)^{1/2}$$

Using these equations we can show that

$$D_P'^2 > D_P^2$$

and so all points in this plane are expanded. Information as to the expansion or compression of points is of great practical importance because it allows an assessment of the applicability or otherwise of polarisation filtering techniques such as those discussed by Poelman. States which are expanded by the target will be more influenced by polarisation filters, while those which are compressed (in the limit tending to random polarisation) will be less amenable to the techniques of filtering. In this way one may assess the potential performance of such filters for the suppression or enhancement of RCS, even in the case of passive imaging where the incident radiation will generally be partially polarised.

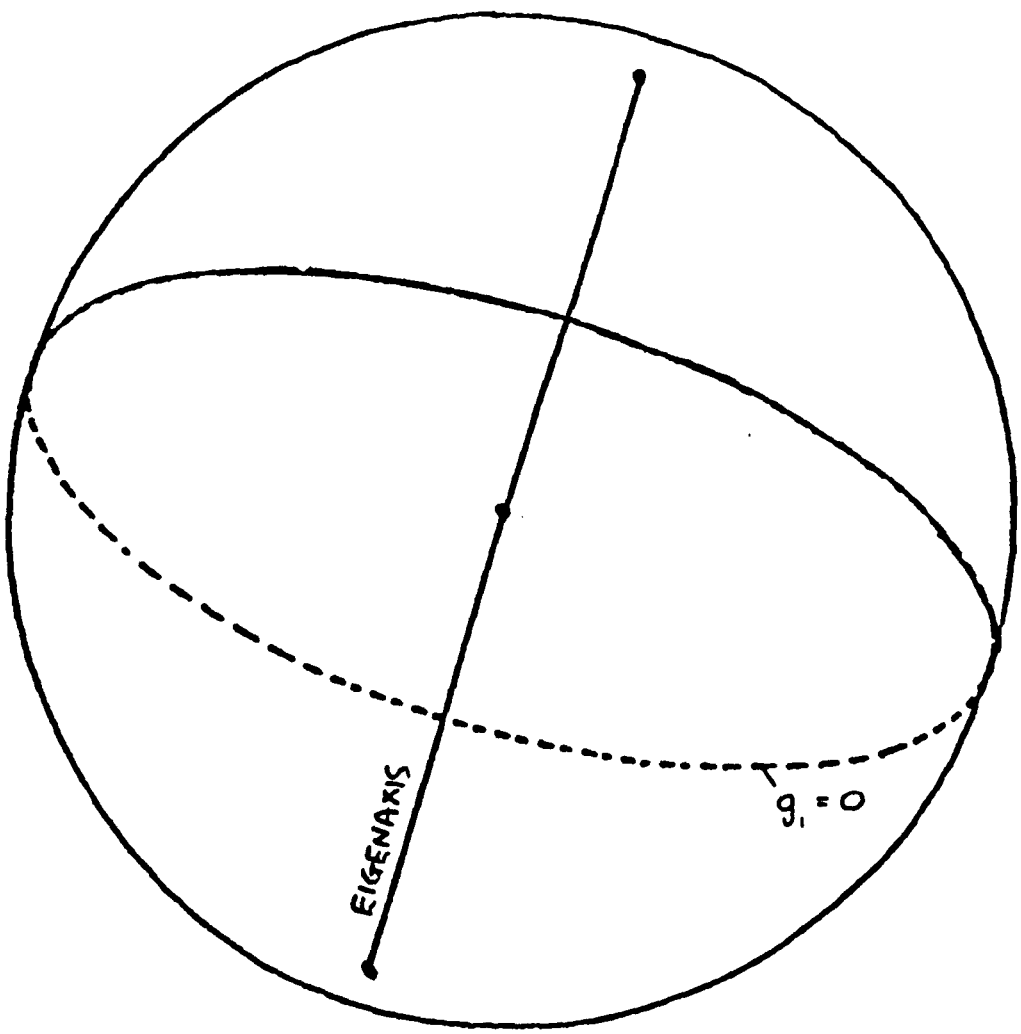

FIGURE 18: $g_1 = 0$ PLANE

5.1 The Pauli Targets

Due to their completeness, we can expand any 2x2 matrix as a linear combination of the 4 Pauli matrices defined in 2.2. When we express the target scattering matrix [S] in this way, we obtain an ordered set of 4 complex numbers forming a complex vector $\hat{k}$, where

$$k_0 = 1/2\mathrm{Tr}([S].\sigma_0) = 1/2(S_{HH} + S_{VV}) \quad - 5.1$$

$$k_1 = 1/2\mathrm{Tr}([S].\sigma_1) = 1/2(S_{HH} - S_{VV}) \quad - 5.2$$

$$k_2 = 1/2\mathrm{Tr}([S].\sigma_2) = 1/2(S_{HV} + S_{VH}) \quad - 5.3$$

$$k_3 = 1/2\mathrm{Tr}([S].\sigma_3) = 1/2(S_{HV} - S_{VH}) \quad - 5.4$$

We will show in this chapter that unitary transformations of the vector $\hat{k}$ are homomorphic to real orthogonal rotations in a 6 dimensional Euclidean space. Thus, just as the wave spinor $\underset{\sim}{E}$ led to mappings on the Poincaré sphere, so the target spinor $\hat{k}$ leads to a mapping onto the surface of a 6-sphere. We will also see that by forming a target coherency matrix $T_C = \hat{k}.\hat{k}^{*T}$, we can relate the elements of the target Mueller matrix [M], to invariants in this target space.

The main reason for following this analysis is that the treatment of statistical fluctuations of the target is most easily interpreted as motion over the surface of this 6-sphere rather than by the dynamics of the null points on the Poincaré sphere. These dynamic effects will be the subject of chapter 6.

The expansion of [S] into its vector coefficients $\hat{k}$ may be viewed as a description of the target in terms of a set of 4 reference base matrices (just as $\underset{\sim}{E}$ was expressed in terms of two base polarisation states $\hat{x}$ and $\hat{y}$). If these reference matrices

are the Pauli set σ (we will see later that they need not be), we describe them as the Pauli targets. The coefficients describing [S] in terms of the Pauli targets are then given by equations 5.1 to 5.4.

Because of their special significance, we devote the rest of this section to a detailed study of the polarisation transformation properties of these Pauli targets. For the sake of simplicity, we will assume they are expressed in the (h,v) polarisation base (being the one most commonly used for reference) and also that the antenna coordinate system is being used (although for comparison we will give the form of the matrices in the conventional coordinates to highlight the differences involved)

1) σ_0

This target appears at first sight to be relatively simple: the identity matrix or matrix corresponding to free space. However, the antenna coordinate system means that its interpretation requires some care. We have

$$[S_A] = \begin{bmatrix} 1 & 0 \\ 0 & 1 \end{bmatrix} \qquad \hat{k} = (1,0,0,0)$$

but its form under a change of polarisation base is

$$[U_2]^T [S_A] [U_2] = A \begin{bmatrix} 1+\rho^2 & 2i\mathrm{Im}(\rho) \\ 2i\mathrm{Im}(\rho) & 1+\rho^{*2} \end{bmatrix} \qquad - 5.5$$

where

$$A = (1+\rho\rho^*)^{-1}$$

We can see that if $\mathrm{Im}(\rho) = 0$ then [S] is diagonal ie. all linear

polarisations are eigenstates. On the other hand, if $\rho = \pm i$ then [S] has a Copol Null ie. for left or right circular polarisation the returned state is orthogonally polarised.

In the conventional coordinate system however

$$[S] = \begin{bmatrix} 1 & 0 \\ 0 & -1 \end{bmatrix} \quad \hat{k} = (0,1,0,0)$$

and under a change of base

$$[U_2]^{*T}[S][U_2] = A \begin{bmatrix} 1 - \rho\rho^* & -2\rho^* \\ -2\rho & \rho\rho^* - 1 \end{bmatrix} \qquad - 5.6$$

and only if $\rho = 0$ (or infinity) does [S] become diagonal and so only h and v are eigenstates. Note however, that $\rho = \pm i$ still gives Copol Nulls.

Returning to the antenna coordinates, we can summarise all the properties of this target by drawing its polarisation fork on the Poincaré sphere (see Figure 19). Since $[S_A]$ has equal eigenvalues, $\tau = 45°$ and the fork is opened out, yielding orthogonal Copol Nulls. The skip angle is zero and so the fork lies in a plane normal to the equator. Finally, since $\tau = 45°$ we can say that all partial states are reflected with an unchanged degree of polarisation.

In Radar terms, this target corresponds to an "odd" bounce reflector such as a flat facet (one "bounce") or trihedral corner reflector (see Figure 20). It also corresponds to the backscatter from a sphere, a result which is used in the design of rain clutter rejection radars (see Skolnik) which use circular polarisation as a Copol Null.

In optics, where the traditional coordinates are more

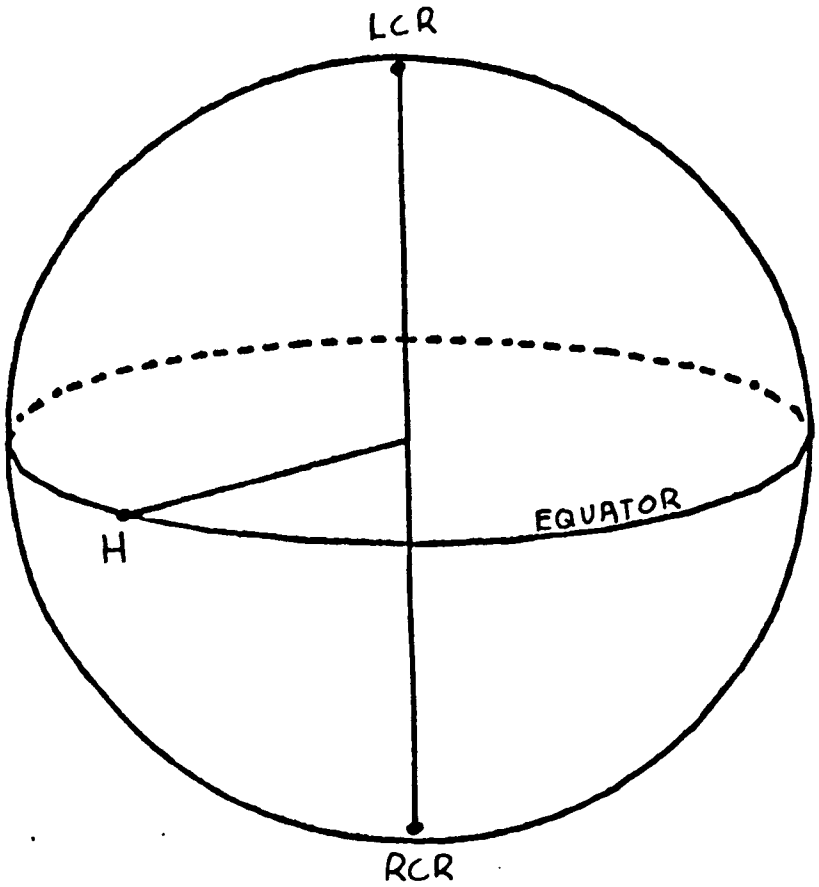

FIGURE 19: FORK FOR σ_o

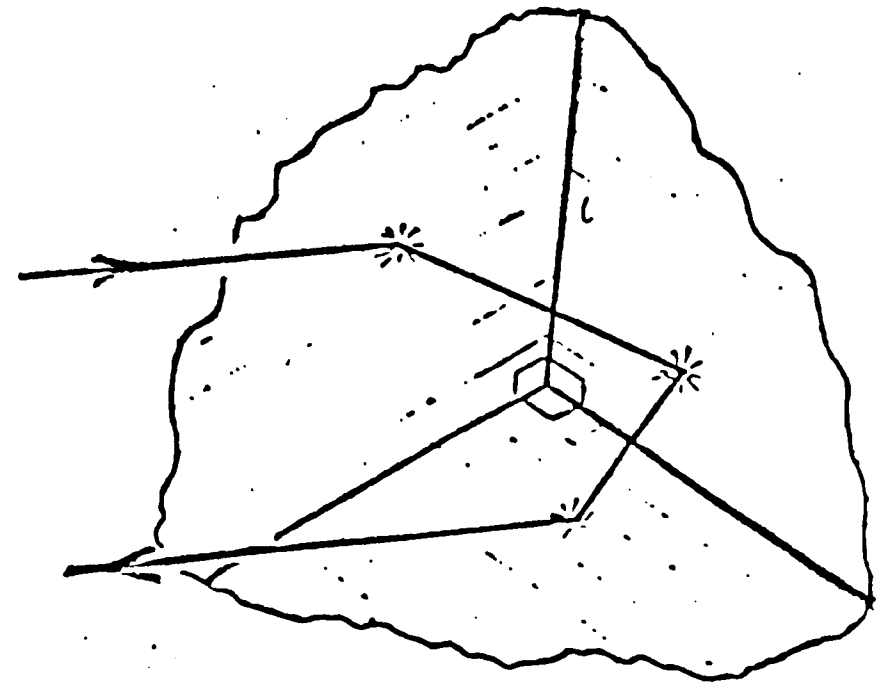

FIGURE 20: TRIHEDRAL CORNER

commonly used, this target corresponds to a half wave plate, used to rotate the plane of linear polarisations and to reverse the sense of elliptical states.

Because of the highly symmetric form of its polar isation fork and the fact that all linear states remain unaltered, we will refer to the coefficient of this component in the expansion of an arbitrary target as target "symmetry".

2) σ_1

For this Pauli target we have

$$[S_A] = \begin{bmatrix} 1 & 0 \\ 0 & -1 \end{bmatrix} \quad \hat{k} = (0,1,0,0)$$

and under a change of base

$$[U_2]^T[S_A][U_2] = A \begin{bmatrix} 1 & -\rho^2 & -2Re(\rho) \\ -2Re(\rho) & \rho^{*2} - 1 \end{bmatrix} \qquad - 5.7$$

This time the set of all states for which $Re(\rho) = 0$ are eigenstates while $\rho = \pm 1$ (ie. $\pm 45°$ linear) defines the Copol Nulls. The target parameters are the same as for σ_0 except that the skip angle is now 90° and so the target fork is rotated into the equatorial plane (Figure 21). The eigenstates lie along a great circle passing through h, v and left and right circular and so this target preserves the sense of circular polarisation while causing linear states with inclination angle θ to be reflected with angle $-\theta$. This property makes $\pm 45°$ linear Copol Nulls, with an apparent rotation of all other linear states. Again there is no change of degree of polarisation for partial states because $r = 45°$.

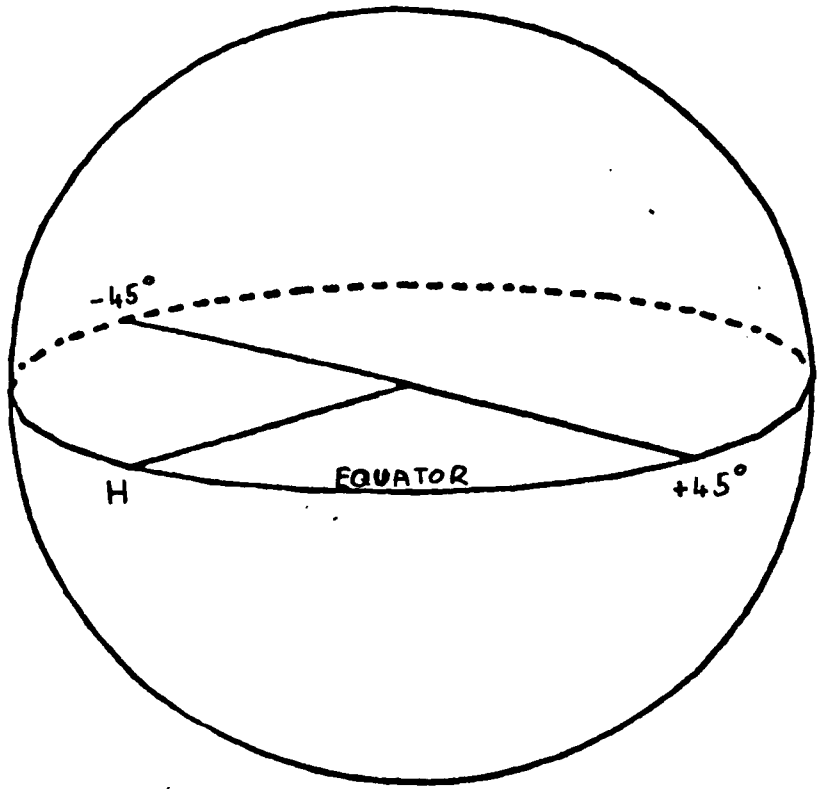

FIGURE 21: FORK FOR σ_1

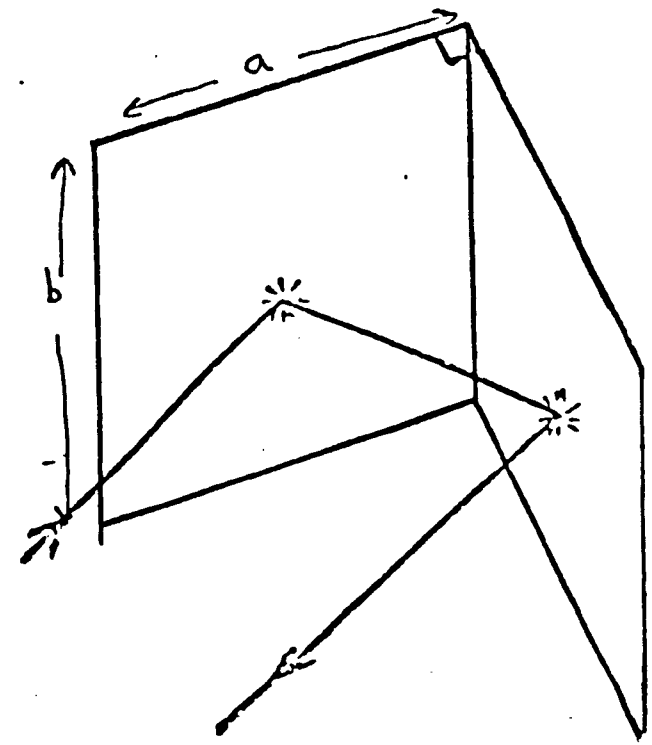

FIGURE 22: DIHEDRAL CORNER

In the conventional coordinates this target corresponds to the identity matrix for <u>all</u> base states and so represents the matrix for free space. In Radar terms however, this matrix is indicative of "even" bounce reflectors such as a dihedral (see Figure 22). σ_1 corresponds to a dihedral with its seam parallel to the incident $\hat{v}$ state. Because of its ability to rotate linear polarisations we will refer to the coefficient of σ_1 as "first quadrant irregularity".

3) σ_2

For this case

$$[S_A] = \begin{bmatrix} 0 & 1 \\ 1 & 0 \end{bmatrix} \quad \hat{k} = (0,0,1,0)$$

and under a change of base

$$[U_2]^T[S_A][U_2] = A \begin{bmatrix} 2\rho & 1-\rho\rho^* \\ 1-\rho\rho^* & -2\rho^* \end{bmatrix} \qquad - 5.8$$

This target is intimately related to σ_1 since we can obtain it from the latter by rotating the reference axes through 45° ie put $\rho = -1$ in 5.7. Its fork is therefore the same as for σ_1 except it is rotated about the polar axis by 90° (see Figure 23). The eigenstates now lie on a great circle passing through the poles and through $\pm$45° linear. The Copol Nulls are now $\hat{h}$ and $\hat{v}$.

We can interpret this target in radar terms as a dihedral with its seam at 45° to the $\hat{v}$ direction. For this reason we call the coefficient of σ_2 "second quadrant irregularity". Its function may be illustrated by noting the similarity between k_1,

k_2 and g_1, g_2, the two corrresponding components of a Stokes vector which <u>together</u> specify the quadrant in which the major axis of the polarisation ellipse lies. In the same way, both k_1 and k_2 are required for a full description of target irregularity.

4) σ_3

For this target

$$[S_A] = \begin{bmatrix} 0 & -1 \\ 1 & 0 \end{bmatrix} \qquad \hat{k} = (0,0,0,1)$$

and under a change of base

$$[U_2]^T [S_A] [U_2] = A \begin{bmatrix} 0 & -i(1 - \rho\rho^*) \\ -i(1 - \rho\rho^*) & 0 \end{bmatrix} \qquad - 5.9$$

We can see immediately that this target has the very unusual property that the Copol Nulls include the whole Poincaré sphere. Because of this we call the coefficient of σ_3 "antisymmetry".

Since σ_3 is not symmetric we cannot represent it by a single fork but must instead use separate forks for transmit and receive (see Chapter 3). If we fix the right singular vectors of $[S_A]$ as (h,v) then we can diagonalise σ_3 by choosing the left singular vectors as i(v,-h) and so

$$[U_{2R}]^T [S_A] [U_{2T}] = \begin{bmatrix} 1 & 0 \\ 0 & 1 \end{bmatrix} \qquad - 5.10$$

The transmitter fork is identical to that for σ_0 but the receiver fork is obtained by a 180° rotation of the transmitter

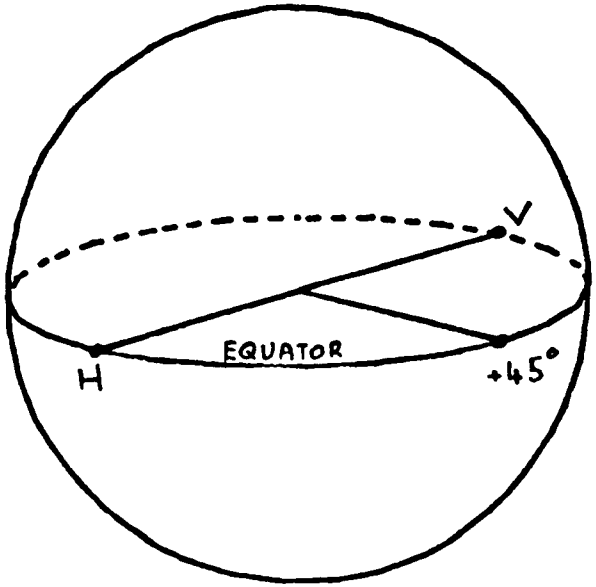

FIGURE 23

FORK FOR σ_2

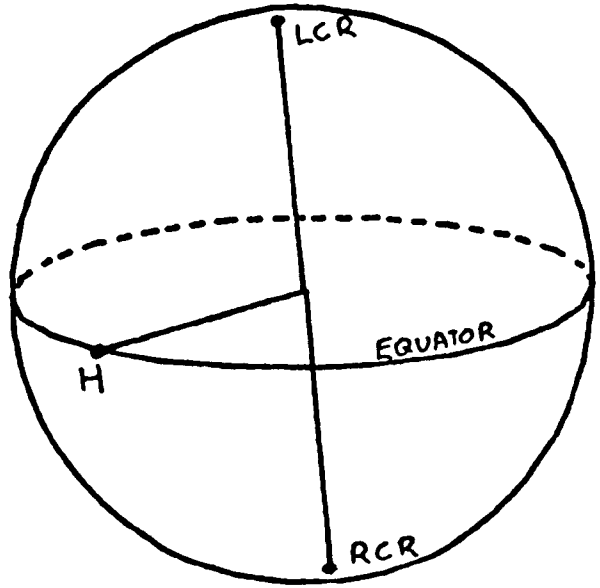

FIGURE 24

TRANSMIT FORK FOR σ_3

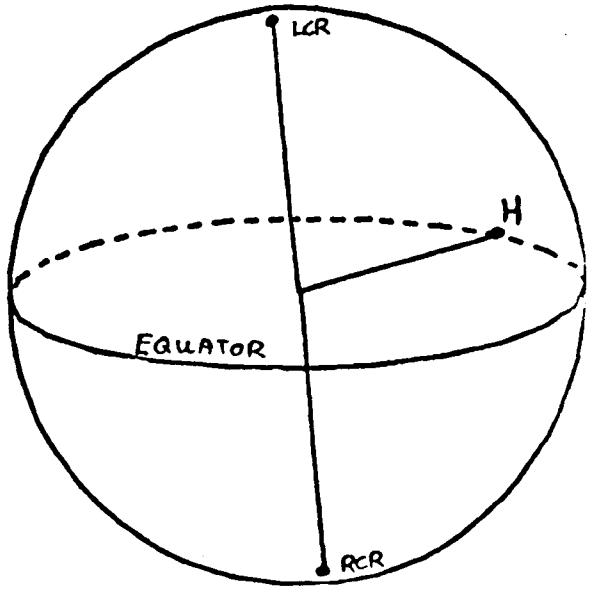

FIGURE 25

RECEIVE FORK FOR σ

fork about the Copol axis (see Figures 24 and 25).

In summary, any single target, given by a scattering matrix $[S_A]$, may be expressed as a linear combination of the 4 Pauli base targets and hence may be specified by its symmetry, irregularity and antisymmetry. For example, the set of all symmetric matrices are characterised by $k_3 = 0$ ie. they have no antisymmetric component in their decomposition. For this special case we need only three Pauli targets to analyse a given target. Notice that in all cases the decomposition is coherent ie. the coefficients $\underset{\sim}{\hat{k}}$ are complex.

5.2 Unitary Transformations of the Target Spinor

In the last section we discussed the properties of the Pauli targets and noted how they form a complete set of basis vectors such that any scattering matrix can be represented as a linear combination of just these 4 matrices. As basis vectors, they satisfy the usual conditions for orthogonality and normalisation:

$$\hat{k}_i^{*T} . \hat{k}_j = \delta_{ij} \qquad - 5.11$$

Evidently, we can construct an infinite number of other sets of four reference matrices by taking linear combinations of the Pauli targets (with the constraint that each base must satisfy 5.11). In this section we will study the details of such target base transformations and show that $\hat{k}$ is a spinor in a 6 dimensional real space.

In matrix notation, two single targets $[S_1]$ and $[S_2]$ are orthogonal if

$$[S_1] = \begin{bmatrix} S_{AX} & S_{XY} \\ S_{YX} & S_{YY} \end{bmatrix} \qquad [S_2] = \begin{bmatrix} S_{AA} & S_{AB} \\ S_{BA} & S_{BB} \end{bmatrix}$$

and

$$S_{\chi\chi^*} S_{\alpha\alpha}^* + S_{\gamma\gamma^*} S_{\beta\beta}^* + S_{\chi\gamma} \cdot S_{\alpha\beta}^* + S_{\gamma\chi} \cdot S_{\beta\alpha}^* = 0 \qquad - 5.12$$

Equation 5.12 provides 2 constraint equations for orthogonality. In addition, both matrices are to be normalised, so adding a further constraint for each matrix. Hence, in constructing an arbitrary set of 4 basis matrices, we begin with a normalised target $[S_1]$, having 6 degrees of freedom (taking into account the normalisation constraint). The second target must be chosen so as to satisfy 5.12 and normalisation, so has only 5 degrees of freedom. Similarly, the third and fourth components have 3 and 1 degrees of freedom respectively. In all, there are 6 + 5 + 3 + 1 = 15 degrees of freedom in constructing a new base. Note that for symmetric matrices, only three basis targets are required, so the change of base has only 8 degrees of freedom. Finally, if we deal only with the set of diagonal matrices $[S_{\alpha\alpha}]$, only 2 (diagonal) base matrices are required and the transformation has only 3 degrees of freedom.

In general, we may write the change of target base as a matrix equation relating the new base $\underline{\sigma}'$ to the Pauli targets $\underline{\sigma}$ as

$$\underline{\sigma}' = [U_4] . \underline{\sigma} \qquad - 5.13$$

where $[U_4]$ is a 4x4 unitary matrix with unit determinant. In this case the target vector $\hat{k}$ transforms as

$$\hat{k} = [U_4]^T . \hat{k}' \qquad - 5.14$$

(see equation 2.35) where

$$k_i' = \frac{1}{2}\,\mathrm{Tr}([S].\sigma')$$

As an example, we may choose the new base

$$[S_1] = \begin{bmatrix} 1 & 0 \\ 0 & 0 \end{bmatrix} [S_2] = \begin{bmatrix} 0 & 0 \\ 0 & 1 \end{bmatrix} [S_3] = \begin{bmatrix} 0 & 1 \\ 0 & 0 \end{bmatrix} [S_4] = \begin{bmatrix} 0 & 0 \\ 1 & 0 \end{bmatrix}$$

which corresponds to a unitary change of base matrix

$$[U_4] = 2^{-1/2} \begin{bmatrix} 1 & 1 & 0 & 0 \\ 1 & -1 & 0 & 0 \\ 0 & 0 & 1 & 1 \\ 0 & 0 & 1 & -1 \end{bmatrix} \qquad - 5.15$$

and gives rise to a target vector

$$\hat{k} = (S_{HH}, S_{VV}, S_{HV}, S_{VH})^T$$

Note that there is only one invariant under unitary transformations of target base, namely

$$\hat{k}^{*T}.\hat{k} = \mathrm{Span}([S]) \qquad - 5.16$$

To emphasise the degrees of freedom inherent in change of target base transformations, we will now consider the change of reference polarisation base, which we discussed in 2.3, as a special case of our matrix $[U_4]$.

In terms of the scattering matrix $[S_A]$, we can write the

change of polarisation base as

$$[S_A]' = [U_2]^T [S_A] [U_2]$$

but

$$\hat{k}' = \sum k_i' \sigma_i \qquad \hat{k} = \sum k_i \sigma_i$$

By using the results of Appendix 1, we can derive a 4x4 matrix relating $\hat{k}'$ to $\hat{k}$ ie.

$$\hat{k}' = [U_{4P}] \hat{k} \qquad - 5.17$$

where the elements of $[U_{4P}]$ are given by

$$u_{ij} = \frac{1}{2} Tr(\sigma_{i8} \sigma_j) \qquad - 5.18$$

and

$$\sigma_{i8} = [U_2] \sigma_i [U_2]^T \qquad - 5.19$$

By using

$$[U_2] = A \begin{bmatrix} 1 & -\rho^* \\ \rho & 1 \end{bmatrix} \qquad - 5.20$$

the elements of $[U_{4P}]$ may be obtained as follows:

Row 1

$$[U_2] \sigma_0 [U_2]^T = [U_2] [U_2]^T = A^2 \begin{bmatrix} 1 + \rho^{*2} & 2i\,Im(\rho) \\ 2i\,Im(\rho) & 1 + \rho^2 \end{bmatrix} \qquad - 5.21$$

so

$$u_{11} = 1 + Re(\rho^2) \qquad u_{12} = -i\,Im(\rho^2)$$

$$u_{13} = 2i\,Im(\rho) \qquad u_{14} = 0$$

The other rows may be obtained in a similar manner to yield

$$[U_{4P}] = A^2 \begin{bmatrix} 1 + Re(\rho^2) & -iIm(\rho^2) & 2iIm(\rho) & 0 \\ iIm(\rho^2) & 1 - Re(\rho^2) & 2Re(\rho) & 0 \\ 2iIm(\rho) & -2Re(\rho) & 1 - \rho\rho^* & 0 \\ 0 & 0 & 0 & 1 + \rho\rho^* \end{bmatrix} \quad - 5.22$$

Notice that k_3 is a transformation invariant ie. $S_{XY} - S_{YX}$ is invariant under a change of polarisation reference base (we met a special case of this when we discussed the transformation of symmetric scattering matrices in chapter 3). We can also show that

$$\det([S_A]) = k_0^2 - k_1^2 - k_2^2 - k_3^2 \quad - 5.23$$

is an invariant under $[U_{4P}]$. Note that neither of these quantities will be invariant under the more general change of target base.

In chapter 2 we saw how the group SU(2) is homomorphic to O_3^+ and hence how we can define the wave spinor $\underset{\sim}{E}$ as a point on a 3-sphere (the Poincaré sphere). We will now investigate further the general properties of the groups SU(n) and O_n^+ with a view to showing that the target vector $\hat{k}$ is a spinor in a 6 dimensional Euclidean space.

The sets of Unitary and rotation matrices are examples of Lie groups, meaning that all group properties follow from considering infinitessimal transformations in the neighbourhood of the identity element. It follows that we can represent a unitary matrix U as a power series

$$U = 1 + iaH + (iaH)^2/2 + ... = \exp(iaH) \quad - 5.24$$

where H is called a generator and for unitary matrices U, will be hermitian ie. $H^{\dagger} = H$ (if U has unit determinant then H will be traceless as well as hermitian). The number of generators required to represent an n dimensional unitary matrix is one problem we will solve shortly but, the set of all such generators will satisfy a commutation relation

$$[H_i, H_j] = ia_{ijk}H_k \qquad - 5.25$$

where the set of numbers a_{ijk} are called the structure constants. Commutation is a very important property of group structures and the number of mutually commuting generators is known as the rank of the group. In addition, there will also exist nonlinear functions of the generators, called Casimir operators, which commute with all the group generators. The number of Casimir operators equals the rank of the group.

As an example of this theory consider SU(2), the group of 2x2 unitary matrices with unit determinant. It has 3 generators which satisfy the commutation

$$[H_iH_j] = i\varepsilon_{ijk}H_k$$

ε_{ijk} is called the permutation operator and is defined as $\varepsilon_{ijk} = 1(-1)$ if ijk are a cyclic (anticyclic) permutation of 123 (otherwise $\varepsilon_{ijk} = 0$).

There are many possible representations of this group (see Arfken 1970) but for the fundamental representation, the generators are the Pauli matrices considered earlier. The rank is given by the number of diagonal traceless generators, which for SU(2) is just 1 (σ_3) and so there is only 1 Casimir

operator, namely

$$H^2 = H_1^2 + H_2^2 + H_3^2 \qquad - 5.26$$

In order to find the number of generators required for SU(n), we note that an nxn Unitary matrix has n^2 degrees of freedom so SU(n) has $n^2 - 1$. Hence, knowing n we can calculate the number of generators eg.

n	$n^2 - 1$
1	0
2	3
3	8
4	15
5	24
6	35

As an example, SU(3) has 8 generators (we may choose any set of eight linearly independent traceless 3x3 hermitian matrices). It turns out that only two of these can be diagonal and so SU(3) has rank 2 (and 2 Casimir operators).

In order to describe an n element complex vector as a spinor, we must do more than identify the generators of SU(n); we must find a homomorphic relationship between the group of transformations SU(n) and some rotation group O_n'. We can easily show that an m x m real orthogonal matrix has m(m-1)/2 degrees of freedom and, clearly, for such a homomorphism to exist, the degrees of freedom in O_n' must match those in SU(n). We have

m	m(m-1)/2
1	0
2	1
3	3
4	6
5	10
6	15
7	21

From this table we can clearly see the SU(2)-O_3^+ homomorphism but also note that O_6^+ may be homomorphic to SU(4). This is an interesting result: if it is true, we can describe the target vector $\hat{k}$ as a spinor in a 6 dimensional real space and so map targets onto the surface of a 6-sphere (we will see in chapter 6 the physical benefit of doing just this).

It is shown in Appendix 3 that this homomorphism does indeed exist and we will now use the results derived therein to develop the 15 generators of SU(4).

We begin by noting that just as we could write the real matrix O_3^+ in terms of three composite plane rotations (the Euler angles), we can likewise write the 6 x 6 rotation matrix as the product of 15 composite plane rotations:

$$O_6^+ = \prod_{ij} O_{ij} \qquad - 5.27$$

where i = 5,4....1 and j = 6,5..i+1. Of the 15 angles, 5 are longitude angles $-180° < \theta < 180°$ ($\theta_{16}, \theta_{26}, \theta_{36}, \theta_{46}$ and θ_{56}) while the other 10 are latitude angles $-90° < \beta < 90°$. Each matrix O_{ij} corresponds to a rotation in the ij plane. For example

$$O_{16} = \begin{bmatrix} \cos(\theta) & 0 & 0 & 0 & 0 & -\sin(\theta) \\ 0 & 1 & 0 & 0 & 0 & 0 \\ 0 & 0 & 1 & 0 & 0 & 0 \\ 0 & 0 & 0 & 1 & 0 & 0 \\ 0 & 0 & 0 & 0 & 1 & 0 \\ \sin(\theta) & 0 & 0 & 0 & 0 & \cos(\theta) \end{bmatrix} \qquad - 5.28$$

It is shown in Appendix 3 that O_6^+ may also be written

$$O_6^* = QWQ^{-1}$$

where W is a 6 x 6 complex matrix (not necessarily orthogonal) whose elements are related to the minors of a corresponding matrix in SL(4). Q is a 6 x 6 transformation matrix given by

$$Q = (1 - i)/2 \begin{bmatrix} I_3 & iI_3 \\ iI_3 & I_3 \end{bmatrix} \qquad - 5.29$$

where I_3 is the 3 x 3 identity matrix. If we write O_6^* in the block form

$$O_6^* = \begin{bmatrix} A & B \\ C & D \end{bmatrix} \qquad - 5.30$$

then we can calculate W as

$$W = -i/2 \begin{bmatrix} (C - B) + i(A + D) & (D - A) + i(B + C) \\ (A - D) + i(B + C) & (B - C) + i(A + D) \end{bmatrix} \qquad - 5.31$$

If we do this for O_{16} we obtain

$$W = \begin{bmatrix} 1+\cos(\theta) & 0 & -i\sin(\theta) & -i(1-\cos(\theta)) & 0 & -\sin(\theta) \\ 0 & 1 & 0 & 0 & 0 & 0 \\ -i\sin(\theta) & 0 & 1+\cos(\theta) & \sin(\theta) & 0 & i(1-\cos(\theta)) \\ i(1-\cos(\theta)) & 0 & -\sin(\theta) & 1+\cos(\theta) & 0 & i\sin(\theta) \\ 0 & 0 & 0 & 0 & 1 & 0 \\ \sin(\theta) & 0 & -i(1-\cos(\theta)) & i\sin(\theta) & 0 & 1+\cos(\theta) \end{bmatrix}$$

Having obtained W, we can now calculate U_4, the 4 x 4 unitary matrix corresponding to O_6. For O_{16} we obtain

$$U_{14} = \begin{bmatrix} \cos(\theta/2) & 0 & 0 & \sin(\theta/2) \\ 0 & \cos(\theta/2) & i\sin(\theta/2) & 0 \\ 0 & i\sin(\theta/2) & \cos(\theta/2) & 0 \\ -\sin(\theta/2) & 0 & 0 & \cos(\theta/2) \end{bmatrix} \quad - 5.33$$

We can obtain the generator for rotations in the 16 plane by writing U_{14} in the form

$$U_{14} = \exp(i\theta/2.\eta_4) \quad - 5.34$$
$$= \cos(\theta/2)\eta_0 + i\sin(\theta/2)\eta_4$$

where η_4 is the generator, given by

$$\eta_4 = \begin{bmatrix} 0 & 0 & 0 & -1 \\ 0 & 0 & 1 & 0 \\ 0 & 1 & 0 & 0 \\ 1 & 0 & 0 & 0 \end{bmatrix} \quad - 5.35$$

By repeating these calculations for all 15 plane rotation angles, we arrive at the set of generators η as shown in figure 26 (also shown are the corresponding plane rotations in 6 space). Together with the 4 x 4 identity matrix η_0, these matrices form a complete set, so any 4 x 4 matrix A, may be expressed as a linear combination of these matrices. Each matrix may then be represented by a set of ordered coefficients $\underset{\sim}{a}$, where

$$\underset{\sim}{a} = \frac{1}{2} Tr(A\eta_i) \quad - 5.36$$

Most significantly, if A is hermitian then the coefficient

vector $\underset{\sim}{a}$ will be real. We will see in the next chapter that "$\underset{\sim}{a}$" bears a simple relationship to the elements of the target Mueller matrix [M]. For the moment it is sufficient to realise that the elements of $\underset{\sim}{a}$ are invariants under plane rotations in 6-space eg. a_{12} is invariant under all rotations of the type U_{14}

$$\begin{bmatrix} 1 & 0 & 0 & 0 \\ 0 & 1 & 0 & 0 \\ 0 & 0 & 1 & 0 \\ 0 & 0 & 0 & 1 \end{bmatrix} \quad \eta_0$$

$$\begin{bmatrix} 0 & 1 & 0 & 0 \\ 1 & 0 & 0 & 0 \\ 0 & 0 & 0 & i \\ 0 & 0 & -i & 0 \end{bmatrix} \quad \eta_1(26)$$

$$\begin{bmatrix} 0 & 0 & 1 & 0 \\ 0 & 0 & 0 & -i \\ 1 & 0 & 0 & 0 \\ 0 & i & 0 & 0 \end{bmatrix} \quad \eta_2(24)$$

$$\begin{bmatrix} 0 & 0 & 0 & 1 \\ 0 & 0 & i & 0 \\ 0 & -i & 0 & 0 \\ 1 & 0 & 0 & 0 \end{bmatrix} \quad \eta_3(46)$$

$$\begin{bmatrix} 0 & 1 & 0 & 0 \\ 1 & 0 & 0 & 0 \\ 0 & 0 & 0 & -i \\ 0 & 0 & i & 0 \end{bmatrix} \quad \eta_4(35)$$

$$\begin{bmatrix} 1 & 0 & 0 & 0 \\ 0 & 1 & 0 & 0 \\ 0 & 0 & -1 & 0 \\ 0 & 0 & 0 & -1 \end{bmatrix} \quad \eta_5(14)$$

$$\begin{bmatrix} 0 & 0 & 0 & -i \\ 0 & 0 & 1 & 0 \\ 0 & 1 & 0 & 0 \\ i & 0 & 0 & 0 \end{bmatrix} \quad \eta_6(16)$$

$$\begin{bmatrix} 0 & 0 & i & 0 \\ 0 & 0 & 0 & 1 \\ -i & 0 & 0 & 0 \\ 0 & 1 & 0 & 0 \end{bmatrix} \quad \eta_7(12)$$

$$\begin{bmatrix} 0 & 0 & 1 & 0 \\ 0 & 0 & 0 & i \\ 1 & 0 & 0 & 0 \\ 0 & -i & 0 & 0 \end{bmatrix} \quad \eta_8(15)$$

$$\begin{bmatrix} 0 & 0 & 0 & i \\ 0 & 0 & 1 & 0 \\ 0 & 1 & 0 & 0 \\ -i & 0 & 0 & 0 \end{bmatrix} \quad \eta_9(34)$$

$$\begin{bmatrix} 1 & 0 & 0 & 0 \\ 0 & -1 & 0 & 0 \\ 0 & 0 & 1 & 0 \\ 0 & 0 & 0 & -1 \end{bmatrix} \quad \eta_{10}(35)$$

$$\begin{bmatrix} 0 & -i & 0 & 0 \\ i & 0 & 0 & 0 \\ 0 & 0 & 0 & 1 \\ 0 & 0 & 1 & 0 \end{bmatrix} \quad \eta_{11}(23)$$

$$\begin{bmatrix} 0 & 0 & 0 & 1 \\ 0 & 0 & -i & 0 \\ 0 & i & 0 & 0 \\ 1 & 0 & 0 & 0 \end{bmatrix} \quad \eta_{12}(13)$$

$$\begin{bmatrix} 0 & 0 & -i & 0 \\ 0 & 0 & 0 & 1 \\ i & 0 & 0 & 0 \\ 0 & 1 & 0 & 0 \end{bmatrix} \quad \eta_{13}(45)$$

$$\begin{bmatrix} 0 & i & 0 & 0 \\ -i & 0 & 0 & 0 \\ 0 & 0 & 0 & 1 \\ 0 & 0 & 1 & 0 \end{bmatrix} \quad \eta_{14}(56)$$

$$\begin{bmatrix} 1 & 0 & 0 & 0 \\ 0 & -1 & 0 & 0 \\ 0 & 0 & -1 & 0 \\ 0 & 0 & 0 & 1 \end{bmatrix} \quad \eta_{15}(25)$$

FIGURE 26: η MATRICES

CHAPTER 6: TARGET DECOMPOSITION THEOREMS

6.1 The Target Coherency Matrix

In the last chapter we showed that the target vector $\hat{k}$ is a spinor in a six dimensional real space. In this chapter we will study the properties of the target spin matrix

$$[T_C] = \hat{k}.\hat{k}^{*T}$$

which is a 4 x 4 hermitian operator and transforms under a change of target base as

$$[T_C]' = [U_4][T_C][U_4]^{*T} \qquad - 6.1$$

Since $[U_4]$ is unitary and $[T_C]$ hermitian, a target base can always be found for which the target spin matrix is diagonal. We will see in the next section how this result may be used for the analysis of fluctuating targets but first we will examine more closely the properties of $[T_C]$ for single targets.

The simplest targets to consider initially are those represented by the set of all diagonal scattering matrices $[S_{AD}]$ (see equation 3.25). For these targets k may be written

$$\hat{k} = \begin{bmatrix} k_0 \\ k_1 \end{bmatrix} = \begin{bmatrix} m(1 + \tan^2 r \exp(-i2x)) \\ m(1 - \tan^2 r \exp(-i2x)) \end{bmatrix} \qquad -6.2$$

In this case the target spin matrix is analagous to [J], the wave coherency matrix and

$$[T_{C2}] = \begin{bmatrix} k_0 k_0^* & k_0 k_1^* \\ k_0^* k_1 & k_1 k_1^* \end{bmatrix} = \begin{bmatrix} p_0+p_1 & p_2-ip_3 \\ p_2+ip_3 & p_0-p_1 \end{bmatrix}$$

The change of target base is governed by SU(2) and so $\hat{k}$ is a spinor in 3-space and we can map the set of all diagonal targets onto the surface of a 3-sphere (see figure 27). The target 4-vector associated with the spinor $\hat{k}$ is given by $\underset{\sim}{p}$ where

$$p_0 = m^2(1 + \tan^4 r) \qquad - 6.3$$

$$p_1 = 2m^2 \tan^2 r \cos(2x) \qquad - 6.4$$

$$p_2 = m^2(1 - \tan^4 r) \qquad - 6.5$$

$$p_3 = 2m^2 \tan^2 r \sin(2x) \qquad - 6.6$$

From these equations we can see that all targets with a skip angle of 0° or 180° are mapped onto the equator with σ_0 and σ_1 antipodal. At 90° to the σ_0, σ_1 diameter are the two dipole targets with degenerate forks ($r = 0°$).

Moving off the equator, the loci of targets with $r = 45°$ lie along a great circle passing through the poles, σ_0 and σ_1. Note that the quarter wave plates lie at the north and south poles ie $r = 45°$ and $x = \pm 45°$. Finally, note that the upper and lower hemispheres map targets with opposite sign of skip angle (positive in the upper and negative in the lower).

It is most important to note that each point on this sphere corresponds to a <u>target</u>, not to a wave state, and so we can analyse changes in target parameters by plotting the motion of points over a sphere (see section 6.3).

Considering the more general class of symmetric matrices, $\hat{k}$ becomes a 3 element target vector ie.

$$\hat{k} = (k_0, k_1, k_2)^T$$

and the change of target base is governed by SU(3). In this case there is no homorphism with a rotation group and so k is <u>not</u> a spinor. As a result we cannot map these targets onto a real sphere. Nonetheless, we saw in chapter 3 that symmetric matrices

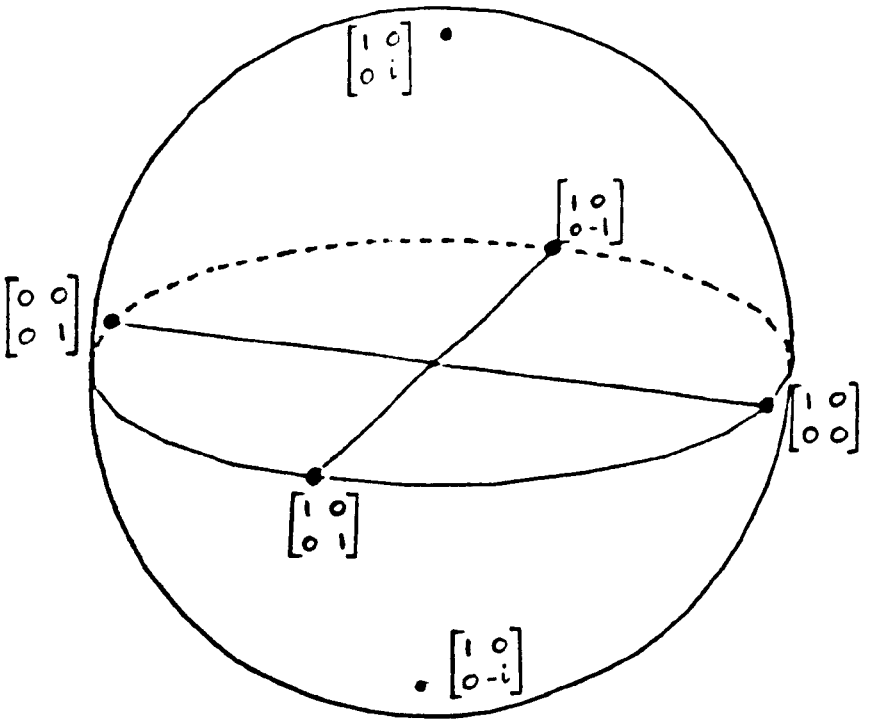

Target Stokes vector $\underline{p}$

$$p_0 = m^2(1+\tan^4\gamma)$$

$$p_1 = 2m^2\tan^2\gamma\cos 2\chi$$

$$p_2 = m^2(1-\tan^4\gamma)$$

$$p_3 = 2m^2\tan^2\gamma\sin 2\chi$$

FIG. 27: TARGET SPHERE

are of special interest in radar scattering because of the combined effects of the reciprocity theorem and the antenna coordinate system. Even though they have no homomorphism of their own, we can map them into the wave space through the multipoint representation known as the polarisation fork.

Finally, we will consider the most general class of targets where the scattering matrix has no specific form other than being 2 x 2 complex. In this case T_c is 4 x 4 hermitian and $\hat{k}$ is a spinor in 6-space. We will write T_c in the parametric form

$$[T_c] = \begin{bmatrix} A_0+A & C-iD & H+iG & I-iJ \\ C+iD & B_0+B & E+iF & K-iL \\ H-iG & E-iF & B_0-B & M+iN \\ I+iJ & K+iL & M-iN & A_0-A \end{bmatrix} \qquad - 6.7$$

This notation is a generalisation of that first introduced by Huynen (1971)(although he does not make explicit reference to the matrix T_c but rather to the Mueller matrix [M]).

We can see that T_c has potentially 16 degrees of freedom (the same as [M]) although for single targets there will be some constraint equations on the elements of T_c due to the fact that a target base exists for which

$$[T_{cb}] = \begin{bmatrix} 1 & 0 & 0 & 0 \\ 0 & 0 & 0 & 0 \\ 0 & 0 & 0 & 0 \\ 0 & 0 & 0 & 0 \end{bmatrix} \qquad - 6.8$$

where 1 is the target eigenvalue (given by the span of [S]) and the corresponding eigenvector is the target vector $\hat{k}$.

We may reexpress this constraint in the form that all minors of T_c must be zero. An n x n matrix has n^2 minors and so potentially $2n^2$ constraint equations. However, since T_c is hermitian, some constraints will be real ($^nC_2$ to be exact) while every complex constraint equation will be matched by its complex conjugate. This means that in all there are only n^2 constraints for an n x n hermitian matrix. We will see shortly that these equations match those mentioned in chapter 4 when discussing the conditions under which the target Mueller matrix represents a single target. However, before we find the connection between [M] and $[T_c]$, we will first examine some of the properties of the parametric elements A.....N.

These coefficients are of 2 types: the leading diagonal terms are positive real ie. A_0+A, A_0-A, B_0+B, B_0-B are all >= 0. Because of their special properties they are termed target generators and clearly represent the magnitudes of the target vector elements k_i. Thus, in the Pauli base they represent the magnitudes of target symmetry, antisymmetry and first and second quadrant irregularity.

The off diagonal terms may be positive or negative real and are called <u>coupling parameters</u> since they couple the symmetry properties of the 4 basis targets chosen for the expansion of [S]. They are controlled by their respective generators in the sense that if one generator is zero then all the coupling parameters in the appropriate row (column) are zero eg. if the target is symmetric $A_0 = A$ and I,J,K,L,M,N are all zero. We may summarise these relationships by drawing a target map (see figure 28). This summarises, in graphical form, the interrelation between the 16 phenomenological target parameters and may be used for the basis of a target classification scheme (see chapter 7 for examples).

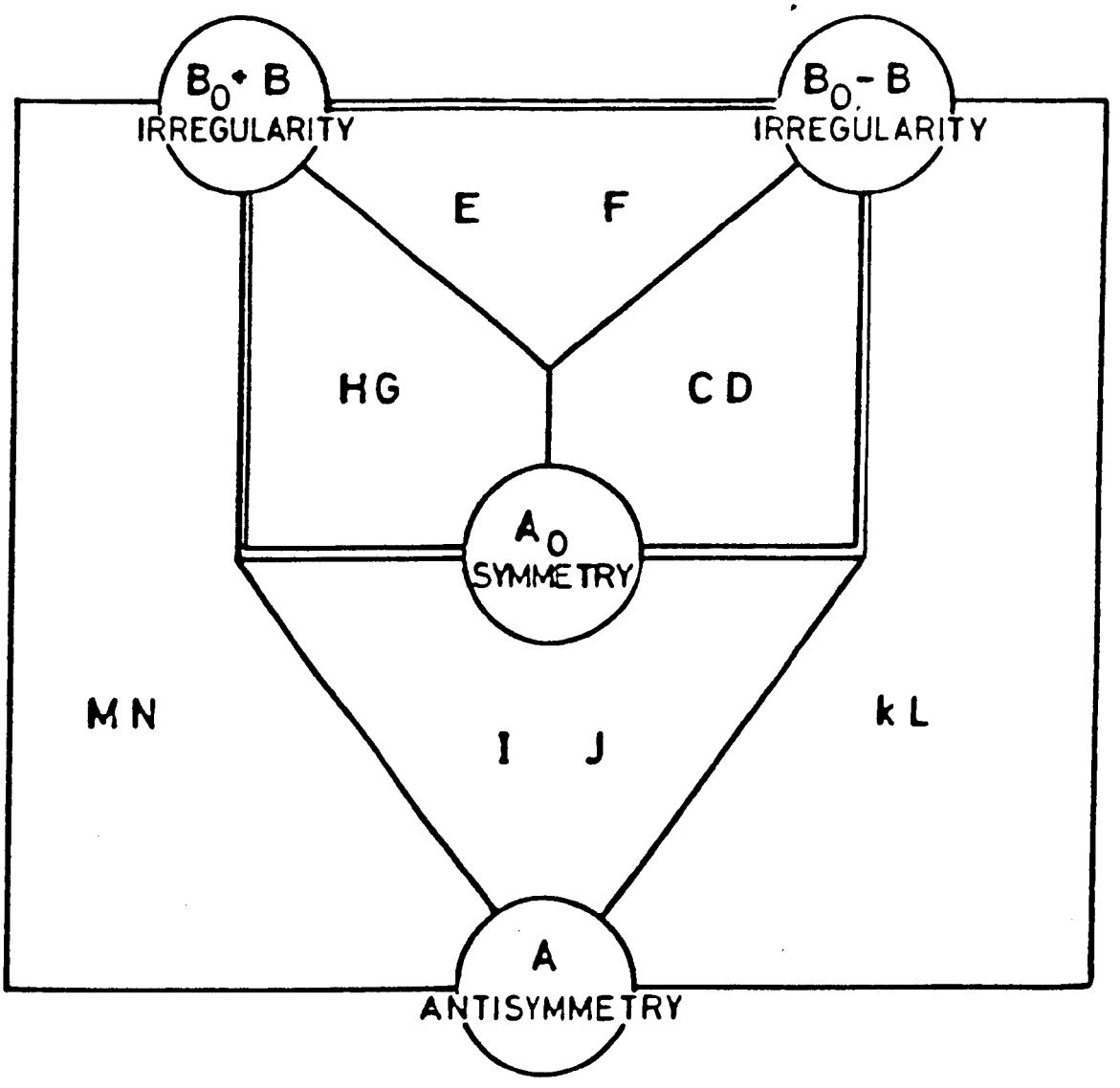

FIG.28 PHENOMENOLOGICAL TARGET PARAMETERS TARGET MAP

We now turn to the problem of relating $[T_c]$ to $[M]$. Clearly these two must be related because both derive from the scattering matrix $[S]$. We will find that the elements of $[M]$ are simply the expansion coefficients of $[T_c]$ in terms of η, the generators of $SU(4)$ and so, geometrically, the elements of the target Mueller matrix are just the set of invariants under plane rotations in a 6 dimensional real space.

To prove this result, we can relate $[M]$ to $[T_c]$ by using the results of Appendix 1 to derive the Mueller matrix in terms of $\hat{k}$ by writing $[S]$ in the parametric form

$$[S] = \begin{bmatrix} k_0+k_1 & k_2-ik_3 \\ k_2+ik_3 & k_0-k_1 \end{bmatrix} \qquad - 6.9$$

After a lengthy but straightforward calculation we can write $[M]$ in terms of the 16 target parameters as

$$[M] = \begin{bmatrix} A_0+B_0 & C+N & H+L & F+I \\ C-N & A+B & E+J & G+K \\ H-L & E-J & A-B & D+M \\ I-F & K-G & M-D & A_0-B_0 \end{bmatrix} \qquad - 6.10$$

Note that $[M]$ is expressed in the conventional coordinates: in the antenna system the fourth row is multiplied by -1.

We can then prove that (see Appendix 4)

$$m_{ij} = \frac{1}{2} \mathrm{Tr}([T_c]\eta_{4i+j}) \qquad - 6.11$$

and hence the result that m_{ij} represent invariants under plane rotations in 6-space. This result is particularly gratifying because of the similarity with the derivation of the Stokes

vector from the wave coherency matrix. Note however that the m_{ij} are not the coordinates of a point in 6-space but rather are related to rotations in 6 dimensions.

6.2 Partial Targets

So far we have considered only single targets ie. those where the elements of [S] are constant. More generally, targets are viewed in a dynamic environment and the elements of the scattering matrix are functions of time and/or position. Such targets will be called partial in direct analogy with the definition of partially polarised waves in chapter 2. Clearly, such targets cannot be represented by a single spinor k and it is the purpose of this section to discuss methods by which these dynamic targets can be included in the spinor formalism of chapter 5.

One approach is to measure the elements of [S] in real time and calculate all the auto and cross correlation functions to characterise the statistics of the fluctuating target. This method may not always be possible: [S] requires a coherent reciever and must be measured on a time or frequency multiplex basis (see chapter 7). Even so, this technique still begs the question: how do we analyse the data so as to extract the important target information and how is this data to be interpreted in the light of the spinor geometry of chapter 5?

We might suggest tracking the loci of null states on the Poincare sphere. Although this can be useful for some applications (such as rain clutter suppression, see Poelman 1983) it becomes very difficult to simultaneously track all the null states (particularly for nonsymmetric matrices) and in particular, it is difficult to assess the cross correlation properties and so detect the presence or otherwise of a dominant

target. This is due to the fact that the scattering matrix has a multipoint representation on the Poincaré sphere. What we need is a single point representation and, as we saw in chapter 5, we can find such a mapping by using the SU(4)-O_6^+ homomorphism. According to this mapping, we represent the target at a given instant as a point on the surface of a 6 dimensional sphere: as time progresses the point moves over the surface, tracing out some locus (which may or may not cover the whole sphere) and resulting in a partial target. However, the advantage of this model is that by using it, we can easily spot the presence of a dominant single target and can even define a formal measure of the statistical disorder of the process by defining the target entropy.

To measure this entropy and assess the correlation properties, we need only form the average Mueller matrix $\langle[M]\rangle$, from which we can calculate $\langle[T_c]\rangle$. It is the latter coherency matrix, being related to the target spinor $\hat{k}$, which provides the basis for our analysis (see chapter 7 for details of the measurement of [M] and $[T_c]$).

To demonstrate the method, we will consider the simple case of a target composed of 2 independent scatterers, each represented by a spinor $\hat{k}$ (see figure 29). The whole target is contained within the coherence volume of some source, the resultant field at the receiver then being given by the coherent sum of the elementary signals from 1 and 2. We can express this result, including polarisation, by writing the resultant target spinor $\hat{k}$ as

$$\hat{k} = \hat{k}_1 + \hat{k}_2 = \hat{k}_1 + \exp(i\phi)\hat{k}_2 \qquad - 6.13$$

where the phase angle ϕ represents the wavelength and spatial

variation through the usual factor

$$\phi = 4.\pi.d.\sin(\theta)/\lambda$$

Clearly, unless $\hat{k}_1$ and $\hat{k}_2$ have the same null states, the resultant fork will be different from that of either $\hat{k}_1$ or $\hat{k}_2$ and will not, in general, be simply related to them. Further, as d, λ or θ change, $\hat{k}$ will change and the target become partial. We can express the instantaneous coherency matrix as

$$\begin{aligned} T_c &= \hat{k}\hat{k}^{*T} \\ &= \hat{k}_1\hat{k}_1^{*T} + \hat{k}_2\hat{k}_2^{*T} + \hat{k}_1\hat{k}_2^{*T} + \hat{k}_2\hat{k}_1^{*T} \\ &= T_{c1} + T_{c2} + T_{c12} + T_{c21} \end{aligned}$$

where T_{c12} is described as a cross coherency matrix which may not itself be hermitian (of course, the sum $T_{c12} + T_{c21}$ will always be hermitian). For a partial target we can form

$$\langle T_c \rangle = T_{c1} + T_{c2} + \langle T_{c12} + T_{c21} \rangle$$

where we have assumed the component spinors $\hat{k}_1$ and $\hat{k}_2$ are constant (note that this may not be true if, for example, we use a broadband source). The time variation of $\hat{k}$ is then caused by interference effects related to the spatial separation of scatterers and so we can easily extend the above formulation to a collection of N different targets contained within the coherence volume of some source to produce

$$\langle T_c \rangle = \sum_{i=1}^{N} T_{ci} + \langle \sum_{j>i}^{N} \sum_{i=1}^{N} (T_{cij} + T_{cji}) \cos(\alpha_i - \alpha_j) \rangle \qquad - 6.14$$

This expression becomes a lot simpler if we can assume the phase

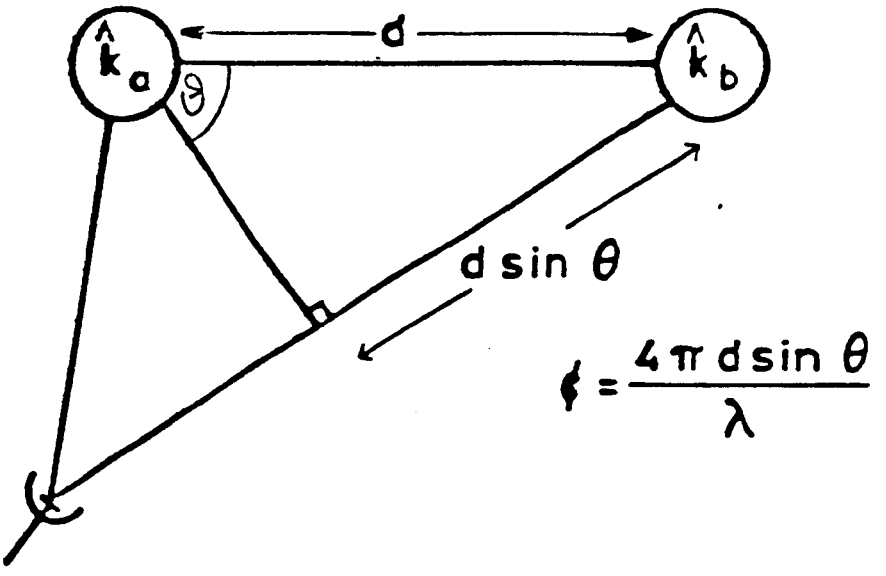

$$\hat{k} = \hat{k}_a + \hat{k}_b = \hat{k}_a + e^{i\phi}\hat{k}_b$$

$$T_C = \hat{k}.\hat{k}^\dagger = \hat{k}_a\hat{k}_a^\dagger + \hat{k}_b\hat{k}_b^\dagger + (\hat{k}_a\hat{k}_b^\dagger e^{-i\phi} + \hat{k}_b\hat{k}_a^\dagger e^{i\phi})$$

For N Scattering Centres

$$T_C = \sum_{i=1}^{N} T_{Ci} + \sum_{j>i}^{N}\sum_{i=1}^{N} (\hat{k}_i\hat{k}_j^\dagger + \hat{k}_j\hat{k}_i^\dagger)\cos(\alpha_i - \alpha_j)$$

Where α_i = Phase of the ith Scattering Centre and $\alpha_1 = 0$

FIG. 29 MODEL FOR COMPOSITE TARGET

angle $\alpha_i - \alpha_j$ to be uniformly random over the interval 0 to 2π, in which case the cross coherency matrices can be ignored and T_c is formed by simply adding the component coherency matrices. This result has important consequences for the analysis of the scattering from clouds of dissimilar particles (see Chapter 7). Note that this decorrelation of scatterers may be caused either by having large N or by intentionally varying λ (or θ) so as to cause the phase angle to average to zero.

In general however, for monochromatic illumination of a target where N is small, the cross terms in 6.14 will be important and the final matrix will bear no simple relationship to the properties of the elementary scatterers.

As a second example of composite target formation, we will consider the case of multiple scattering where the incident wave interacts first with a single target (with spinor $\hat{k}_1$) and then with a second ($\hat{k}_2$), before being detected by a receiver. In the scattering matrix formulation the resultant matrix is simply the product of the composite target matrices (see Jones 1941). We wish to describe this process in terms of the target spinors $\hat{k}_1$ and $\hat{k}_2$.

Unfortunately, we cannot simply form the inner product of the component spinors because matrix multiplication does not map into an inner product in spinor space. Instead, we have to employ a set of 4 matrix operators

$$\Gamma = (\eta_0, \eta_1, \eta_2, \eta_3)$$

where the η matrices are 4 of the SU(4) generators considered earlier (see figure 26). With these defined we can obtain the resultant spinor $\hat{k}$ from the composite spinors $\hat{k}_1$ and $\hat{k}_2$ as

$$\hat{k} = \hat{k}_2^{T} \Gamma \hat{k}_1 \qquad - 6.15$$

so that the ith element of the spinor $\hat{k}$ is given by

$$k_i = \hat{k}_2 . \eta_i \hat{k}_1$$

As an example, consider again the conditions outlined in section 3.2 for the scattering matrix [S] to be diagonalised by a similarity transformation $[Q][S][Q]^{*T}$. We found that in the conventional coordinates this required

$$[S][S]^{*T} = [S]^{*T}[S]$$

We can now use 6.15 to calculate the general form of [S] under this constraint. We begin by noting that if [S] is equivalent to $\hat{k} = (k_0, k_1, k_2, k_3)$ then $[S]^{*T}$ has the target spinor $\hat{k}^*$, $[S]^T$ the spinor $\hat{k}_T = (k_0, k_1, k_2, -k_3)$ and $[S]^*$ the spinor $\hat{k}_T^*$. By using equation 6.15 we can then show that for $[S][S]^{*T} = [S]^{*T}[S]$, the spinor $\hat{k}$ must be constrained such that $\phi_1 = \phi_2 = \phi_3$ ie. that the phases of the spinor elements k_1, k_2 and k_3 are equal. Similarly, we can show that in the antenna coordinates where we require $[S][S]^{*T} = [S]^T[S]^*$, the constraint on $\hat{k}$ is that $k_3 = 0$ or [S] is symmetric.

The extension of 6.15 to higher order multiple scattering is obvious ie.

$$k = k_n^{T} \Gamma k_{n-1}^{T} \Gamma \ldots\ldots \Gamma k_1 \qquad - 6.16$$

Note that the first element of $\hat{k}$ is always given by the hermitian product of the composite target spinors. Hence, if multiple scattering occurs between orthogonal targets then

$\hat{k}_1^{*T}.\hat{k}_2 = 0$, and $k_0 = 0$. In the Pauli target base this may be interpreted as a lack of target symmetry (ie. $S_{xx} = -S_{yy}$).

We can now derive the elements of the resultant coherency matrix as

$$[T_c]_{ij} = \hat{k}_2^T \eta_i \hat{k}_1 (\hat{k}_2^T \eta_j \hat{k}_1)^{*T}$$

and using the fact that hermitian matrices commute, we can express this as

$$[T_c]_{ij} = k_2^T \eta_i \eta_j T_{c1} \hat{k}_2^* \qquad - 6.17$$

where $i,j = 0,1,2,3$ and T_{c1} is the coherency matrix for the first target. This calculation requires knowledge of the commutation properties of $\underline{\eta}$ which we can easily show are

$$[\eta_i, \eta_j] = -2i \varepsilon_{ijk} \eta_k \qquad - 6.18$$

where ε_{ijk} is the permutation symbol ie. +1 for even permutations of 1,2,3 and -1 for odd permutations (an odd number of simple transpositions yields an odd permutation).

In summary, we have seen that the treatment of multicomponent targets is relatively simple using the spinor formalism (especially if we can assume decorrelation) whereas the treatment of multiple scattering is more complicated and requires the use of 4 of the generators of SU(4).

6.3 Target Decomposition Theorems

In chapter 4 we discussed the use of wave decomposition theorems for the representation of partial wave states. We saw that there were two different approaches: the first, to represent the wave

as the noncoherent sum of two pure states while the second involved representing the wave as the sum of a single pure state plus noise (in the form of a randomly polarised component). Both were based on the representation of partial states by a coherency matrix, [J].

In the last section we saw that a partial target may also be represented by a coherency matrix (although 4 x 4 instead of 2 x 2) and consequently, we now seek a set of decomposition theorems, analagous to those developed for the wave states, enabling us to represent a partial target by the sum of one or more statistically independent components. In particular, we wish to discover whether or not there is a target dichotomy.

We will find that there is only one unique decomposition, based on the eigenvectors of $[T_c]$, while there are an infinite number of single target plus noise models. Consequently, there is no target dichotomy (a point which Huynen (1971) failed to realise) and so only one decomposition theorem for partial targets.

Decompositions rely on the statistical significance of diagonal coherency matrices: the absence of off diagonal terms indicating statistical independence between component spinors. In practice we usually begin by using the Pauli reference base, which leads to a diagonal $[T_c]$ only under fortuitous circumstances. However, having measured (or calculated) $[T_c]$ using the Pauli targets, we can change the target base by using a unitary matrix U_c. In particular, we can always find a base which diagonalises $[T_c]$ since the latter is always Hermitian. It is this result which leads to the following decomposition theorems:

1)The 4 target theorem

This is analagous to the 2 state model for waves in that we express the target coherency matrix as the noncoherent sum of 4 statistically independent single targets by performing an eigenvector analysis of $[T_c]$ (note that this decomposition is difficult to derive when using the Mueller matrix formalism). Hence

$$T_c = \sum_{i=1}^{4} a_i T_i \qquad - 6.19$$

The eigenvectors of T_c form a set of normalised orthogonal single targets (T_1 to T_4) while the eigenvalues, a represent their statistical weights.

If T_c represents a single target then its minors are all zero or, equivalently, it has only 1 nonzero eigenvalue. At the other extreme, all 4 eigenvalues are equal, all minors are equal and the target is random ie. there is no correlation in the fluctuations of the elements of [S]. Between these two extremes lies the set of partial targets for which, as a measure of their statistical disorder, we define the target entropy from the eigenvalues of T_c as

$$H_T = -\sum_{i=1}^{4} P_i \log_4 P_i \qquad - 6.20$$

where

$$P_i = a_i / \sum_{j=1}^{4} a_j$$

If T_c has only one nonzero eigenvalue then $H_T = 0$. while if $P = 0.25$ ie. a random target, then $H_T = 1$.

We may interpret the quantities P_i as the probabilities that, on making an instantaneous measurement of the target scattering matrix [S], the result will be the ith eigenvector of

T_c. This result has many important consequences for the measurement and analysis of target data (see chapter 7).

The fact that T_c must have positive eigenvalues imposes certain constraints on the minors of T_c and hence on the elements of the corresponding Mueller matrix. In particular, we note that not every combination of 16 real numbers represents a target Mueller matrix because some combinations lead to negativ eigenvalues for T_c. In order to examine these constraints more closely, we define a 4 x 4 matrix of minors [X], the ijth element of which is the minor obtained by deleting the ith row and jth column of T_c. The condition for singularity then becomes

$$[X] = 0$$

while for a partial target

$$[X] >= 0$$

Note that [X] is 4 x 4 hermitian and so potentially provides 16 constraint equations. However, not all of these are independent For example, single targets have 7 degrees of freedom and so only 9 of the 16 constraints provided by [X] can be independent For symmetric scattering matrices, [X] is 3 x 3 hermitian and yields 9 constraints but again, for single targets, only 4 are independent, leaving $[T_c]$ with the 5 degrees of freedom from [S]. Nonetheless, the matrix [X] may be used as an indicator of the number of independent single targets required to represent matrix: if [X] = 0 then the target is singular, otherwise it is partial.

We may summarise these constraints by saying that the target coherency matrix $[T_c]$ must be positive definite and only

those 4 x 4 real matrices which satisfy this constraint may be described as Mueller matrices. To test for this, we form $[T_c]$ from [M] and then calculate [X]: if any elements (real or imaginary) of [X] are negative then the original real matrix is not a Mueller matrix. If they are zero then the original matrix corresponds to a single target and if positive, to a partial target. This procedure is equivalent to that outlined in chapter 4 (equation 4.24) but is easier to implement, being based on the hermitian coherency matrix rather than [M]. Huynen (1971) derives explicit forms of these equations for symmetric matrices but does not use the coherency matrix formulation.

Note that the decomposition of T_c into one or more single targets will not, in general, yield the real targets physically comprising the object under investigation. Rather the latter are "blended" to produce a set of 4 orthogonal target components. Thus, while we may resolve T_c, we may not attach any physical existence to the composite targets: there will be many different real targets which give the same partial target.

In summary, we have a unique decomposition theorem for modelling any dynamic scattering problem by four independent single targets occurring with known probabilities: the most probable target being the one corresponding to the largest eigenvalue of T_c. This decomposition is analagous to the pure state decomposition of [J], and it is interesting to speculate on the existence of a second decomposition of T_c into 2 components; one which satisfies [X] = 0 and so is a single target and the other, a remainder or "noise" matrix which must be positive definite hermitian.

2)<u>The Single Target Plus Noise Model</u>

In this decomposition we attempt to identify the presence of a

single underlying matrix [S], with all fluctuations being ascribed to a "noise" term. In terms of T_c, we wish to write

$$T_c = T_{cs} + T_{cn}$$

where T_{cs} has an equivalent single target (ie [X] = O) and T_{cn} is positive definite hermitian. This model corresponds to the decomposition of a partially polarised wave into the noncoherent sum of a pure state plus randomly polarised component.

We will show that the above decomposition is possible but <u>not</u> unique ie. there are an infinite number of ways of satisfying the required constraints. This means that there is no physical basis for adopting this decomposition and therefore the only unique and consistent model for targets is that based on the eigenvectors of T_c.

We begin by examining the degrees of freedom in each of the terms of 6.19. On the left hand side, T_c must be positive definite hermitian and so has 16 degrees of freedom (satisfying [X] > O). These must be matched on the right hand side: T_{cs} has 7 degrees of freedom since it must satisfy [X] = O to be a single target. This leaves 9 degrees of freedom for T_{cn}, a positive definite hermitian matrix with potentially 16 degrees of freedom. Clearly, we can satisfy these constraints in an infinite number of ways ie. there are an infinite number of matrices T_{cn} satisfying 6.19 because the noise matrix has only to be positive definite hermitian.

As an example, let us consider Huynen's theorem (1971) which is applicable only to symmetric matrices ie. T_c is 3 x 3. He expressed the coherency matrix in the form

$$\begin{bmatrix} 2A_0 & C-iD & H+iG \\ C+iD & B_0+B-w_1 & E+iF-w_2 \\ H-iG & E-iF-w_2^* & B_0-B-w_3 \end{bmatrix} + \begin{bmatrix} 0 & 0 & 0 \\ 0 & w_1 & w_2 \\ 0 & w_2^* & w \end{bmatrix}$$

where w_1 and w_3 are real and w_2 is complex (giving the noise matri 4 degrees of freedom and the single target, 5). Huynen calls this noise term a canonical N-target (standing for nonsymmetrical noise) and we can see that it certainly has zero target symmetry ($A_0 = 0$). To call it a "noise" target however is a bit of a misnomer; an example of such a target being the dihedral reflector (σ_1). Huynen argues that this decomposition is unique and so is a valid target model. By using the coherency matrix formalism however, we can see that he has chosen only one special case: for example, we could choose to set $B_0 = B$ in the noise matrix and then the decomposition becomes

$$\begin{bmatrix} 2A_0-w_1 & C-iD-w_2 & H+iG \\ C+iD-w_2^* & B_0+B-w_3 & E+iF \\ H-iG & E-iF & B_0-B \end{bmatrix} + \begin{bmatrix} w_1 & w_2 & 0 \\ w_2^* & w_3 & 0 \\ 0 & 0 & 0 \end{bmatrix}$$

which represents a different but equally valid decomposition. Again the noise term has the form of a "canonical target" but we could postulate an infinite number of noncanonical forms by letting T_{cn}have a more general form ie. 4 x 4 hermitian with nonzero diagonal terms but still only 9 degrees of freedom.

We conclude that this decomposition must be rejected as a useful target model on the grounds that it is not unique and so the only valid decomposition theorem for targets is the eigenvector decomposition of T_c.

CHAPTER 7: EXPERIMENTAL POLARIMETRY

7.1 Measurement of Pure and Partial Wave States

In this section we will discuss practical methods for the measurement of both pure and partial wave states and describe the main features of an experimental system used by the author for the verification of some of the key theoretical results outlined in chapters 2 to 6.

Pure states can be measured in many different ways, the most common techniques being two channel coherent detection and null polarimetry.

The measurement of the wave spinor $\underline{E}$ calls for the reception of two orthogonal components (eg. horizontal and vertical linear or left and right circular). By measuring the amplitudes and phases (relative to some common coherent source) of the signals in each of these two channels, both E_1 and E_2 may be determined. However, because this technique requires coherent detection it is limited by cost and technical feasibility, especially at high radar frequencies and in optics. In the latter case, polarimetry is a well developed science with pure state measurement based almost exclusively on nulling techniques.

In null polarimetry, elliptical wave states are first converted to linear polarisation by using a rotatable compensator (which in many instances is just a quarter wave plate). When followed by linear polaroid, a null signal can then always be obtained for arbitrary elliptical incident state. The only restriction is that θ and τ stay constant during the measurement period. The attractive feature of this technique is that no calibration of the detector is required because only null signals are to be detected.

Null polarimetry suffers from 2 main drawbacks: firstly,

for multiple measurements the nulling procedure becomes tedious and is not easily automated. Secondly, when dynamic events are to be analysed, θ and τ change with time and the need to rotate devices to measure the wave state becomes too restrictive.

Because of the drawbacks of both coherent 2 channel and null polarimetry, an alternative measurement technique was sought for use in this thesis. The requirements are for a system which may be easily automated and capable of (near) instantaneous measurement of the wave state. With these in mind a parallel processor was designed for instantaneous measurement of the wave Stokes vector. Like null polarimetry, this technique is based on intensity measurements and so coherent detection is not required. Unlike null polarimetry however, it is capable of (near) instantaneous measurement of θ and τ and is easily interfaced to a microcomputer for automation and analysis.

A block diagram of the Stokes receiver is shown in figure 30. The wave is first split into four parallel channels by passing it through a diffraction grating (300 lines/mm). The signals then pass through four filters matched to the following wave states: horizontal, vertical, +45° linear and circular. By solving the resultant set of four linear equations in four unknowns, the Stokes vector of the incident wave can be measured. The detection was performed by an array of four photodiodes interfaced to a BBC microcomputer via a lock in amplifier (LIA) and integrating ADC. Since only one LIA was available, the outputs from the array where multiplexed into the receiver under program control.

Because the system relies on <u>relative</u> intensity measurements, a calibration procedure is required. This involves transmitting 2 known wave states (h and +45°) through the receiver and matching the signal amplitudes in each channel.

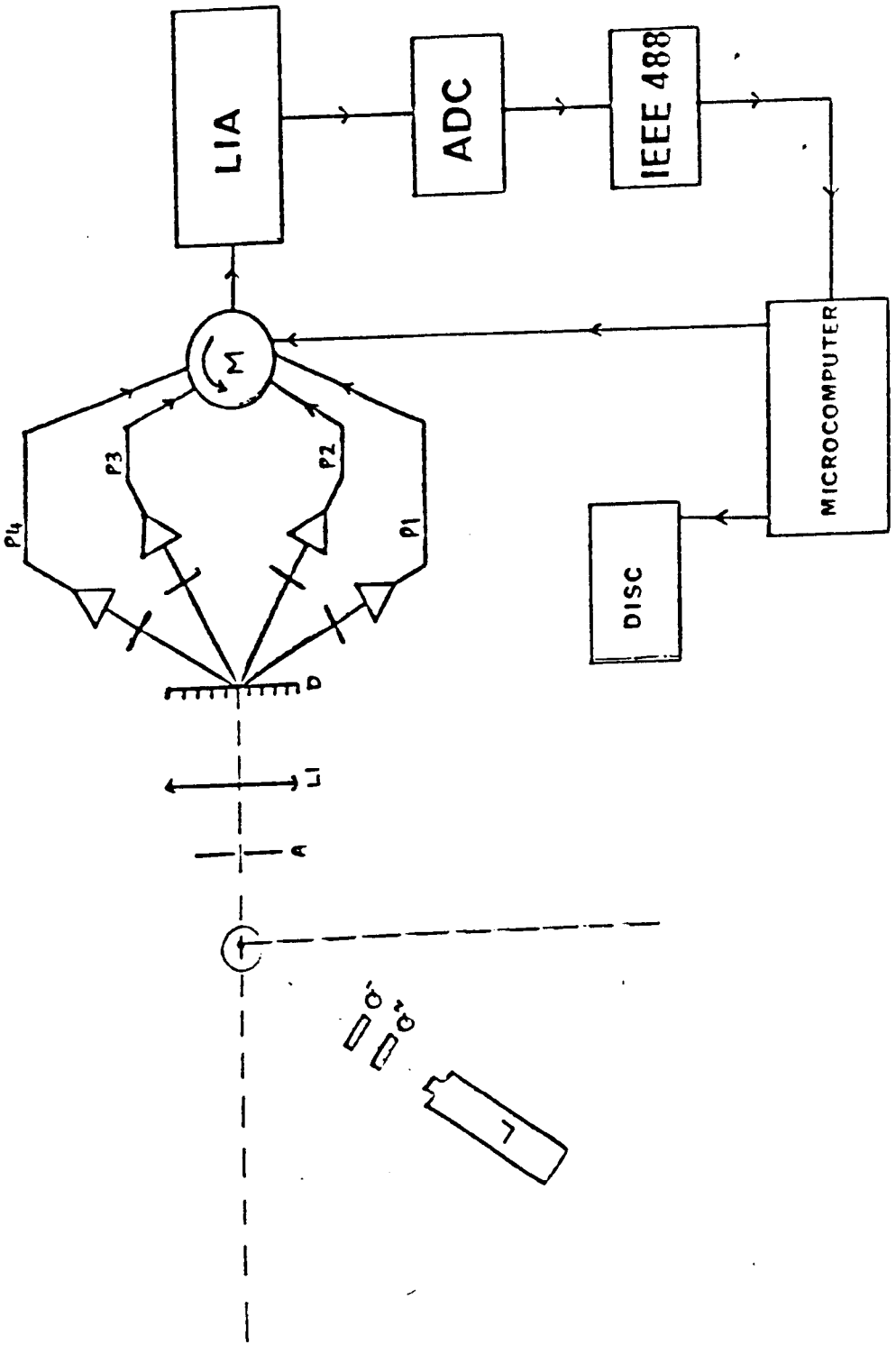

FIGURE 30: OPTICAL POLARIMETER

The transmitter consists of a linearly polarised HeNe laser (λ=632.8nm) with a pair of quartz retardation plates, the first of which is a half wave plate with nominal transmission matrix

$$[S] = \begin{bmatrix} 1 & 0 \\ 0 & -1 \end{bmatrix}$$

Figure 31 shows the locus of available polarisation states on an orthographic projection of the Poincaré sphere for rotations of this plate from 0 to 90° with a linearly polarised input. Note that this plate allows movement around the equator of the sphere and hence the generation of arbitrary linear polarisation. The second plate is a quarter wave retarder with matrix

$$[S] = \begin{bmatrix} 1 & 0 \\ 0 & i \end{bmatrix}$$

For linear horizontal input this plate allows generation of all those states shown in figure 32 (note that at $\pm$45° rotation , left and right circular are available). By cascading both plates we can obtain any state on the Poincaré sphere.

The receiver was constructed from 3 appropriately cut pieces of HN22 linear sheet polaroid, the fourth channel containing a piece of circular polaroid. The dynamic range of the receiver was approximately 32dB and a typical time series output for an incident h wave is shown in figure 33. Each measurement of wave state requires a cycle of 4 intensity measurements from the multiplexer. The latter was limited to a maximum rate of 1Khz so yielding a maximum Stokes measurement rate of 250Hz. For pure state measurement a slower rate of 4Hz

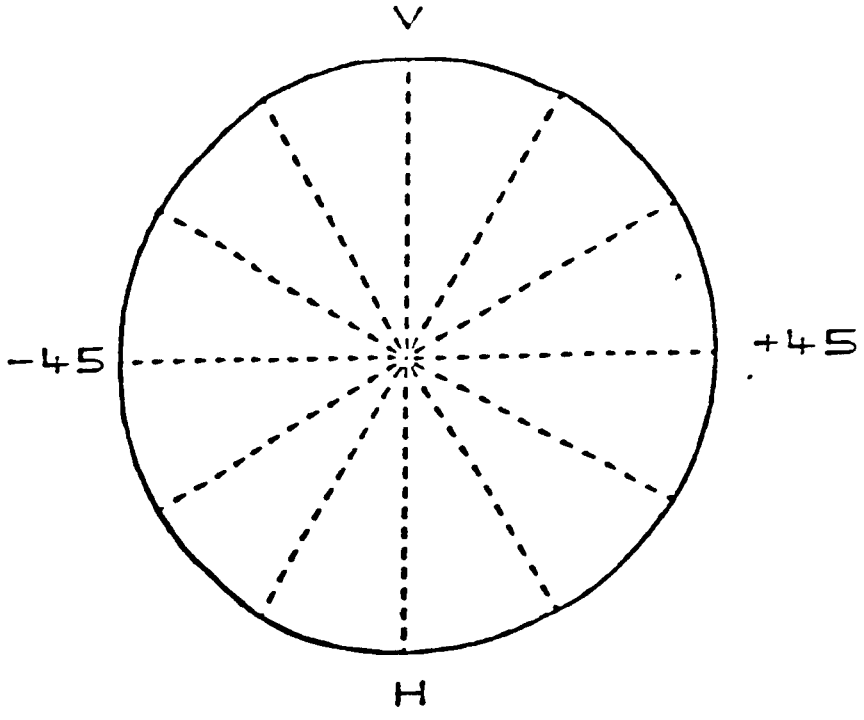

FIGURE 31: LOCUS FOR ROTATION OF HALF WAVE PLATE

FIGURE 32: LOCUS FOR ROTATION OF QUARTER WAVE PLATE

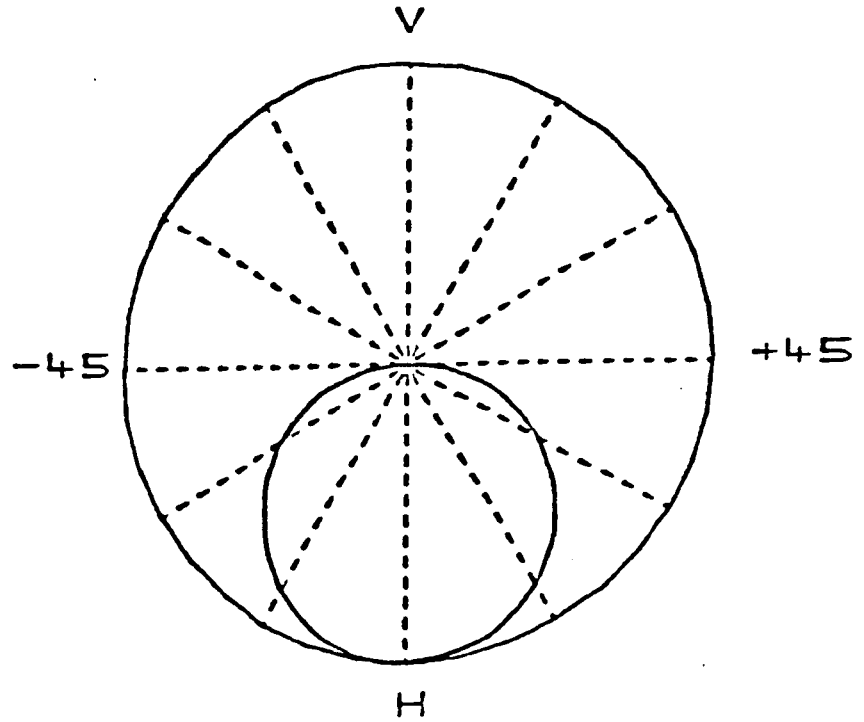

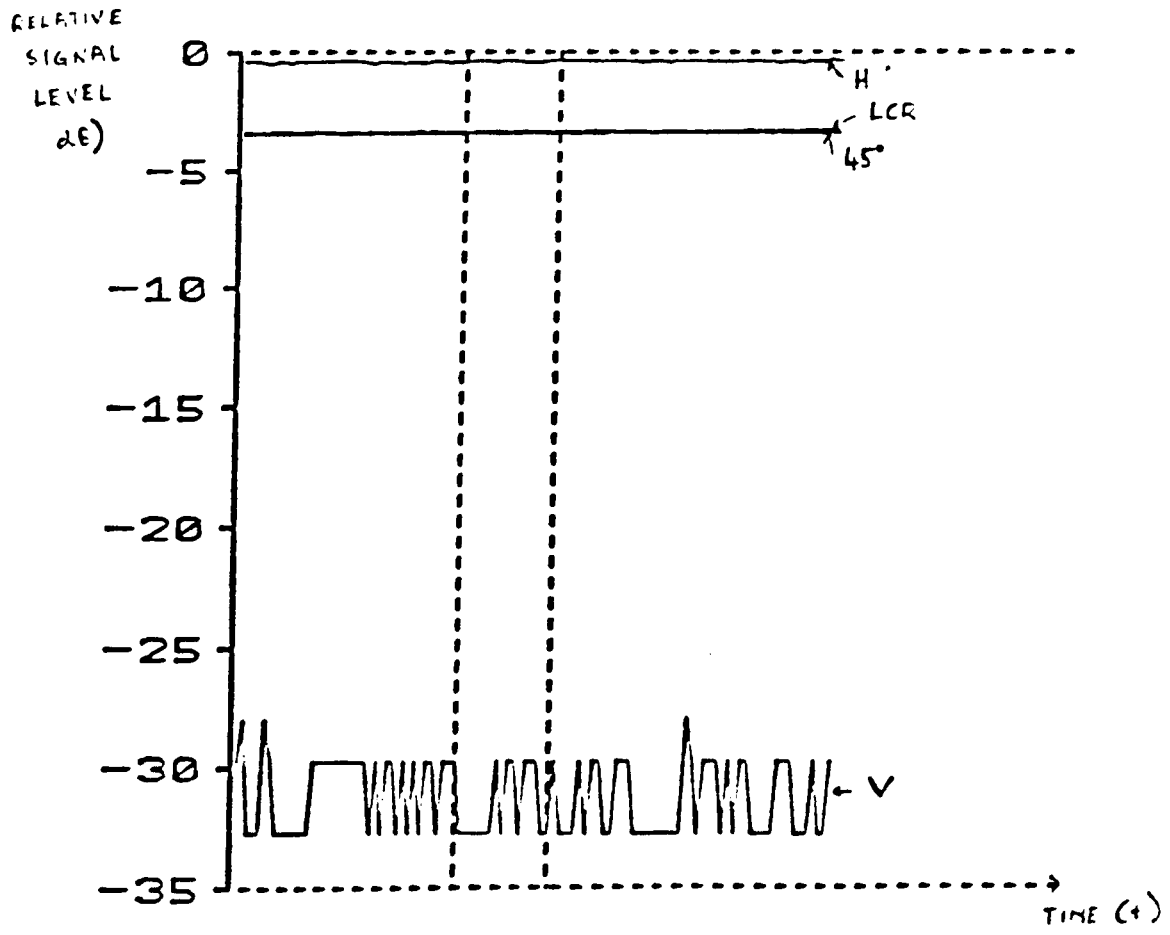

FIGURE 33: OUTPUT FROM PHOTODIODES

(1Hz Stokes measurement) was used with a mixture of analogue and digital integration in the LIA to improve the signal to noise ratio.

The receiver was fixed in position but the transmitter could be rotated to obtain bistatic scattering angles ranging from 0° (forward scatter) to ±90°. Note that it is not possible to measure backscatter with this system, mainly because it is CW and isolation of transmitter and receiver is difficult (note that the use of beamsplitting mirrors is to be avoided because they cause polarisation transformations which distort the target information and have to be calibrated using a more elaborate procedure than that described above). Given this limitation, the system was used for the measurement of pure states and for the determination of the scattering matrix of several test targets formed from combinations of retardation plates and polaroid. Results from this system will be discussed in the next section.

One key advantage of interfacing the receiver to a computer is that we can use it as an adaptive polarisation filter ie. we can measure the wave Stokes vector and form its inner product with a chosen test vector whose form we can change at will. The result of this product is then the same as passing the light through a single filter matched to the test state and so the system represents a piece of "programmable polaroid". This feature is useful for validating the calculated null states of test targets.

7.2 Measurement of Single and Partial Targets

In the last section we discussed details of a coherent optical system designed for the generation and measurement of wave states covering the whole Poincaré sphere. In this section we describe the use of such a system for measurement of the target

scattering matrix via the Mueller and coherency matrix formulations.

Since the system measures the Stokes vector of incident waves, it is natural to begin by forming the Stokes reflection or Mueller matrix [M]. This can be obtained by sequentially transmitting 4 wave states and measuring the Stokes vector of the scattered light. This yields 16 equations in 16 unknowns (the elements of [M]), which can be solved by the usual techniques (Gaussian elimination with pivotal condensation was used in this project). However, care has to be taken over the choice of incident wave states to ensure that all equations are independent. The set of states chosen were nominally h, v, +45° and left circular although, in practice, the wave states are first measured without the target in position for calibration purposes (this is necessary because the quartz plates are not perfect: their fast and slow axes are well aligned, yielding low crosspolar terms, but the phase difference between orthogonal components is not exactly 90° or 180°). Having measured the four"probe" states, the target was inserted and the measurements repeated. The resulting data was then used to solve for the elements of [M].

The next stage is to calculate $[T_c]$ from the Mueller matrix. This can be done using the results of 6.1 and yields a 4 x 4 hermitian matrix. For the extraction of [S], we need to find the eigenvectors of $[T_c]$. Since we expect one dominant eigenvalue for single targets, we could use routines for finding only the maximum eigenvector but, since $[T_c]$ is only 4 x 4, a routine was used (Jacobi iteration) which calculates all eigenvectors and eigenvalues of the coherency matrix.

As a result, an eigenvalue spectrum is obtained which can be used for the calculation of target entropy and for the

identification of the "optimum" single target. Knowing [S], we can then perform a singular value decomposition to find the null states. These null states can then be programmed into the adaptive filter and the transmitter adjusted to obtain a null result. According to the theory of chapter 3, the null states should form 2 orthogonal pairs.

To illustrate the measurement and analysis procedure, we will consider results for the following 3 test targets:

1) Free space

2) A mica half wave plate ($\lambda/2$ at 560nm $\pm$ 40nm)

3) A mica quarter wave plate ($\lambda/4$ at 560nm $\pm$ 80nm)

1) In the first instance, measurements were carried out without a target in position so as to measure the matrix for free space propagation. The measured Mueller matrix was

$$[M] = \begin{bmatrix} 1.000 & 0.000 & 0.000 & 0.000 \\ 0.000 & 1.000 & 0.000 & 0.016 \\ 0.010 & 0.011 & 0.990 & 0.008 \\ -0.005 & -0.003 & -0.003 & 1.006 \end{bmatrix} \qquad - 7.1$$

which corresponds to a coherency matrix

$$[T_c] = \begin{bmatrix} 1998[0^\circ] & 5[269^\circ] & 11[61^\circ] & 6[-244^\circ] \\ 5[-269^\circ] & 2[0^\circ] & 6[27^\circ] & 8[38^\circ] \\ 11[-61^\circ] & 6[-27^\circ] & -8[0^\circ] & 2[1^\circ] \\ 6[244^\circ] & 8[-38^\circ] & 2[-1^\circ] & 8[0^\circ] \end{bmatrix} \qquad - 7.2$$

where all magnitudes are x 10^{-3} and we have written complex components in the form amplitude[phase]. Figure 34 shows the calculated eigenvalue spectrum for $[T_c]$. The spectrum is

FIGURE 34: FREE SPACE

1.0 EIGENVALUE = -21.2 dB
2.0 EIGENVALUE = -22.6 dB
3.0 EIGENVALUE = -29.6 dB

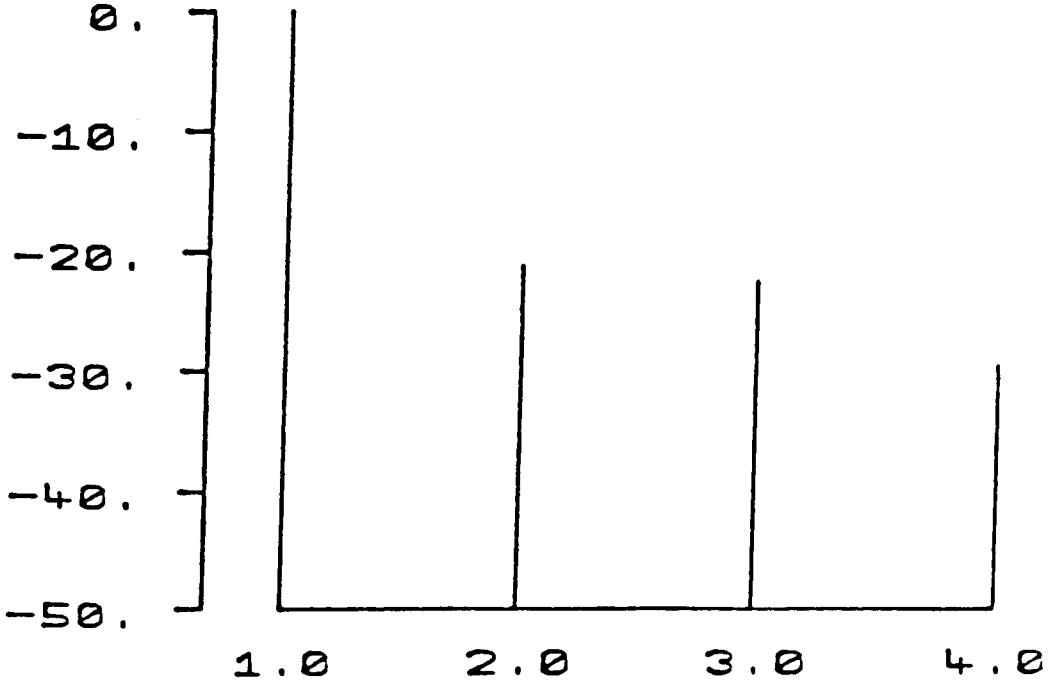

normalised to the maximum eigenvalue and plotted on a logarithmic scale. We can immediately see the presence of a dominant eigenvalue, corresponding to a dominant scattering matrix [S] specified by the eigenvector

$$k = \begin{bmatrix} 1.000[0^\circ] \\ 0.003[90^\circ] \\ 0.005[-62^\circ] \\ 0.003[-116^\circ] \end{bmatrix} \qquad - 7.3$$

This vector corresponds to a scattering matrix

$$[S] = \begin{bmatrix} 1.000[0^\circ] & 0.008[-49^\circ] \\ 0.004[-92^\circ] & 1.000[0^\circ] \end{bmatrix} \qquad - 7.4$$

which closely corresponds to that for free space.

Having established the procedure we now turn our attention to measurement of the scattering matrix for transmission through some simple optical elements.

2) Shown in figure 35 is the eigenvalue spectrum for a mica half wave plate. Note that the entropy is finite despite the singular nature of the target. This is due to experimental error (depending on the nature of these errors some of the eigenvalues of $[T_t]$ may in fact be negative). Nonetheless, there is a strongly dominant eigenvalue with corresponding eigenvector

$$k = \begin{bmatrix} 0.176[0^\circ] \\ 0.984[-90^\circ] \\ 0.018[68^\circ] \\ 0.028[-36^\circ] \end{bmatrix} \qquad - 7.5$$

FIGURE 35: HALF WAVE PLATE

1.0 EIGENVALUE = -12.6 dB
2.0 EIGENVALUE = -14.8 dB
3.0 EIGENVALUE = -19.5 dB

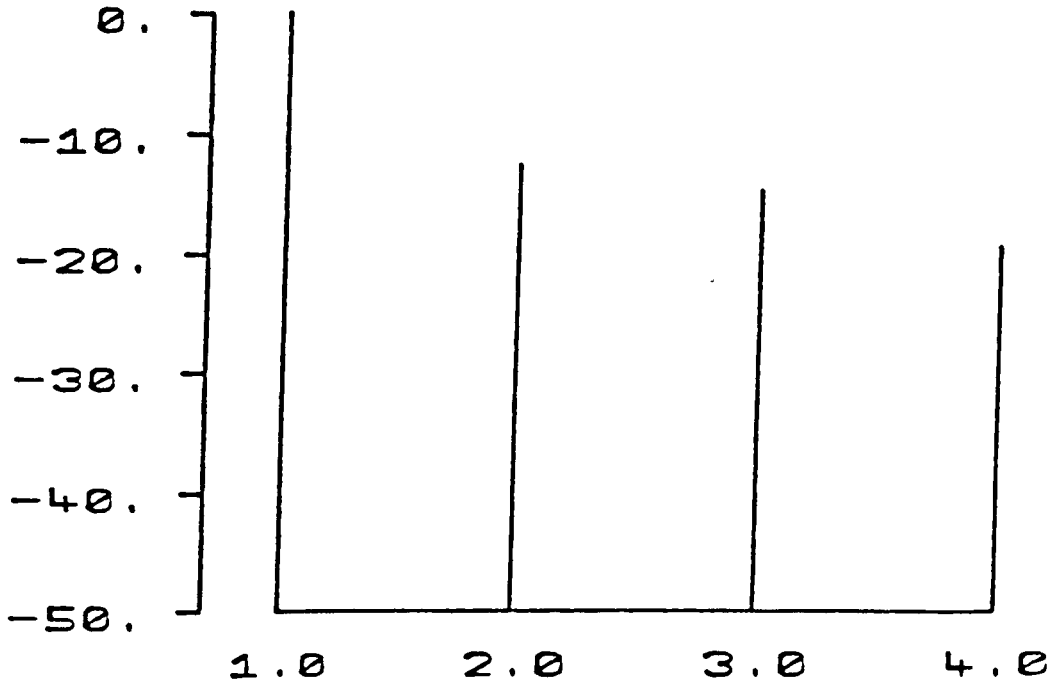

This spinor corresponds to a scattering matrix

$$[S] = \begin{bmatrix} 1.00 & 0.04[140^\circ] \\ 0.01[-68^\circ] & 1.00[160^\circ] \end{bmatrix} \qquad - 7.6$$

These results are to be compared with the nominal spinor

$$\hat{k} = (0,1,0,0)$$

and scattering matrix

$$[S] = \begin{bmatrix} 1 & 0 \\ 0 & -1 \end{bmatrix}$$

Figure 36 shows the predicted locus of available wave states for h input and rotation of the plate from 0° to 90°. (compare with figure 31). The maximum deviation from linear states occurs at a rotation of 45°, where the predicted output has an ellipticity of $\tau = 11°$. We can check this result by noting that $\lambda = 632.8$nm and so the plate thickness (280 $\pm$20 nm) corresponds to 0.443λ ± 0.03 or a phase difference of 159° $\pm$11°. The measured value clearly lies within these bounds.

Having obtained the scattering matrix [S], we can perform a singular value analysis and express it in diagonal form. To do this we form the hermitian matrices $[S].[S]^{*T}$ and $[S]^{*T}.[S]$ and find the 2 unitary matrices which diagonalise them by similarity transformations. In this way we can express [S] as

$$\begin{bmatrix} 0.69[0^\circ] & -0.73[-6^\circ] \\ 0.73[6^\circ] & 0.69[0^\circ] \end{bmatrix} \begin{bmatrix} 1.02 & 0 \\ 0 & 0.98[161^\circ] \end{bmatrix} \begin{bmatrix} 0.67[0^\circ] & 0.74[154^\circ] \\ -0.74[-154^\circ] & 0.67[0^\circ] \end{bmatrix}$$

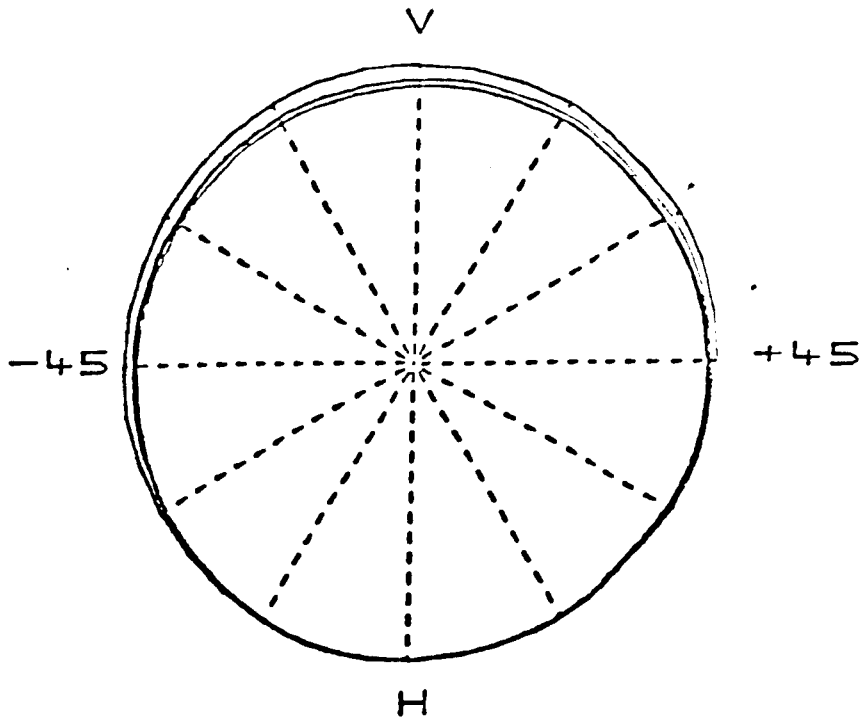

FIGURE 36: TRUE LOCUS FOR HALF WAVE PLATE

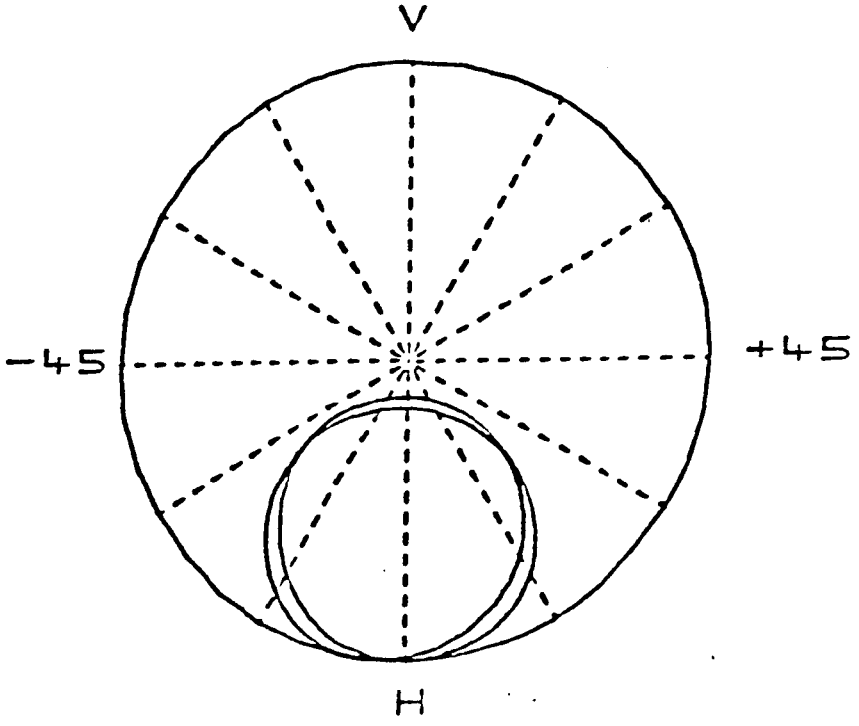

FIGURE 37: TRUE LOCUS FOR QUARTER WAVE PLATE

From the 2 unitary matrices we can calculate the normalised Stokes vectors for the transmit base as

$$g = (1.00, -0.09, -0.89, -0.44) \quad - 7.7$$

and

$$g = (1.00, 0.09, 0.89, 0.44) \quad - 7.8$$

and for the receiver base

$$g = (1.00, -0.05, 0.99, 0.10) \quad - 7.9$$

and

$$g = (1.00, 0.05, -0.99, -0.10) \quad - 7.10$$

Note that all these vectors are expressed in the conventional coordinate system.

To check these results, the receiver states were used in an adaptive filter and the transmitter state manually altered to obtain a minimum signal. The target was then removed and the transmitter polarisation measured. The transmitter states so obtained were

$$g = (1, -0.08, -0.95, -0.30)$$

and

$$g = (1, 0.05, 0.98, 0.20)$$

which are to be compared with 7.7 and 7.8 and confirm the orthogonality of singular vectors.

2) The eigenvalue spectrum for the mica quarter wave plate is shown in figure 38. Again the entropy is nonzero because of

FIGURE 38: QUARTER WAVE PLATE

1.0 EIGENVALUE = -13.3 dB
2.0 EIGENVALUE = -16.0 dB
3.0 EIGENVALUE = -23.6 dB

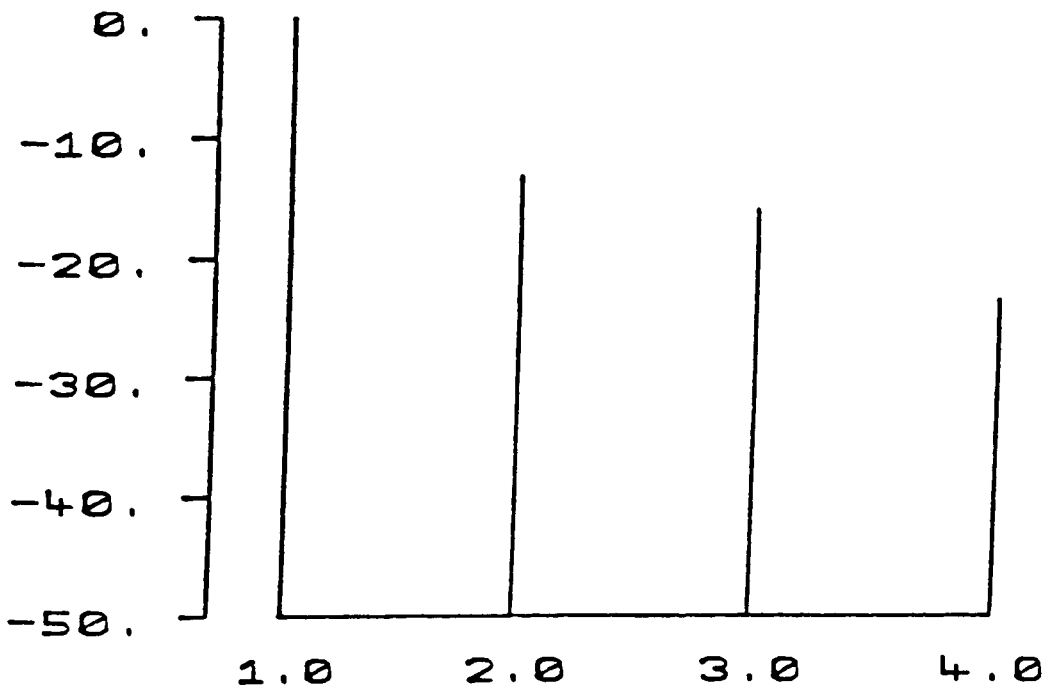

experimental error, but the dominant eigenvalue has a corresponding eigenvector

$$\hat{\underline{k}} = \begin{bmatrix} 0.761[0°] \\ 0.646[-90°] \\ 0.047[101°] \\ 0.019[-19°] \end{bmatrix} \qquad - 7.11$$

and scattering matrix

$$[S] = \begin{bmatrix} 1.00 & 0.06[133°] \\ 0.03[159°] & 1.00[81°] \end{bmatrix} \qquad - 7.12$$

The predictive locus for rotation of the plate is shown in figure 37 (to be compared with figure 32). Note that we cannot generate circular polarisation with this plate at this wavelength. Again we can check the measured phase difference by noting that at λ = 632.8nm, the plate is $0.221\lambda \pm 0.032$ wavelengths thick. The expected phase angle is then $79.5° \pm 11.5°$. Again, the measured value lies within these bounds.

7.3 Applications to target classification

In this section we will discuss a classification scheme for targets based on their polarisation transformation properties. The classification will depend on structural properties of the target spinor and corresponding coherency matrix. As such, we will consider 3 basic target types:

1) Linear targets, having linear singular vectors and showing only properties of linear birefringence and/or dichroism.
2) Circular targets, having circular singular vectors and

displaying circular birefringence (optical activity) and/or dichroism.

3) Elliptical targets, being the most general classification and including as special cases 1) and 2).

Finally, we will consider the application of these results to the problem of radar target identification and to the characterisation of radar backscatter from a cloud of linear dipoles.

1) Linear targets are defined as all those having linear transmit and receive eigenstates. The corresponding singular values may have either a finite phase difference (corresponding to linear birefringence) or different magnitudes (linear dichroism), but in either event, we may write the scattering matrix for such targets in the form

$$[S] = \begin{bmatrix} \cos\theta_1 & \sin\theta_1 \\ -\sin\theta_1 & \cos\theta_1 \end{bmatrix} \begin{bmatrix} t_1 & 0 \\ 0 & t_2 \end{bmatrix} \begin{bmatrix} \cos\theta_2 & -\sin\theta_2 \\ \sin\theta_2 & \cos\theta_2 \end{bmatrix} \qquad - 7.13$$

where t_1 and t_2 are the complex singular values of [S], expressed in the (h,v) base. From this we can readily calculate the target spinor $\hat{k}$ with elements

$$k_0 = \tfrac{1}{2}\cos(\theta_1-\theta_2)(t_1+t_2) \qquad k_1 = \tfrac{1}{2}\cos(\theta_1+\theta_2)(t_1-t_2)$$
$$k_2 = -\tfrac{1}{2}\sin(\theta_1+\theta_2)(t_1-t_2) \qquad k_3 = \tfrac{i}{2}\sin(\theta_1-\theta_2)(t_1+t_2)$$

We can then make the following observations:

a) The target spinor for linear targets has the general property that k_0 and k_3 are in phase quadrature, k_1 and k_2 are either in phase or antiphase.

b) If $\emptyset_1 = \emptyset_2$ then $k_3 = 0$ ie. the scattering matrix is symmetric. In this case, k_0 (the trace of the scattering matrix) is a transformation invariant (under a change of polarisation base).

c) For pure birefringence ie. $|t_1| = |t_2|$, k_0 and k_1 are in phase quadrature, while for pure dichroism, t_1 and t_2 are in phase and k_0, k_1 and k_2 are all in phase or antiphase. However, for a mixture of the two processes (dichroism plus birefringence) the phase of k_0 bears no simple relationship to that of k_1.

d) The coherency matrix for linear targets has several specific symmetries: the coupling parameters I and F (the real and imaginary parts of the 03 and 12 elements respectively) are zero. For symmetric matrices, T_c is 3 x 3 and, in general, only F will be zero.

2) Circular targets are characterised by having circular polarisation eigenstates with the corresponding singular values representing circular birefringence (optical activity) and/or circular dichroism. In the conventional coordinate system, these targets have a scattering matrix of the form

$$[S] = \begin{bmatrix} 1 & i \\ i & 1 \end{bmatrix} \begin{bmatrix} t_1 & 0 \\ 0 & t_2 \end{bmatrix} \begin{bmatrix} 1 & -i \\ -i & 1 \end{bmatrix} \qquad - 7.14$$

with a corresponding target spinor

$$\hat{k} = (t_1+t_2,\ 0,\ 0,\ t_1-t_2) \qquad - 7.15$$

In the antenna coordinates the scattering matrix for circular targets becomes

$$[S_A] = \begin{bmatrix} 1 & i \\ i & 1 \end{bmatrix} \begin{bmatrix} t_1 & 0 \\ 0 & t_2 \end{bmatrix} \begin{bmatrix} 1 & i \\ i & 1 \end{bmatrix} \qquad - 7.16$$

which has a corresponding spinor

$$\hat{k} = (0,\ t_1 - t_2,\ i(t_1 + t_2),\ 0)$$

We can see that circular targets have $S_{HH} = \pm S_{VV}$ (+ for conventional and - for antenna coordinates) and $S_{HV} = \pm S_{VH}$ (+ for antenna and - for conventional coordinates). In either case the target coherency matrix is sparse: only 2 generators and 2 coupling parameters being nonzero.

3) Elliptical targets represent the most general class. They have elliptical eigenstates and show no particular symmetry in $\hat{k}$ nor in T_c. The singular values of such targets represent elliptical birefringence and dichroism. Clearly, linear and circular targets are special cases of this class but, for convenience, we exclude them from membership and include only those targets which do not satisfy the constraints of 1) or 2).

We will now consider 2 specific examples of the use of polarisation information for target classification: both involve radar backscatter and so the antenna coordinate system will be used.

The first concerns the classification of targets using short wavelength radar (eg mm wave and short microwave). In this limit, the backscatter is dominated by specular reflection from

flat surfaces (facets) normal to the radar line of sight and by multiple scattering from corner reflectors (the latters importance stems from its wider beamwidth when compared with specular reflection from a flat surface). We can describe all such returns, polarimetrically, using just 3 component matrices:

1) specular reflection at normal incidence may be represented by

$$[S_A] = a \begin{bmatrix} 1 & 0 \\ 0 & 1 \end{bmatrix}$$

where

$$a = (4.\pi.A^2/\lambda^2)^{1/2}$$

A is the area of the facet and λ the radar wavelength. It must be emphasised that although a strong reflection can occur at normal incidence, the reflection decreases dramatically for a small shift away from the normal. The half power beamwidth is approximately

$$\theta = \lambda/2a \text{ radians}$$

where a is the length of facet.

2) A trihedral corner reflector can be represented by the same scattering matrix as 1), the main difference being a larger 3dB beamwidth (up to approximately 40° in azimuth and elevation). Polarimetrically it is indistinguishable from the facet (NB we are assuming metallic reflectors. If the corner is made of dielectric material it will behave in a different manner to the facet). Note that both the facet and the trihedral are rotation invariant in a plane normal to the radar line of sight.

3) The dihedral reflector is formed by 2 intersecting planes at right angles. It has a wide beamwidth in a plane perpendicular to the seam (approximately 30°), but the same narrow beamwidth

as the facet in the elevation plane. However, because it is a double bounce scatterer, it has a different scattering matrix from the other two targets considered. It is characterised by a skip angle of 180° and is dependent on its orientation angle relative to the radar vertical reference. It is a linear target with $t_1 = -t_2$ and $\emptyset_1 = \emptyset_2$. Hence it has a scattering matrix

$$[S] = x\begin{bmatrix} \cos 2\emptyset & -\sin 2\emptyset \\ -\sin 2\emptyset & -\cos 2\emptyset \end{bmatrix}$$

and target spinor

$$\hat{k} = (0,\ \cos 2\emptyset,\ -\sin 2\emptyset,\ 0)$$

where $\emptyset$ represents the angle of the dihedral relative to the reference vertical.

We now come to the task of classifying targets made from combinations of these 3 reflector types.

The first point to note is that for monochromatic illumination at fixed aspect there will be a coherent summation of target spinors and, from examination of the component targets, we can see that the object may appear to be <u>any</u> symmetric matrix at all (depending simply on the spatial separation of scatterers and the wavelength). Hence, target classification at a single aspect and for fixed frequency is not possible, at least using this model for radar targets. The only hope in classifying such targets is to use frequency agility or variable aspect data so as to decorrelate the component targets and obtain a coherency matrix which is the sum of component matrices. In this way we arrive at a coherency matrix of the general form

$$[T_c] = \begin{bmatrix} \alpha & 0 & 0 & 0 \\ 0 & \chi & \gamma & 0 \\ 0 & \gamma & \chi & 0 \\ 0 & 0 & 0 & 0 \end{bmatrix}$$

which has 3 parameters α, χ and γ. The first 2 relate to the relative amplitudes of scattering from dihedral and trihedral components, while γ relates to the correlation in rotation angle of dihedrals. In any case, we can see that the coherency matrix is sparse and there is not a lot of target polarisation information present in the return signal. Of course, it remains to be seen whether such a model is accurate for real radar targets: it may well be that the deviation from perfect di and trihedral scattering is sufficient to provide more structure in the coherency matrix than expected. This may be particularly true at lower radar frequencies where the simple specular scattering approach is expected to be less accurate.

Finally, there is the added complication that as target aspect changes, so the distribution and amplitudes of the specular scattering centres will change. This means that the 3 parameters α, χ and γ will be aspect dependent, making classification more difficult.

As a second example of this classification scheme, consider the general problem of scattering from a cloud of particles. Such scattering has been examined from a polarimetric point of view by Van De Hulst but never before using the target decomposition theorems outlined in this thesis.

The significance of a cloud of scatterers is that the resultant coherency matrix for monochromatic illumination will be given by the sum of all component matrices, simply because

the large number of scattering elements in the cloud causes a decorrelation (as explained in section 6.1). Hence, in the most trivial case when all scatterers are the same (eg. a cloud of spheres) the integrated coherency matrix will just be n times the coherency matrix of an individual target (where n is the number of scatterers in the cloud). Evidently, such a matrix will have only 1 nonzero eigenvalue corresponding to the single target comprising the cloud.

In general a cloud will contain many different targets or, at the very least, a large number of similar objects in various orientations. For bistatic scattering there are a large number of permutations; Van De Hulst has summarised some of these by considering reflection properties in the plane of scattering and in the bisectrix. Fortunately, for backscatter, the geometry simplifies and we can generate the coherency matrix quite easily. In this section, we will derive the matrix for a cloud of identical scatterers distributed over a range of orientation angles in a plane normal to the radar line of sight.

If we let the "parent" target comprising the cloud have a spinor k, then the spinor for rotation of the object through $\emptyset^\circ$ is

$$k(\emptyset) = (k_0,\ \sin 2\emptyset k_2 + \cos 2\emptyset k_1,\ \cos 2\emptyset k_2 - \sin 2\emptyset k_1,\ 0)$$

If we denote the ijth element of the coherency matrix of the parent as t_{ij}, then the elements of $[T_c(\emptyset)]$, the coherency matrix for the rotated target will be

$$t_{00} = t_{00}$$

$$t_{01} = \cos 2\theta t_{01} + \sin 2\theta t_{02}$$

$$t_{02} = \cos 2\theta t_{02} - \sin 2\theta t_{01}$$

$$t_{03} = 0$$

$$t_{11} = \cos^2 2\theta t_{11} + \sin^2 2\theta t_{22} + \sin 2\theta \cos 2\theta \mathrm{Re}(t_{12})$$

$$t_{12} = \cos^2 2\theta t_{12} - \sin^2 2\theta t_{21} + \sin 2\theta \cos 2\theta (t_{22} - t_{11})$$

$$t_{13} = 0$$

$$t_{22} = \cos^2 2\theta t_{22} + \sin^2 2\theta t_{11} - \sin 2\theta \cos 2\theta \mathrm{Re}(t_{12})$$

$$t_{23} = 0$$

The variable θ will have some distribution of values depending on the nature of the cloud. In the simplest case, we can assume θ is uniformly distributed over the range 0 to 2π, in which case we can simplify the above using

$$\langle \sin 2\theta \rangle = \langle \cos 2\theta \rangle = \langle \sin 2\theta \cos 2\theta \rangle = 0$$

$$\langle \sin^2 \theta \rangle = \langle \cos^2 \theta \rangle = 0.5$$

In this case the coherency matrix becomes

$$[T_C] = \begin{bmatrix} 2t_{00} & 0 & 0 & 0 \\ 0 & t_{11}+t_{22} & i\mathrm{Im}(t_{12}) & 0 \\ 0 & -i\mathrm{Im}(t_{12}) & t_{11}+t_{22} & 0 \\ 0 & 0 & 0 & 0 \end{bmatrix}$$

which has the same degrees of freedom as the trihedral/dihedral target model discussed earlier.

As an example, consider backscatter from a cloud of dipole scatterers: the parent spinor is

$$\hat{k} = (1,\ 1,\ 0,\ 0)$$

and the coherency matrix for a cloud of such particles is

$$[T_c] = \begin{bmatrix} 2 & 0 & 0 & 0 \\ 0 & 1 & 0 & 0 \\ 0 & 0 & 1 & 0 \\ 0 & 0 & 0 & 0 \end{bmatrix}$$

Clearly the eigentargets are the Pauli set (ie. trihedral and dihedral symmetry) and the target eigenvalues indicate a stronger correlation of trihedral than dihedral type symmetry. This result could provide the basis for discriminating such a target from others with different matrix structure.

In summary, we have seen that for radar backscatter from a cloud of identical but randomly oriented scatterers, the coherency matrix is sparse, making the classification of such targets difficult. As an example we considered a trihedral/dihedral target model for high frequency radar scattering and found that there were (in the worst case) only 3 factors available for target discrimination. We also considered a cloud of randomly oriented dipoles and showed that it has the same average reflection properties as a combination of dihedrals and trihedrals (with the latter target being slightly more predominant).

It must be emphasised that our target models are grossly simplified: in practice there may well be significantly more structure in the coherency matrix than implied by the results of this section. These simple targets are meant only as an illustration of the potential application of the target spinor formalism to the classification problem. Its most important

feature is that it allows a processing framework in which to analyse experimental data and judge quantitatively the information contained within the polarisation signature.

One of the main aims of this thesis has been the development of a phenomenological theory for the classification of targets based on their polarisation transformation properties. Towards this end, we have seen that we can describe the degrees of freedom available in the polarisation signature in 3 different ways.

For single targets we can use the coherent scattering matrix [S] with its 8 degrees of freedom. Further, we saw that by using the antenna coordinates and considering only backscatter, we could interpret these degrees of freedom as null points on the Poincaré sphere which, together, form a structure called the polarisation fork. For the more general case we found, however, that 2 forks are needed; destroying somewhat the simplicity of the fork geometry.

The basic problem with the fork analysis is that the Poincaré sphere is a wave representation space and we can only represent targets as multipoint objects in this space. One of the central themes of this thesis has been the search for a target representation space, a space where each target has a single point representation. This search has lead successfully (for the first time) to a target sphere in 6 dimensions.

Despite their clumsy representation on the Poincaré sphere, the null states themselves are of great practical significance because of their special symmetry and the possibility of using them to maximise or minimise the radar cross section of a target.

The second approach is again well documented in the literature and invloves the use of Stokes vectors for the representation of incident and scattered waves. The resulting 4

x 4 Mueller matrix follows from the simple assumption of linearity in the scattering process. However, this matrix bears a complicated relationship to [S], making difficult the interpretation of the Mueller matrix elements in terms of the target null states. The main attraction of this formalism is that in experiments we very often measure the Stokes vectors directly and so can easily calculate [M] using simple linear algebra.

Another important difference between the Mueller calculus and the coherent scattering matrix is the ability of the former to represent partial targets. However, because of the complicated relationship between [S] and [M], interpretation of the extra information on target correlations is difficult to extract from [M] directly.

All of these difficulties are relieved by adopting the target spinor and coherency matrix approach to the scattering problem and it is this approach which represents the core of original research in this thesis.

By using the simple expedient of changing the scattering matrix into a target vector, we open up a whole new approach to the characterisation of polarisation problems. By studying the transformation properties of this vector, we have shown it to be a very interesting geometrical quantity, a spinor in a 6 dimensional real space. This result is strongly analogous to the Poincaré sphere representation of waves and this similarity is formally explored using group theory.

With this mapping of the target vector onto a real sphere we are able to do 2 things: first to generate a target coherency matrix which describes the correlation properties of partial targets in a much clearer way than [M] and secondly, we can formally relate the elements of the Mueller matrix to those of

this coherency matrix by interpreting the former as invariants under plane rotations in this 6 dimensional target space.

A third important result of using the coherency matrix formulation is the development of a target decomposition theorem which expresses a partial target as the noncoherent sum of up to 4 single targets, given by the eigenvectors of the coherency matrix. This theorem has important implications for the use of polarisation information in remote sensing systems and also allows the extraction of scattering matrix data in the presence of experimental noise. To demonstrate the advantages of this method an experimental coherent optical polarimeter was constructed capable of measuring the scattering matrix for a range of bistatic scattering angles (except backscatter). The results obtained from this system showed clearly the advantages of the coherency matrix formulation over the Mueller matrix.

Finally we compared the target decomposition theorem with the only other one developed in the literature (by J Huynen) and have shown that the latter theorem is nonphysical in the sense that it is not unique. We conclude therefore that the only fundamental decomposition of partial targets is via the eigenvector analysis outlined in this thesis.

APPENDIX 1: DERIVATION OF THE STOKES REFLECTION MATRIX FROM [S]

If the target has scattering matrix [S] then

$$\underline{E}_s = [S]\underline{E}_i$$

and the wave coherency matrix transforms as

$$[J_s] = [S][J_i][S]^{*T}$$

From the properties of the Pauli matrices

$$[J_s] = \sum_{i=0}^{3} g_i \sigma_i$$

where

$$g_i = \tfrac{1}{2}\,\mathrm{Tr}([J_s]\sigma_i)$$

Writing this in compact form and using the cyclic property of the trace operator yields

$$\begin{aligned} \underline{g}_s &= \tfrac{1}{2}\,\mathrm{Tr}([J_s]\underline{\sigma}) \\ &= \tfrac{1}{2}\,\mathrm{Tr}([S][J_i][S]^{*T}\underline{\sigma}) \\ &= \tfrac{1}{2}\,\mathrm{Tr}([J_i][S]^{*T}\underline{\sigma}[S]) \\ &= \tfrac{1}{2}\,\mathrm{Tr}([J_i]\underline{\sigma}_s) \end{aligned} \qquad \text{- A1.1}$$

where

$$\underline{\sigma}_s = [S]^{*T}\underline{\sigma}[S]$$

The coherency matrix of the incident wave may also be written in terms of the Pauli matrices as

$$[J_i] = \frac{1}{2}\sum_{k=0}^{3} Tr([J_i]\sigma_k)\sigma_k$$

and similarly

$$\underline{\sigma}_s = \frac{1}{2}\sum_{k=0}^{3} Tr(\underline{\sigma}_s \sigma_k)\sigma_k$$

substituting in A1.1 yields

$$\underline{g}_s = \frac{1}{8}\sum_{k=0}^{3} Tr(\underline{\sigma}_s \sigma_k)Tr([J_i]\sigma_k)$$

NB. $\sigma_k^2 = \sigma_0$

This may be written in terms of the Stokes parameters of incident and scattered waves to yield

$$\underline{g}_s = \frac{1}{4}\sum Tr(\underline{\sigma}_s \sigma_k)g_k$$
$$= \sum m_{jk} g_k$$

where m_{jk} relates the kth Stokes parameter of the incident Stokes vector to the jth parameter of the scattered Stokes vector. Together they form a matrix [M], relating the Stokes vector of the incident wave to that of the scattered wave ie.

$$\underline{g}_s = [M]\underline{g}_I$$

where

$$[M] = \frac{1}{4} Tr(\underline{\sigma}_s \underline{\sigma})$$

and

$$\underline{\sigma} = [S]^{*T}\underline{\sigma}[S]$$

In particular

$$\underline{\sigma}_s \underline{\sigma} = \begin{bmatrix} \sigma_{0s} \\ \sigma_{1s} \\ \sigma_{2s} \\ \sigma_{3s} \end{bmatrix} (\sigma_0, \sigma_1, \sigma_2, \sigma_3)$$

which can be written

$$\begin{bmatrix} \sigma_{0s}\sigma_0 & \sigma_{0s}\sigma_1 & \sigma_{0s}\sigma_2 & \sigma_{0s}\sigma_3 \\ \sigma_{1s}\sigma_0 & \sigma_{1s}\sigma_1 & \sigma_{1s}\sigma_2 & \sigma_{1s}\sigma_3 \\ \sigma_{2s}\sigma_0 & \sigma_{2s}\sigma_1 & \sigma_{2s}\sigma_2 & \sigma_{2s}\sigma_3 \\ \sigma_{3s}\sigma_0 & \sigma_{3s}\sigma_1 & \sigma_{3s}\sigma_2 & \sigma_{3s}\sigma_3 \end{bmatrix}$$

By taking the trace of these matrices we obtain a real matrix [M], the Stokes reflection or Mueller matrix.

Note that for the antenna coordinate system [M] has to be multiplied by

$$\begin{bmatrix} 1 & 0 & 0 & 0 \\ 0 & 1 & 0 & 0 \\ 0 & 0 & 1 & 0 \\ 0 & 0 & 0 & -1 \end{bmatrix}$$

to yield a modified matrix [M_a] (this is to account for the conjugate nature of the backscattered wave).

If we write the matrix [S] in the general form

$$[S] = \begin{bmatrix} a & b \\ c & d \end{bmatrix}$$

then we can use the above result to show that the elements of [M] are given by

$$2m_{00} = a^2+b^2+c^2+d^2 \qquad 2m_{01} = a^2-b^2+c^2-d^2$$

$$m_{02} = \mathrm{Re}(a^*b+c^*d) \qquad m_{03} = \mathrm{Im}(a^*b+c.d)$$

$$2m_{10} = a^2+b^2-c^2-d^2 \qquad 2m_{11} = a^2-b^2-c^2+d^2$$

$$m_{12} = \mathrm{Re}(a^*b-c^*d) \qquad m_{13} = \mathrm{Im}(a^*b-c^*d)$$

$$m_{20} = \mathrm{Re}(a^*c+b^*d) \qquad m_{21} = \mathrm{Re}(a^*c-b^*d)$$

$$m_{22} = \mathrm{Re}(a^*d+b^*c) \qquad m_{23} = \mathrm{Im}(a^*d-b^*c)$$

$$m_{30} = -\mathrm{Im}(a^*c+b^*d) \qquad m_{31} = -\mathrm{Im}(a^*c-b^*d)$$

$$m_{32} = -\mathrm{Im}(a^*d+b^*c) \qquad m_{33} = \mathrm{Re}(a^*d-b^*c)$$

where we have written a^2 for aa^* etc. and $\mathrm{Re}(a) = (a+a^*)/2$, $\mathrm{Im}(a) = i(a-a^*)/2$.

APPENDIX 2: LORENTZ TRANSFORMATION OF STOKES VECTORS

The scattering of eigenstates from a single target may be written as a Lorentz transformation of the form

$$g_0' = \cosh(\alpha)g_0 + \sinh(\alpha)g_1$$

$$g_1' = \sinh(\alpha)g_0 + \cosh(\alpha)g_1$$

If $g_1 = D_p g_0$ then we can rewrite this as

$$g_0' = g_0(\cosh(\alpha) + \sinh(\alpha)D_p)$$

$$g_1' = g_0(\sinh(\alpha) + \cosh(\alpha)D_p)$$

hence the degree of polarisation of the scattered wave is

$$D_p' = \frac{g_1'}{g_0'} = \frac{D_p + \tanh(\alpha)}{1 + \tanh(\alpha)D_p} = G$$

The derivative of this function with respect to D_p is given as

$$\frac{dG}{dD_p} = \frac{1 - \tanh^2(\alpha)}{(1 + \tanh(\alpha)D_p)^2} > 0$$

The value of D_p for which the derivative is unity is then given by

$$1 + D_p\tanh(\alpha) = (1 - \tanh^2(\alpha))^{1/2} \qquad \text{- A2.1}$$

We can relate this to the target fork angle γ by using the relation

$$\tanh(\alpha) = \frac{1 - \tan^4\gamma}{1 + \tan^4\gamma}$$

from which

$$1 - \tanh^2(\alpha) = \frac{4\tan^4\gamma}{(1 + \tan^4\gamma)^2}$$

thus from A2.1 we have

$$\frac{2\tan^2\gamma}{1 + \tan^4\gamma} = 1 + \frac{1 - \tan^4\gamma}{1 + \tan^4\gamma}D_p$$

or

$$D_p = \frac{2\tan^2\gamma - 1 - \tan^4\gamma}{1 - \tan^4\gamma}$$

$$= \frac{(\cos^2\gamma - \sin^2\gamma)^2}{\sin^4\gamma - \cos^4\gamma}$$

$$= -(\cos^2\gamma - \sin^2\gamma)$$

$$= -\cos 2\gamma$$

This is the value of incident wave degree of polarisation that marks the boundary between compression and expansion.

APPENDIX 3: THE SU(4)-O_6^+ HOMOMORPHISM

In this Appendix we consider the mathematical details of the homomorphism between the groups SU(4) (ie.the set of 4 x 4 unitary matrices with unit determinant) and O_6^+ (the set of 6 x 6 real orthogonal matrices). This homomorphism is used in chapter 5 to develop the target coherency matrix.

We begin by considering 2 vector spaces U and V. The tensor product U ⊗ V consists of a vector space with basis vectors

$$\underset{\sim}{u}_i \otimes \underset{\sim}{v}_j$$

where i = 1,2,3...N and j = 1,2,3...M and N,M are the dimensions of U and V respectively. We can write a vector in such a space as

$$x = \sum_{i=1}^{N}\sum_{j=1}^{M} x_{ij}\, \underset{\sim}{u}_i \otimes \underset{\sim}{v}_j$$

Note that dim(U ⊗ V) = dim(U).dim(V).

Typically, we take the tensor product of a space with itself ie.

$$U \otimes U \otimes .....\otimes U = L^r(U_n)$$

which has basis vectors

$$\underset{\sim}{e}_{i1} \otimes \underset{\sim}{e}_{i2} \otimes .....\underset{\sim}{e}_{ir}$$

with i = 1,2,3.....N. An element in this rth order space is known as an rth order tensor and $L^r(U_n)$ is called the carrier

space for rth order tensor product representations.

In particular, in second order tensor space $L^2(U_N)$, it is possible to form new tensors as linear combinations of the basis vectors $e_i \times e_j$, which are antisymmetric under an interchange of order of subscripts. We do this by defining a <u>wedge product</u> or <u>bivector</u> as

$$\underset{\sim}{e}_i \wedge \underset{\sim}{e}_j = \underset{\sim}{e}_i \otimes \underset{\sim}{e}_j - \underset{\sim}{e}_j \otimes \underset{\sim}{e}_i = -\underset{\sim}{e}_j \wedge \underset{\sim}{e}_i$$

In general, the number of independent basis vectors existing in a fully antisymmetric subspace of $L^r(U_N)$ is given by

$$\dim L^r(U_N) = \begin{bmatrix} N \\ r \end{bmatrix} = \frac{N!}{r!(N-r)!}$$

For our second order tensor space there are therefore $\frac{N}{2}(N-1)$ such basis vectors. In particular, we note that if $N = 4$ then $\dim L^2(U_4) = 6$.

This is our first important result towards establishing the required homomorphism: by letting $U = C_4$ (the 4 dimensional complex space) and forming the exterior algebra $L^2(C_4)$, we can establish a mapping from a 4 into a 6 dimensional (complex) space.

Let the basis in C_4 be $\underset{\sim}{e}_1$, $\underset{\sim}{e}_2$, $\underset{\sim}{e}_3$ and $\underset{\sim}{e}_4$. The basis in $L^2(C_4)$ is then

$$\underset{\sim}{t}_1 = \underset{\sim}{e}_1 \wedge \underset{\sim}{e}_2 \qquad \underset{\sim}{t}_2 = \underset{\sim}{e}_2 \wedge \underset{\sim}{e}_3 \qquad \underset{\sim}{t}_3 = \underset{\sim}{e}_3 \wedge \underset{\sim}{e}_1$$

$$\underset{\sim}{t}_4 = \underset{\sim}{e}_3 \wedge \underset{\sim}{e}_4 \qquad \underset{\sim}{t}_5 = \underset{\sim}{e}_1 \wedge \underset{\sim}{e}_4 \qquad \underset{\sim}{t}_6 = \underset{\sim}{e}_2 \wedge \underset{\sim}{e}_4$$

Given a matrix [A] in SL(4), we have

$$\underset{\sim}{e}_i \wedge \underset{\sim}{e}_j \rightarrow [A]\underset{\sim}{e}_i \wedge [A]\underset{\sim}{e}_j$$

where [A]e is the ith column of [A] and so

$$[A]\underset{\sim}{e}_i \wedge [A]\underset{\sim}{e}_j = \left(\sum a_{ri}\,\underset{\sim}{e}_i\right)\left(\sum a_{sj}\,\underset{\sim}{e}_j\right)$$
$$= \sum\sum a_{ri}\,a_{sj}\,(\underset{\sim}{e}_r \wedge \underset{\sim}{e}_s)$$

This mapping corresponds to a 6 x 6 matrix [W], the 36 elements of which are derived from the 36 2 x 2 minors of [A] eg. w_{11} comes from $(\underset{\sim}{e}_1 \wedge \underset{\sim}{e}_2)$ with $(\underset{\sim}{e}_1 \wedge \underset{\sim}{e}_2)$ and is given by the minor formed by rows 1 and 2 with columns 1 and 2 ie.

$$w_{11} = a_{11}a_{22} - a_{12}a_{21}$$

In general, the ijth element of [W] is found by calculating the 2 x 2 minor formed from the corresponding rows and columns of [A]. Note that [W] will not in general be orthogonal.

To extend this result we now consider the higher exterior products of C^4 ie $L^r(C_4)$. In particular, $L^4(C_4)$ has a basis

$$\underset{\sim}{e}_1 \wedge \underset{\sim}{e}_2 \wedge \underset{\sim}{e}_3 \wedge \underset{\sim}{e}_4$$

and

$$[A]\underset{\sim}{e}_1 \wedge [A]\underset{\sim}{e}_2 \wedge [A]\underset{\sim}{e}_3 \wedge [A]\underset{\sim}{e}_4 = \det([A])(\underset{\sim}{e}_1 \wedge \underset{\sim}{e}_2 \wedge \underset{\sim}{e}_3 \wedge \underset{\sim}{e}_4)$$

In general, r x r minors are involved in the exterior algebra $L^r(U_N)$. If r = N, there is only 1 basis vector, called the <u>volume element</u> associated with the basis $(\underset{\sim}{e}_1, \underset{\sim}{e}_2, \ldots\ldots \underset{\sim}{e}_N)$. For $[A] \in SU(4)$, det([A]) = 1 and so when all 4 terms in the volume element are distinct their coefficient is 1, whereas the coefficient is 0 for all combinations which have repeated indices (because $\underset{\sim}{e}_i \wedge \underset{\sim}{e}_i = 0$).

If 2 bivectors $\underset{\sim}{x}$ and $\underset{\sim}{y}$ are identified with 2 vectors in

C_4 ie.

$$x = \sum x_j \underset{\sim}{t}_j$$
$$y = \sum y_j \underset{\sim}{t}_j$$

then the 4-vector $\underset{\sim}{x} \wedge \underset{\sim}{y}$ is given by

$$f(x,y)(\underset{\sim}{e}_1 \wedge \underset{\sim}{e}_2 \wedge \underset{\sim}{e}_3 \wedge \underset{\sim}{e}_4)$$

where the basis can be identified as the volume element of $L^2(C_3)$ and

$$f(x,y) = x_1 y_4 + x_2 y_5 + x_3 y_6 + x_4 y_1 + x_5 y_2 + x_6 y_3$$

This can be shown quite easily by forming the wedge product of the six basis vectors $\underset{\sim}{t}_i$ given earlier and noting that any term containing components of the form $\underset{\sim}{e}_i \wedge \underset{\sim}{e}_i = 0$.

Note that there is a cyclic permutation of ordering in $\underset{\sim}{y}$ and so to obtain a scalar product in C_4 we consider not $[W]^T[W]$, but

$$[W]^T[P][W]$$

where

$$P = \begin{bmatrix} 0 & I_3 \\ I_3 & 0 \end{bmatrix}$$

I_3 is the 3 x 3 identity matrix and [P] permutes the rows of [W] as required. Since we are considering SU(4), the matrix product $[W]^T[P][W]$ will have 1 in positions 14, 25 etc. where 4 distinct basis vectors occur and zero elsewhere, hence

$$[W]^T[P][W] = [P]$$

Now, if [A] is unitary $[A]^{*T}[A] = I_4$ and we know $[A] \rightarrow [W]$, $[A]^{*T} \rightarrow [W]^{*T}$ then

$$I_4 = [A]^{*T}[A] \rightarrow [W]^{*T}[W]$$

but $I_4 \rightarrow I_6$ and so [W] is unitary. In order to show the mapping of SU(4) into O_6, we have to develop a mapping of [A] into a real orthogonal matrix, not into [W]. We can develop such a matrix as follows: define a matrix [Q] by

$$[Q]^2 = [P] \qquad [Q] = [Q]^T$$

Note that $[P]^2 = I_6$ the 6 x 6 identity and so

$$[Q]^4 = [P]^2 = I_6$$

therefore

$$[Q]^{-1} = [Q]^3$$

Now consider a similarity transformation of [W] by [Q] ie.

$$[Q][W][Q]^{-1}$$

then (dropping the brackets around matrices for notational convenience)

$$(QWQ^{-1})^T(QWQ^{-1}) = Q^3W^TPWQ^3$$

$$= Q^3PQ^3 = I_6$$

and so QWQ^{-1} is orthogonal. Thus $A \rightarrow QWQ^{-1}$ is a mapping from

SL(4) to SO(6) over C. We will define [Q] explicitly as

$$Q = (1-i)/2 \begin{bmatrix} I_3 & iI_3 \\ iI_3 & I_3 \end{bmatrix}$$

We now have only to prove that QWQ^{-1} is <u>real</u> orthogonal. To do this, we need to show that it is unitary as well as orthogonal ie. that

$$(QWQ^{-1})^{*T}(QWQ^{-1}) = I_6$$

<u>Proof</u>

$$(QWQ^{-1})^{*T} = Q^{3*T}W^{*T}Q^{*T}$$

but

$$Q^3 = PQ = (1-i)/2 \begin{bmatrix} iI_3 & I_3 \\ I_3 & iI_3 \end{bmatrix}$$

and

$$Q^* = Q^{*T} = (1+i)/2 \begin{bmatrix} I_3 & -iI_3 \\ -iI_3 & I_3 \end{bmatrix} = Q^3$$

also

$$Q^{3*} = Q^{3*T} = (1+i)/2 \begin{bmatrix} -iI_3 & I_3 \\ I_3 & -iI_3 \end{bmatrix} = Q$$

therefore

$$\begin{aligned} (QWQ^{-1})^{*T}.(QWQ^{-1}) &= Q^{3*}W^{*T}Q^{*}QWQ^{-1} \\ &= Q^{3*}W^{*T}I_6WQ^3 \\ &= QI_6Q^3 = I_6 \end{aligned}$$

hence QWQ^{-1} is both unitary and orthogonal and so must be real orthogonal as required for the homomorphism.

In summary, we can map an element of SU(4) into a 6 x 6 real orthogonal matrix by

1) Forming a 6 x 6 complex matrix [W] from the minors of [A].

2) Calculating QWQ^{-1}, which is a real 6 x 6 orthogonal matrix.

APPENDIX 4: RELATIONSHIP BETWEEN $[T_c]$ and $[M]$

By expanding the scattering matrix S (we will drop the brackets around matrices for notational convenience) in terms of the Pauli ring, we can express it as a vector $\underset{\sim}{k}$

$$\underset{\sim}{k} = \frac{1}{2} Tr(S\underset{\sim}{\sigma})$$

The Mueller matrix M is related to S by

$$m_{ij} = \frac{1}{2} Tr(S^{*T} . \sigma_i . S . \sigma_j)$$

In this Appendix we will show that this can also be written

$$m_{ij} = \frac{1}{4} Tr(T_c \eta_{4i+j})$$

where the sixteen matrices η are the generators of SU(4) plus the 4x4 identity (see figure 26). To prove this we need one key result: the product of 2 matrices S_1 and S_2 yields a new matrix S_3 which has a corresponding vector $\underset{\sim}{k}_3$ given by

$$\underset{\sim}{k}_3 = \underset{\sim}{k}_1^T . \Gamma . \underset{\sim}{k}_2$$

where Γ are the set of matrices η_0 to η_3 (see Figure 26) and $\underset{\sim}{k}_1$, $\underset{\sim}{k}_2$ are the target vectors corresponding to S_1 and S_2.

With this result we can write

$$S . \sigma_j = \eta_j . \underset{\sim}{k}$$

where $\underset{\sim}{k}$ corresponds to S. Similarly

$$\sigma_i . S . \sigma_j = \eta_i^T \eta_j . \underset{\sim}{k}$$

We now note that if $S \rightarrow \underset{\sim}{k}$ then $S^{*T} \rightarrow k^*$ and the trace of the matrix product $S_1 . S_2$ is given by

$$Tr(S_1 . S_2) = \underset{\sim}{k}_1^T . \underset{\sim}{k}_2$$

Hence we have that

$$2\, m_{ij} = \underset{\sim}{k}^{*T} . \eta_i^T \eta_j . \underset{\sim}{k}$$

but m_{ij} is a scalar, so we can take its trace and use the cyclic property of trace operators to rewrite this as

$$m_{ij} = Tr(m_{ij}) = \frac{1}{2} Tr(\underset{\sim}{k} . \underset{\sim}{k}^{*T} . \eta_i^T \eta_j)$$

Finally we note that

$$\eta_i^T \eta_j = m_{4i+j}$$

and hence our desired result that the elements of the Mueller matrix are given by the expansion of the coherency matrix in terms of the set of generators $\underset{\sim}{\eta}$.

REFERENCES

G. Arfken "Mathematical Methods For Physicists" Chapter 4 Academic press 1970

K Atkinson "Introduction to Numerical Analysis" Wiley 1978

R M Azzam "Propagation of Partially Polarised Light Through Anisotropic Media..." J. Opt. Soc. Am. Vol 68, No. 12, pp 1756-1767 Dec 1978

R. Barakat "Theory of the Coherency Matrix for Light of Arbitrary Spectral Bandwidth" J. Opt. Soc. Am Vol 53, No 3, pp317-323 March 1963

R.A.Beth "Mechanical detection and measurement of the angular momentum of light" Phys Rev 50, 115 (1936)

A. Blanchard "Antenna Effects in Depolarisation Measurements" IEEE Trans Geo and Rem Sens Vol GE-21, No 1, pp 113-117 Jan 1983

W.M. Boerner "Polarisation dependence in EM inverse problems" IEEE Trans AP-29, pp262-271 March 1981

F. Bolinder "Radio Engineering uses of the Minkowski Model of Lorentz space" Proc IRE p 450, March 1959

M. Born E. Wolf "Principles of Optics" Pergamon press 1965

J. Byrne "Classification of Electron and Optical Polarisation transfer matrices" J Phys B Vol 4, pp 940-953 1971.

S.Chandrasekhar "Radiative transfer" Dover 1960

S.K. Chaudhuri Foo and Boerner "A validation of Huynens target descriptors..." Proc IEEE AP34 No 1 pp11-21 Jan 1986

H.Chen "Theory of Electromagnetic Waves: a Coordinate Free Approach" McGraw Hill 1985

S. Cloude "Polarimetric Techniques in Radar Signal Processing" Microwave Journal Vol 26 No 7 July 1983

S. Cloude "Target Decomposition theorems in radar target scattering" Electronics letters Vol 21 No 1 pp 22-24 Jan 1984

S.Cloude "Group theory and polarisation algebra" OPTICS 86, The Hague, Netherlands, May 1986

S. Cloude "Target Decomposition theorems in radar polarimetry" IEE colloquium on Discrimination and Identification methods in Radar, 6th May 1986

M.H. Cohen "Radio Astronomy Polarisation Measurements" Proc IRE Vol 46 pp 172-183 Jan 1958

J. Copeland "Radar target classification by polarisation properties" Proc IRE Vol 48 pp1260-1296 July 1960

J. Crispin K.Siegel "Methods of radar cross section analysis" Academic Press 1968

I. Craig and J. Brown "Inverse problems in Astronomy" Adam Hilger 1986

G. Deschamps "Geometrical representation of plane polarised waves" Proc IRE Vol 39, p540 May 1951

G. Deschamps "Poincare Sphere representation of partially polarised waves" Proc IEEE Vol AP-21(4) p 474 1973

J. Dieudonne "Treatise on Analysis" Vol 5 p 103 Academic press 1977

U. Fano "Description of states by the density matrix" Revs Mod PhysVol 29 No. 1 pp74-93 Jan 1957

P. S. Farago " Electron Spin Polarisation" Reports on Prog in Phys Vol 34 Pt 3 pp 1055-1124 1971

A.P French "Special relativity" Nelson 1982

H. Gent "Elliptically polarised waves and their reflection from radar targets" TRE memo No 584 Telecommunications Research Establishment Malvern, March 1954

H.Goldstein "Classical Mechanics" 2nd ed. Addison-Wesley 1980

C. Graham "Symmetry indications of the polarisation of light scattered by fluids..." Proc R Soc A 369 pp517-535 1980

C. D. Graves "Radar Power Polarisation scattering matrix" Proc IRE Feb 1956 pp248-257

R.Loudon "Quantum theory of light" Oxford Science pub. 1983

Ludwig "Definition of cross polarisation" IEEE trans Ap-21 pp116-119 1973

A.Marathay "Operator formalism in the theory of partial polarisation" J.Opt.Soc.Am. p969 Aug 1965

G.Mie Ann. Physik 25,377 (1908)

C.Misner et al "Gravitation" Chapter 41 Freeman 1973

M.Morgan "Synthesis and analysis of elliptic polarisation" Proc IRE Vol 39 pp552-556 May 1951

H.Mueller "Foundations of optics" J.Opt.Soc.Am Vol38 1948

F. Murnaghan "The Unitary and Rotation Groups" Lectures on Applied Maths Vol 3 Spartan Books 1962

J.F.Nye "Lines of circular polarisation in EM wave fields" Proc.R.Soc A 389, pp 279-290 1983

N.Parke "Matrix Optics" Phd thesis MIT (1948)

W.T.Payne "Elementary spinor theory" Am.J.Phys Vol 20 No.5 pp253-262 May 1952

W.T.Payne" "Spinor Theory of Four terminal networks" J. Math Phys Vol 32 pp19-33 April 1953

K. Gruner "Polarisation Dependence in Microwave Radiometry" IGARSS 82 International Remote Sensing Symposium

E. Hecht A. Zajac "Optics" Addison Wesley 1980

P Hillion "Spinor representation of EM fields" J. Opt. Soc Am. Vol 66 No 8 p 865 Aug 1976

P. Hillion "The spinor helmholtz equation" J. Math Phys 19(1) p 264 Jan 1978

J. R. Huynen "Phemomenolgical theory of radar targets" Phd thesis Drukkery Bronder-Offset, N.V. Rotterdam 1970

J.R.Huynen "Measurement of target scattering matrix" Proc IRE 53(8) pp 936-946 1965

I.Ionaddis "Optimum antenna polarisation for target discrimination in clutter" IEEE Trans AP 27 pp 357-363 May 1979

R.C.Jones J.Opt.Soc Am Vol31 pp488-499 (1941), Vol32 pp486-493 (1943), Vol37 pp107-110 (1947), Vol38 pp671-685 (1948), Vol 46 pp126-131 (1956)

H.Ko "On the reception of quasimonochromatic waves" Proc IRE Vol50 pp 1950-1957 Sept 1962

E.M.Kennaugh "Polarisation properties of radar reflections" MSc thesis Ohio State University 1952

F.Perrin "Polarisation of light scattered by isotropic media" J.Chem.Phys Vol10, p415 (1942)

A.J.Poelman "Polarisation vector translation in radar systems" Proc IEE Pt F Vol 130 pp 161-165 March 1983

H.Poincare "Theorie Mathematique de la Lumiere" Chapter 12 Paris 1892

Lord Rayleigh Phil. Mag. 12,81 (1881)

P.Roman "Generalised Stokes parameters for waves with arbitrary form" Nuove Cimento Vol 13 No. 5 pp974-982 Sept 1959

V.Rumsey et al "Techniques for handling elliptically polarised waves" Proc IRE Vol 39 pp533-556 May 1951

R.Schmeider "Stokes Algebra Formalism" J.Opt.Soc Am Vol 59 pp297-302 March 1969

W.Schurcliff "Polarised light:production and use" Harvard University press 1962

Scientific American "Haidinger Brush" Amateur Scientist July 1976

G.Sinclair Report 302-19 Antenna Lab Columbus Ohio 1945

M. Skolnik "Introduction to Radar Systems" McGraw Hill 1980

G. Sinclair Report 302-19 Antenna Lab Columbus Ohio 1945

Special Issue on Radar Reflectivity, Proc IEEE Vol 53(8) Aug 1965

Special Issue on Partial Coherence, Proc IEEE AP-15 Jan 1967

Special Issue on Inverse Methods in EM imaging, Proc IEEE AP-29 March 1981

G.Stokes "Mathematical and Physical papers" Cambridge University Press 1901

H. van de Hulst "Light scattering by small particles" Dover Press 1981

R.Wehner "Polarised light navigation by insects" Scientific American July 1976

N.Wiener "Generalised harmonic analysis" Acta math Vol55, p117 (1930)